Session 11

NUCLEAR WASTE TREATMENT

TUESDAY: October 21, 1980
CHAIRMAN: Russell Brown

VOLATILITIES OF RUTHENIUM, IODINE, AND TECHNETIUM ON CALCINING FISSION PRODUCT NITRATE WASTES

S. J. Rimshaw and F. N. Case
Oak Ridge National Laboratory*
Oak Ridge, Tennessee

Abstract

Various high-level nitrate wastes were subjected to formic acid denitration. Formic acid reacts with the nitrate anion to yield non-condensable, inert gases according to the following equation:

$$4\ HCOOH + 2\ HNO_3 \rightarrow N_2O + 4\ CO_2 + 5\ H_2O\ .$$

These gases can be scrubbed free of ^{106}Ru, ^{131}I, and ^{99}Tc radioactivities prior to elimination from the plant by passage through HEPA filters. The formation of deleterious NO_x fumes is avoided. Moreover, formic acid reduces ruthenium to a lower valence state with a sharp reduction in RuO_4 volatility during subsequent calcination of the pretreated waste. Comparative tests showed that on calcining an acidic thorium nitrate at 250 and 350°C, the percent ^{106}Ru volatilities were 26.2 and 27.5% for the untreated waste, and only 0.07 and 0.15%, respectively, for the same waste pretreated with 2.0 moles of formic acid per mole of nitrate. Other acidic nitrate wastes containing aluminum nitrate or (Zr, Al) fluoride-nitrate showed a substantial decrease in RuO_4 volatility on pretreatment with formic acid. The percent ^{106}Ru volatility is relatively low ($\sim$1.0%) on calcining untreated acidic wastes at high calcination temperatures of 600°C or on calcining alkaline wastes (sludge and sodium nitrate supernate). It is shown that a minimum of 3% of RuO_4 in an off-gas stream reacts with Davison silica gel (Grade 40) to give a fine RuO_2 aerosol having a particle size of 0.5 μ. This RuO_2 aerosol passes through water or weak acid scrub solutions but is trapped by a caustic scrub solution. Iodine volatilizes almost completely on calcining an acidic waste, and the iodine volatility increases with increasing calcination temperature. On calcining an alkaline sodium nitrate waste the iodine volatility is about an order of magnitude lower, with a relatively low iodine volatility of 0.39% at a calcination temperature of 250°C and a moderate volatility of 9.5% at 600°C. Volatilities of ^{99}Tc were generally <1% on calcining acidic or basic wastes at temperatures of 250 to 600°C. Data are presented to indicate that ^{99}Tc concentrates in the alkaline sodium nitrate supernatant waste, with $\sim$10 mg ^{99}Tc being associated with each curie of ^{137}Cs present in the waste. It is shown that lutidine (2,4 dimethyl-pyridine) extracts Tc(VII) quantitatively from alkaline supernatant wastes. The distribution coefficient (K_D) for Tc(VII) going into the organic phase in the above system is 102 for a simulated West Valley waste and 191 for a simulated Savannah River Plant (SRP) waste.

I. Introduction

Denitration

The nitrate anion is the predominant constituent in most, high-level, liquid wastes. In ([1]) it is shown that the most satisfactory

*Operated by Union Carbide Corporation under contract W-7405-eng-26 with the U.S. Department of Energy.

method of decomposing HNO_3 and minimizing toxic NO_x production involves addition of the acidic fission-product nitrate solution to formic acid. Formic acid is a reducing agent that reacts with nitric acid at 80 to 100°C to form CO_2, N_2O, and H_2O according to the following equation:

$$4\ HCOOH + 2\ HNO_3 \rightarrow N_2O + 4\ CO_2 + 5\ H_2O \qquad (1)$$

Because of the possible presence of volatile radioactive compounds such as I_2, Tc_2O_7, and RuO_4 in the off-gas stream, it is desirable that the gaseous byproducts (CO_2 and N_2O) be subjected to aqueous scrubbing prior to passage through HEPA filters and elimination from the plant. This process was developed and carried to the pilot plant stage at Karlsruhe, Germany.[2,3] Continuous chemical denitration can be carried out by premixing the formic acid with the high-level waste prior to injection into a spray calciner. In this case N_2 is likely to be formed rather than the N_2O that is formed by reaction of nitric acid with excess formic acid in aqueous solution.

When formic acid is added to the acidic nitrate solution in the presence of excess nitric acid, Orebaugh and Healy[4,5] show that the main reactions are as follows:

$$2\ HNO_3 + HCOOH \rightarrow CO_2 + 2\ NO_2 + 2\ H_2O \text{ at } HNO_3 > 4\ M \qquad (2)$$

and

$$2\ HNO_3 + 3\ HCOOH \rightarrow 3\ CO_2 + 2\ NO + 4\ H_2O \text{ at } HNO_3 < 2\ M \qquad (3)$$

Healy urged the application of these reactions to the removal and recycle of nitric acid from fission-product waste solutions. However, the recovery of NO_x gases introduces engineering and processing difficulties because of the slow absorption kinetics of hydrating the NO_x vapors to produce HNO_3 and HNO_2. The escaping NO_x vapors have an adverse environmental effect, with the threshold limiting value (TLV) for nitrogen dioxide being set at 0.05 ppm (0.10 mg/m^3) as an average annual value[6] because of the deleterious effects of NO_x vapors on lung function. Thus, the present technology has moved toward NO_x abatement rather than to HNO_3 recovery and recycle. Pence and Thomas[7,8] introduce ammonia gas, which reduces NO_2 to N_2 or N_2O according to the following reactions:

$$4\ NH_3 + 3\ NO_2 \rightarrow 7/2\ N_2 + 6\ H_2O + \text{heat} \qquad (4)$$

and

$$6\ NH_3 + 8\ NO_2 \rightarrow 7\ N_2O + 9\ H_2O \qquad (5)$$

Because of the inert nature of the reaction products (N_2 or N_2O gases), these gases can be scrubbed and filtered through HEPA filters before being eliminated from the plant. It should be noted that these same gases are produced by reacting nitrate in the presence of excess formic acid. The harmless inert, noncondensable gases (N_2 and N_2O) produced in both cases serve the goal of NO_x abatement.

Ruthenium Behavior

The high volatility of ruthenium when calcining HNO_3 solutions can be explained([1]) by the existence of a highly nitrated ruthenium complex that decomposes at higher temperatures with RuO_4 volatilization.([9,10,11]) Formic acid interacts with the nitrated octahedral complexes of ruthenium to yield formate complexes that decompose and form nonvolatile RuO_2, or possibly ruthenium metal, instead of the volatile RuO_4. On calcining a 4.0 *N* HNO_3 solution the RuO_4 volatility is decreased from ~35% to 0.007% after pretreatment with a 15% excess above two moles of formic acid per mole of nitrate.([1]) Thus, formic acid decreases the intrinsic volatility by reacting with and removing nitrato and nitro groups from ruthenium complexes.

The volatilized RuO_4 has a high solubility (0.07 to 0.10 mol/liter) in weak acid solutions([12]) and is easily scrubbed from an off-gas stream, with 99.9% trapping of RuO_4 in the first two scrubbers of an all-glass system.([1]) The RuO_4 is reduced to a nonvolatile, lower-valence state by hydrogen peroxide or nitrous acid present in the scrub solution.([13,14]) In studying the vapor pressure of RuO_4, Myuller and Nikol'skii([15]) found it necessary to work in all-glass equipment and to remove any grease film by pretreating the glass surfaces with strong oxidizing agents. Because of its reactivity, RuO_4 reacts with stainless steel to form black deposits of RuO_2.([16]) This reaction is rapid and complete even at room temperature. The author has observed the immediate coating of stainless steel surfaces with a black RuO_2 deposit after a strong oxidant is added to an acidic ruthenium solution contained in a Pyrex glass vessel fitted with a stainless steel head and stainless steel lines. Special precautions must be taken to eliminate vapor condensation because it is possible for RuO_4 to react with H_2O_2 or HNO_2 in the condensate. Hence, in addition to the use of glass equipment, the off-gas stream is passed through a filter enclosed in an electric heating mantle to prevent vapor condensation. Under these conditions, where precautions are taken to avoid reaction of RuO_4 with stainless steel or other materials, it is possible to define an intrinsic RuO_4 volatility, and to break down the problem of RuO_4 volatility into its component parts. Thus, for example, in ([1]) we have shown that the intrinsic volatility of RuO_4 is much greater on calcining nitric acid solutions than on calcining formic acid solutions. In this study the intrinsic volatilities of RuO_4 are compared between acidic nitrate wastes and the same wastes pretreated with formic acid. A low intrinsic RuO_4 volatility is desirable for the safe operation of a calcination plant.

Little light has been shed on the characteristics of RuO_2 aerosols formed by decomposition of RuO_4 in the gas phase or by interaction of RuO_4 with stainless steel or silica gel. Feber([17]) has observed the formation of particulate RuO_2 with a mean diameter of 0.05 μ or less as a result of RuO_4 decomposition in the gas phase. In this study, gaseous RuO_4 is reacted with silica to form a fine RuO_2 aerosol, which can pass through a series of four acid scrubbers without significant absorption, but which can be scrubbed from the off-gas stream by caustic scrubbing. Agglomerated particles of RuO_2 were observed in the acid traps after 15 to 30 min. This behavior indicates that ruthenium can spread throughout an off-gas system in the form of an RuO_2 aerosol as well as in the form of gaseous RuO_4.

Actually, ruthenium may be present predominantly in the off-gas system as a RuO_2 aerosol. Our observations in ([1]) and in this study show that it is possible to distinguish between gaseous RuO_4 and particulate RuO_2 in an off-gas stream by passing the gas through a series of four scrubbers with weak acid in the first two scrubbers and caustic in the last two scrubbers.

Rapid denitration of a salt at high temperatures leads to lower RuO_4 volatilities in a number of nitrate systems.([1]) The nitrate salt decomposes to an acid vapor (NO_x fumes) with formation of an alkaline residual calcine (the metal oxide). The alkaline oxide matrix fixes ruthenium as the ruthenate, and thus the formation of volatile RuO_4 is suppressed. Calcination of alkaline solutions also yields low ruthenium volatilities because of the fixation of ruthenium as ruthenate in an alkaline oxide matrix. In this study we report on the denitration of acidic solutions containing high concentrations of thorium nitrate, aluminum nitrate, and (Zr, Al) nitrate-fluoride mixture. On calcining the thorium nitrate and aluminum nitrate wastes, the intrinsic RuO_4 volatility is high (20 to 60%) at temperatures of 250 to 450°C, but decreases to a low value of 0.5 to 1.0% at the higher calcination temperature of 600°C. However, the (Zr, Al) fluoride-nitrate waste yields high RuO_4 volatilities (55 to 99%) at all temperatures from 250 to 600°C. Pretreatment of all acidic wastes with two moles of formic acid per mole of nitrate led to low intrinsic RuO_4 volatilities of 0.1 to 3.0% at calcination temperatures of 250 to 600°C. Calcination of alkaline wastes from the Savannah River Plant gave low RuO_4 volatilities.

A number of incidents involving the emission of particulate RuO_2 activity at various reprocessing sites have been reviewed.([18]) In these cases, the ruthenium was initially evolved as RuO_4, which reacted with the stainless steel equipment to form RuO_2. Caustic solutions were more effective than acid solutions in solubilizing the black RuO_2 deposits and in scrubbing RuO_2 aerosols from the off-gas stream. Because of the safety hazards, the processes involving the evolution of RuO_4 were evaluated, and then modified to decrease the risk of dealing with large amounts of volatile radioactive RuO_4. Usually the addition of a strong oxidant to an acid solution was eliminated to avoid the formation of volatile RuO_4. Idaho personnel have had extensive experience in operating a waste calcinator. Christian([16,19]) has described the difficulties encountered in controlling RuO_4 volatility. Since RuO_4 is formed during the calcination process and is converted to particulate RuO_2 by interaction of volatile RuO_4 with the stainless steel equipment, a final caustic scrubber at the end of the off-gas system in front of the HEPA filters of the off-gas system should be included to trap RuO_2 particulate activity. Giraud and LeBlaye([20]) report on the use of efficient caustic scrubbers in the off-gas system of a pilot plant calcining high-level waste with a high RuO_4 volatility of 15%. High decontamination factors (DF) for ^{106}Ru on the order of 10^9 to 10^{10} were obtained in spite of the high intrinsic RuO_4 volatility. Even higher DFs are obtainable at lower intrinsic RuO_4 volatilities.

Technetium Behavior

Smith, Cobble, and Boyd([21]) report vapor pressures so high for technetium heptoxide (Tc_2O_7), pertechnic acid ($HTcO_4$), and aqueous solutions

of $HTcO_4$ that almost complete volatility of ^{99}Tc would be expected on calcining an acid solution at 350°C. The boiling point of Tc_2O_7 is estimated to be 311°C, and the melting point is 118°C. The volatilities of Tc_2O_7 and $HTcO_4$ have been widely used to concentrate and isolate the long-lived ^{99}Tc by distillation from concentrated H_2SO_4 or perchloric acid at 200°C.([22,23]) However, our study([1]) shows less than 1% ^{99}Tc volatilization on calcining a fission-product HNO_3 solution over a range of temperatures from 250 to 600°C. These unexpectedly low ^{99}Tc volatilities can be correlated to the high thermal stability limits of various metal pertechnetates and technetates reported in ([24]) and which are presented in Table I.

Table I. High melting technetium oxide compounds.[a]

Compounds	Thermal stability limit (°C)	Comment
$Ba(TcO_4)_2$	700	
$Ba_3(TcO_5)_2$	850	
$Ba_5(TcO_6)_2$	850	Mixed oxide with BaO
$Sr(TcO_4)_2$	680	
$Sr_5(TcO_6)_2$	850	Mixed oxide with SrO
$Ca(TcO_4)_2$	650	
$Ca_5(TcO_6)_2$	800	Mixed oxide with CaO
Sr_2LiTcO_6	900	
$BaTcO_3$	800	
$SrTcO_3$	1200	

[a]Source: KFK-341 (July 1965).

It can be calculated that 10 µg of ^{99}Tc are associated with each mCi of ^{137}Cs as a result of ^{235}U fission. A total of 80 to 90% of fission ^{99}Tc is found associated with ^{137}Cs in alkaline sodium nitrate supernatant waste. Kelley([25]) notes that the alkaline SRP supernate contains 200 megacuries of ^{137}Cs in 100 megaliters of solution. Thus, the total amount of ^{99}Tc in the SRP alkaline supernate is 2000 kg. It is estimated that the solids would contain 865 nCi of ^{99}Tc per gram of solids.

It would be desirable to remove the long-lived ^{99}Tc (half-life of 2.05×10^5 y) from the alkaline sodium nitrate supernate. The removal of ^{99}Tc from alkaline solutions by solvent extraction with lutidine (2,4-dimethylpyridine) is described in ([26,27]). The distribution coefficient (K_D) for the extraction of Tc(VII) by lutidine is 102 for a simulated West Valley waste and 191 for a simulated SRP alkaline sodium nitrate waste. Lutidine can be used to recover or remove Tc(VII) from liquid alkaline wastes.

Iodine Behavior

Iodine is readily volatilized from acid solution during dissolution of fuel elements in heated acid. Thus, Yarbro([28,29]) reports that 98 to 99% of the iodine is evolved during dissolution and feed adjustment. With NO injection and reflux([30]), it is possible to evolve 99.8% of the iodine during dissolution. Thus, the main fission product liquid waste will contain only a small fraction of the iodine formed in fission, which is 0.10 Ci of ^{129}I per metric ton of

uranium irradiated at 30,000 Mwd. The volatilized iodine can be trapped by wet scrubbing([1,31]) at a yield of 95 to 99% (DF of 20 to 100). Wet scrubbing has been used to trace the fate of iodine during calcination.([1]) Iodine volatility is lower on evaporating an alkaline solution than on evaporating an acid solution.([32]) Iodine can also react with stainless steel equipment at elevated temperatures.([33]) On calcining a HNO_3 waste the iodine volatility increases with increasing temperature,([1]) as shown in Fig. 1 and Table II. An appreciable fraction of the iodine is retained in the solid residue only at the lower temperatures (350°C and lower). Almost all the iodine is volatilized at the higher temperatures (650°C and higher). Wastes containing a high fraction of the iodine should be segregated and treated separately.

Table II. Iodine distribution in the pot calciner off-gas scrubber system.

	Calcination temperature (°C)						Row[b]
	350	450	550	650	350[a]	650[a]	
Total distribution of iodine (%)							
Residues	70.2	44.6	41.2	22.6	37.0	2.3	A
Particulates[d]	1.2	9.7	2.3	2.6	3.3	1.0	B
Volatiles	28.6	45.7	56.5	74.8	59.7	96.7	C
Distribution of volatiles (%)							
Formic acid scrubber							
Trap 1	19.2	33.0	52.6	63.9	48.3	76.1	D
Trap 2	7.8	10.2	3.5	9.9	9.6	19.5	E
Trap 3	1.1	0.8	0.2	0.6	0.5	0.7	F
Trap 4	0.3	0.2	0.07	0.2	0.2	0.2	G
NaOH scrubber	0.03	1.3	0.06	0.1	0.1	0.02	H
HEPA							I
Adsorbents							
1st charcoal filter	0.17	0.2	0.07	0.2	1.0	0.18	J
2nd charcoal filter							K
Silica gel				0.08[c]			L

[a] Pretreated with formic acid (2 moles per mole of nitrate).
[b] Rows A–C total 100%; rows D–L total to line C.
[c] The silica gel was placed ahead of the charcoal filter.
[d] Iodine found on rinsing the filter in front of the wet scrubbers.

II. Description of Equipment and Experimental Procedure

A small quartz pot calciner is mounted inside a 10×10×10-cm cavity in a laboratory furnace. The solution to be calcined is added dropwise to the calciner, which is held at a constant temperature. Evaporation takes place by flash evaporation. The vapors are drawn off through a sidearm and passed through a 9-cm-diam fritted glass

disk of medium porosity (10- to 15-μ pore size) encased in a heating mantle to prevent condensation of RuO_4. The off-gas is also pulled through four water (weak acid) scrubbers filled with glass Rashig rings and connected to each other with glass ball joints. Since the equipment is of all quartz and Pyrex construction and no grease was used in the ball joints, no black deposits of RuO_2 were ever observed. A caustic scrubber, a silica gel column, and a HEPA filter followed by a vacuum pump complete the off-gas scrubbing train. More details are given in ([1]). A sketch of the equipment is shown in Fig. 2.

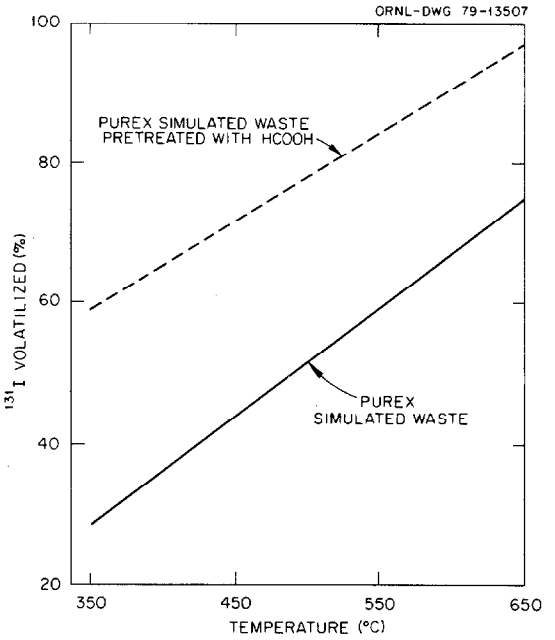

Fig. 1. Iodine-131 volatilization (%) vs temperature (°C).

The solution in the first two water scrubbers was sampled and gamma-emitting radioactivities were analyzed by gamma scanning to determine ^{106}Ru or ^{103}Ru, ^{95m}Tc and ^{131}I; ^{134}Cs, ^{144}Ce, and ^{152}Eu, as well as ^{106}Ru were routinely determined in a mixture of aged fission products by gamma scanning. Strontium-90 and ^{99}Tc were determined radiochemically after addition of a carrier. Nitrate was determined by reduction to ammonia with the use of Devarda's alloy. Other cations were determined by emission spectroscopy.([1])

A highly radioactive nitric acid waste was prepared as described in ([1]). The composition of waste constituents and radioactivity concentrations is given in Table III. This high-level radioactive waste was used in the preparation of other highly radioactive wastes. Generally, one part of this waste was added to nine parts of a waste containing the major stable components in order to prepare a simulated high-level waste. The composition and activity concentrations of the waste are given in the section in which the waste is discussed. The results of tracer level activity runs were generally confirmed by the results obtained in the high-level activity runs.

ORNL-DWG 79-13506

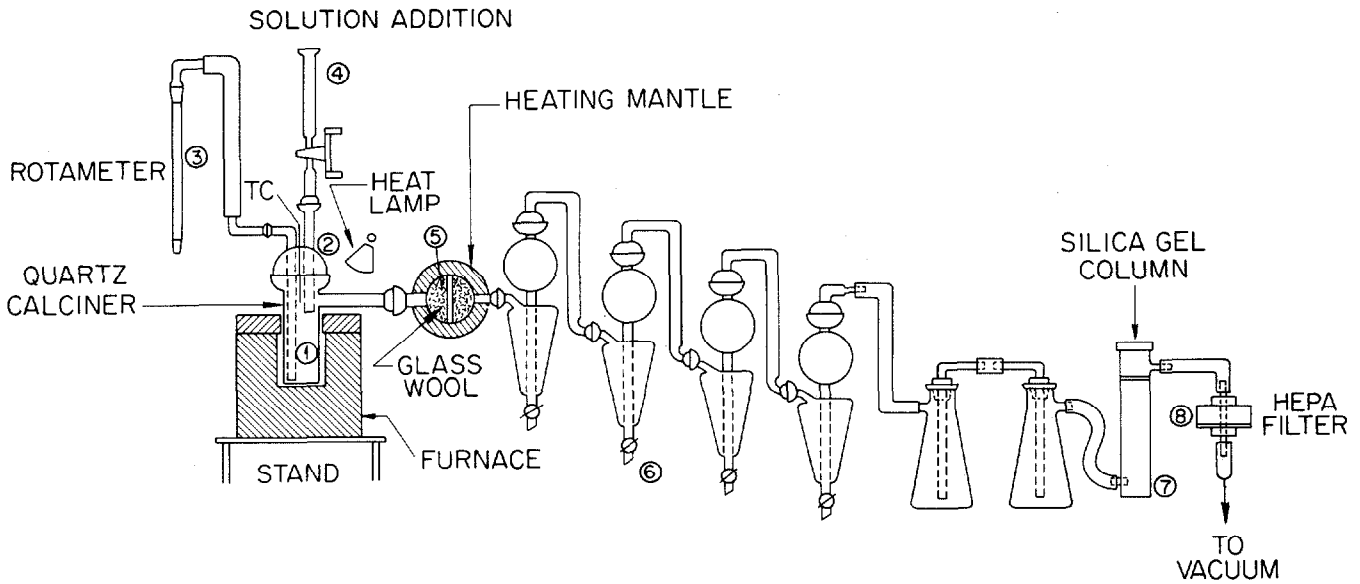

Fig. 2. Quartz pot calciner and off-gas scrubber train.

Table III. Composition of actual and simulated HNO_3 waste (100 gallons waste per 1000 kg of U)

Constituent	Formula	Concentration, molar	
Nitric acid	HNO_3	4.0	
Uranium nitrate	$UO_2(NO_3)_2$	0.123	(1% of original U)
Ruthenium nitrate	$Ru(NO_3)_3$	0.061	
Cesium nitrate	$Cs(NO_3)$	0.062	
Rare earth nitrates	$M(NO_3)_3$	0.1608	
Gadolinium nitrate	$Gd(NO_3)_3$	0.1512	(added as a neutron poison)
Strontium nitrate	$Sr(NO_3)_2$	0.0246	
Barium nitrate	$Ba(NO_3)_2$	0.0336	
Cerium nitrate	$Ce(NO_3)_3$	0.0477	
Sodium nitrate	$NaNO_3$	0.0114	
Iron nitrate	$Fe(NO_3)_3$	0.0945	(Stainless steel corrosion products)
Nickel nitrate	$Ni(NO_3)_2$	0.0036	
Chromium nitrate	$Cr(NO_3)_3$	0.0102	
Zirconium nitrate	$Zr(NO_3)_4$	0.1074	
Molybdenum oxide	MoO_3	0.0981	

Activity concentrations

Isotope	Activity curies/liter
Ruthenium-106	120
Cesium-137	177
Cesium-134	75.3
Strontium-90	158
Cerium-144	159
Europium-154	9.1
Technetium-99	86.9 (mg)

III. Calcining Acidic Thorium Nitrate Waste

At present a total of 45,000 liters of this waste is stored at the West Valley site in New York. The waste composition is as follows: $Th(NO_3)_4$ = 1.46 *M*; $Al(NO_3)_3$ = 0.36 *M*; HNO_3 = 1.03 *M*; F = 0.10 *M*; and P = 0.04 *M*. Two series of calcination experiments were run at 250, 350, 450, and 600°C. In one series the simulated liquid waste was converted to a solid by adding the liquid at a controlled rate to the quartz pot calciner held at the indicated temperature without any pretreatment. In the second series the nitrate in the waste was subjected to the reducing action of formic acid by adding the nitrate waste to 90% formic acid held at 80 to 100°C. Then this pretreated waste (two moles of formic acid per mole of nitrate) was converted to a dry solid by flash evaporation in the quartz pot calciner. The results of these two series of experiments are presented in Fig. 3 and Table IV. The simulated waste was made up by adding one part of acid waste in Table III to nine parts of acid thorium nitrate waste. Only tracer-level experiments were run. No high-level experiments were performed with the acidic thorium nitrate waste.

Table IV. Tracer studies of ruthenium volatility as a function of temperature on calcining acidic thorium nitrate waste with and without formic acid pretreatment.

Temperature (°C)	^{106}Ru volatility (%)		Nitrate in residual solid (%)	
	Untreated[a]	Treated with formic acid[b]	Untreated	Treated with formic acid
250	26.2	0.07	1.6	0.5
350	27.5	0.15	1.1	0.1
450	0.6	0.10	0.2	0.1
600	0.5	0.18	0.1	0.07

[a] Composition of initial thorium nitrate waste: $Th(NO_3)_4$ = 1.46 *M*; $Al(NO_3)_3$ = 0.36 *M*; HNO_3 = 1.03 *M*; F = 0.10 *M*; and P = 0.04 *M*.

[b] Thorium nitrate waste was added to a formic acid solution heated to 80 to 100°C and containing two moles of formic acid per mole of nitrate in the waste.

One tracer level experiment with ^{131}I, on calcining an untreated thorium nitrate waste at 250°C, showed a high iodine volatility of 28%.

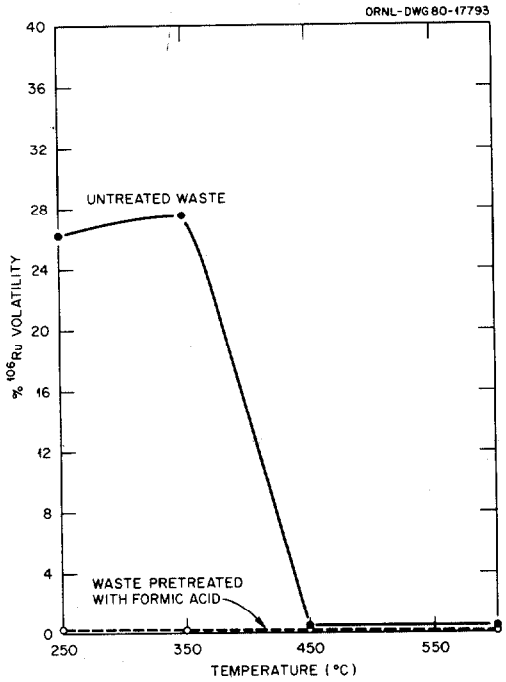

Fig. 3. Ruthenium volatility on calcining thorium nitrate waste (tracer studies).

Thermal denitration precedes ruthenium fixation in an alkaline oxide matrix. The thermal decomposition of thorium nitrate is discussed in ([34]), where it is noted that thorium nitrate decomposes directly to thorium oxide without the formation of an intermediate basic nitrate salt. The equation for the decomposition of the anhydrous thorium nitrate salt is as follows: $Th(NO_3)_4 = ThO_2 + 4\ NO_2 + O_2$. The decomposition pressure is 119 torr at 134°C, 199 torr at 145°C, and 359 torr at 161°C.

In this case the ThO_2 serves as the alkaline oxide matrix. If denitration is rapid, the incoming acid waste is neutralized, and ruthenium is fixed in the alkaline oxide matrix as ruthenate. If the denitration is slow, insufficient ThO_2 is formed and RuO_4 can evolve under the conditions of high local acidity. Thus, high RuO_4 volatilities of 26.2 and 27.5% are noted at 250 and 350°C, even though the nitrate contents of the residual salt are low (1.6 and 1.1%, respectively). In contrast, the pretreatment of the acidic thorium nitrate waste with formic acid gives low RuO_4 volatilities at all calcination temperatures. Formic acid reduces ruthenium to a lower valence state and interacts with nitrato and nitro groups of the octahedral ruthenium complexes. Decarboxylation at higher temperatures then gives RuO_2 or ruthenium metal rather than volatile RuO_4.

IV. Calcining Acidic Aluminum Nitrate Waste

Acidic aluminum nitrate waste is produced at the Idaho reprocessing plant from aluminum-clad, spent fuel. Its composition is given by Christian([16]) as follows: $Al(NO_3)_3$ = 2.1 *M*; HNO_3 = 1.3 *M*; and $NaNO_3$ = 0.15 *M*. The volume of this waste is only 10% of the total volume of high-level waste generated at the Idaho plant. This waste is usually blended with the zirconium fluoride waste to decrease the fluoride corrosion on the equipment.

Simulated high-level waste was made up by adding one part of waste having a composition given in Table III to nine parts of aluminum nitrate waste. The radioactivity levels were a factor of 20 to 100 times higher for our simulated high-level waste than they were for an authentic aluminum-zirconium blend given in ([35]). Tracer-level and high-level runs were carried out at calcination temperatures of 250, 350, 450, and 600°C on the untreated waste and on the aluminum nitrate waste pretreated with two moles of formic acid per mole of nitrate. The results of ^{106}Ru and ^{99}Tc volatilities from these runs are presented in Tables V, VI, and VII, and in Fig. 4.

Table V. Tracer-level experiments to determine ^{106}Ru volatility as a function of temperature from the pot calcination of aluminum nitrate waste with and without formic acid pretreatment.[a]

Temperature (°C)	^{106}Ru volatility (%)		Nitrate in residual salt (%)	
	Untreated	Pretreated with formic acid[b]	Untreated	Pretreated with formic acid[b]
250	31.6	0.06	3.6	2.7
350	21.0	0.20	13.5	4.2
450	57.2	0.09	4.1	1.0
600	0.9	0.13	2.6	7.5

[a]Composition of initial aluminum nitrate waste: $Al(NO_3)_3$ = 2.1 *M*; $NaNO_3$ = 0.15 *M*; HNO_3 = 1.3 *M*.
[b]Aluminum nitrate waste was added to formic acid solution that was heated to 80 to 100°C and that contained two moles of formic acid per mole of nitrate.

Table VI. High-level experiments to determine ^{106}Ru volatility as a function of temperature from the pot calcination of aluminum nitrate waste.[a]

Temperature (°C)	^{106}Ru volatility (%)		Nitrate in residual salt (%)	
	Untreated	Pretreated with formic acid[b]	Untreated	Pretreated with formic acid[b]
250	11.0	1.5	25.4	14.5
350		1.0		7.9
450	45.3	0.8	0.2	9.0
600	17.5	2.8	0.6	3.1

[a]Composition of initial aluminum nitrate waste: $Al(NO_3)_3$ = 2.1 *M*; $NaNO_3$ = 0.15 *M*; HNO_3 = 1.3 *M*.
[b]Aluminum nitrate waste was added to formic acid solution that was heated to 80 to 100°C and that contained two moles of formic acid per mole of nitrate.

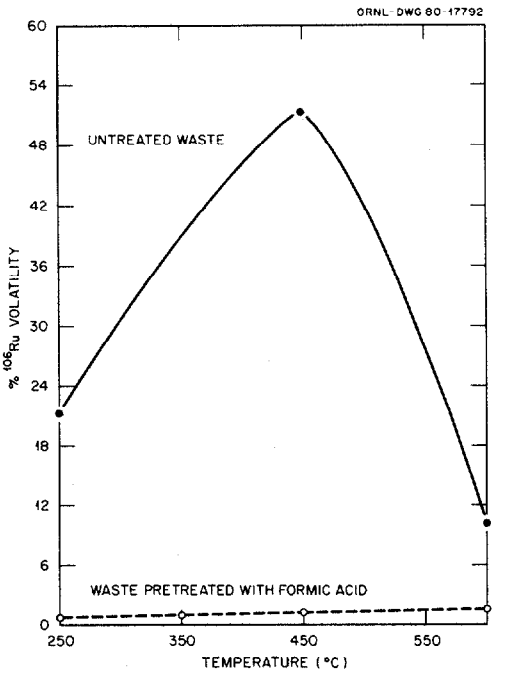

Fig. 4. Ruthenium volatility vs temperature on calcining aluminum nitrate waste.

Table VII. Results of high-level experiments to determine ^{99}Tc volatility as a function of temperature and pretreatment conditions during the pot calcination of aluminum nitrate waste.[a]

Temperature (°C)	^{99}Tc volatility (%)	
	Untreated	Treated with formic acid[b]
250	<1.1	<0.1
350		<0.1
450	<0.7	<0.2
600	<1.0	<0.1

[a]Composition of initial aluminum nitrate waste: $Al(NO_3)_3$ = 2.1 *M*; $NaNO_3$ = 0.15 *M*; HNO_3 = 1.3 *M*.

[b]Aluminum nitrate waste was added to a formic acid solution that was heated to 80 to 100°C and contained two moles of formic acid per mole of nitrate.

The ^{99}Tc volatilities are all low (<1.0%) on calcining the aluminum nitrate waste over a temperature range of 250 to 600°C, whether or not the waste has been pretreated with formic acid. Although no experiments with ^{131}I tracer were run, our previous experience in calcining acidic nitrate wastes([1]) indicates that the ^{131}I volatility should be high and should increase with temperature on calcining an acidic aluminum nitrate waste.

As can be seen from Fig. 4, the calcination of acidic $Al(NO_3)_3$ waste pretreated with formic acid gives much lower RuO_4 volatilities than those obtained on calcining the untreated $Al(NO_3)_3$ waste. The formic acid serves a double function. It reacts directly with the nitrate anion to give N_2 or N_2O. It also reduces ruthenium to a lower valence state and prevents the formation of volatile RuO_4 during calcination.

Thermal denitration of the untreated $Al(NO_3)_3$ waste proceeds with the formation of lower basic aluminum nitrates and the evolution of NO_x fumes([36]). Under calcination conditions ruthenium forms a highly nitrated complex that decomposes with RuO_4 volatilization. In this case moderate amounts of RuO_4 are evolved at 250 and 350°C, with a maximum at 450°C. At a higher temperature of 600°C the alkaline oxide matrix fixes ruthenium as the ruthenate,([1]) and the amount of evolved RuO_4 is decreased.([1]) Our results agree with those of Christian,([16]) who reports a RuO_4 volatility of 65% at 400°C and 2% at 500°C on calcining an $Al(NO_3)_3$ waste in a fluidized bed reactor.

V. Calcining (Zr,Al) Fluoride-Nitrate Waste

The bulk of the high-level waste produced at the Idaho Falls plant is (Zr, Al) fluoride-nitrate waste. Its composition is given in ([16]) as follows: $Al(NO_3)_3$ = 0.6 *M*; $Zr(NO_3)_4$ = 0.35 *M*; HNO_3 = 3.2 *M*; HF = 3.0 *M*. This waste was calcined directly without adding a calcium salt to fix fluoride. A simulated high-level waste was prepared by blending nine parts of waste of the above composition with one part of waste of a composition given in Table III. The activity levels in the simulated high-level waste were a factor of 20 to 100 higher than in the actual waste. Tracer-level and high-level experiments were performed by flash evaporation of the untreated and formic-acid-treated wastes in the quartz pot calciner at temperatures of 250, 350, 450, and 600°C. The results of these experiments are presented in Tables VIII, IX, and X, and in Fig. 5.

Table VIII. Results of high-level experiments to determine ^{99}Tc volatility as a function of temperature and pretreatment conditions during the pot calcination of (Zr,Al) fluoride-nitrate waste.[a]

Temperature (°C)	^{99}Tc volatility (%)	
	Untreated	Treated with formic acid[b]
250	<2.6	8.1
350	1.3	5.1
450	9.2	3.0
600	21.1	12.9

[a] Composition of initial (Zr,Al) fluoride-nitrate waste: $Al(NO_3)_3$ = 0.6 *M*; $Zr(NO_3)_4$ = 0.35 *M*; HNO_3 = 3.2 *M*; HF = 3.0 *M*.

[b] (Zr,Al) fluoride-nitrate waste was added to a formic acid solution containing two moles of formic acid per mole of nitrate, heated to 80 to 100°C.

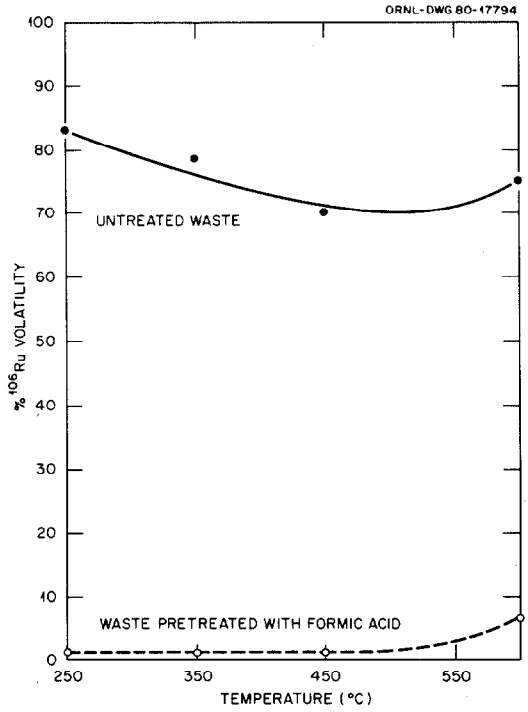

Fig. 5. Ruthenium volatility vs temperature on calcining a (Zr,Al) fluoride-nitrate waste.

Table IX. Tracer-level experiments to determine ^{106}Ru volatility as a function of temperature and pretreatment conditions during the flash evaporation of (Zr,Al) fluoride-nitrate waste.[a]

Temperature (°C)	Ru volatility (%)		Nitrate in residual salt (%)	
	Untreated	Treated with formic acid[b]	Untreated	Treated with formic acid[b]
250	83.4	0.7	0.16	0.026
350	61.0	0.5	0.13	0.012
450	60.6	0.5	0.024	0.018
600	55.4	12.5	0.024	0.012

[a]Composition of initial (Zr,Al) fluoride-nitrate waste: $Al(NO_3)_3$ = 0.6 *M*; $Zr(NO_3)_4$ = 0.35 *M*; HNO_3 = 3.2 *M*; HF = 3.0 *M*.
[b](Zr,Al) fluoride-nitrate waste was added to a formic acid solution containing two moles of formic acid per mole of nitrate, heated to 80 to 100°C.

From Tables IX and X and Fig. 5, it can be seen that the use of formic acid dramatically reduces the volatility of ruthenium. From an almost quantitative evolution of ruthenium of 50 to 99%, the volatility of ruthenium is decreased to a percent or two on pretreating the (Zr,Al) fluoride-nitrate waste with two moles of formic acid per mole of nitrate. The percent nitrate in the residual salt remains low regardless of the calcination temperature or the pretreatment conditions. The low nitrate content of the salt would seem to point to a reaction between HNO_3 and HF under calcination conditions, but it is not clear at the present stage of investigation what this reaction

Table X. High-level experiments to determine ^{106}Ru volatility as a function of temperature and pretreatment conditions during the flash evaporation of a (Zr,Al) fluoride-nitrate waste in a quartz pot calciner.[a]

Temperature (°C)	^{106}Ru volatility (%)		Nitrate in residual salt (%)	
	Untreated	Treated with formic acid[b]	Untreated	Treated with formic acid[b]
250		1.8		1.9
350	99.1	2.2	0.5	0.7
450	80.0	1.3	1.8	0.7
600	93.1	0.8	0.65	1.9

[a]Composition of initial (Zr,Al) fluoride-nitrate waste: $Al(NO_3)_3$ = 0.6 *M*; $Zr(NO_3)_4$ = 0.35 *M*; HNO_3 = 3.2 *M*; HF = 3.0 *M*.
[b](Zr,Al) fluoride-nitrate waste was added to a formic acid solution containing two moles of formic acid per mole of nitrate, heated to 80 to 100°C.

would be. It is possible that ruthenium is being volatilized as RuF_5 and that ruthenium is reduced to a lower valence state by formic acid to prevent volatilization of RuF_5. It was found that 5 to 20% of the initial fluoride was volatilized during calcination of the acid fluoride waste. Fluoride is usually tied up by previous addition of a calcium salt to the acid fluoride waste.

VI. Calcining Alkaline Sodium Nitrate Supernate and Sludge

Alkaline Sodium Nitrate Waste

At present megaliters of alkaline sodium nitrate supernate are stored in mild steel tanks at Hanford, Savannah River, and West Valley.[37,38] The compositions of this waste stored at the Savannah River Plant (SRP) and the West Valley plant are given in Tables XI and XII, respectively.

Table XI. Composition of alkaline sodium nitrate supernatant waste at Savannah River Plant, South Carolina

Constituent	Formula	Concentration (moles)	Constituent	Formula	Concentration (moles)
Sodium nitrate	$NaNO_3$	2.2	Sodium sulfate	Na_2SO_4	0.3
Sodium nitrite	$NaNO_2$	1.1	Sodium chloride	NaCl	0.022
Sodium aluminate	$NaAlO_2$	0.5	Sodium fluoride	NaF	0.002
Sodium hydroxide	NaOH	0.75	Mercury	Hg	0.001
Sodium carbonate	Na_2CO_3	0.3			

Table XII. Composition of alkaline sodium nitrate waste at West Valley, New York

Constituent	Formula	Concentration (moles)
Sodium nitrate	$NaNO_3$	6.0
Sodium sulfate	Na_2SO_4	0.32
Disodium phosphate	Na_2HPO_4	0.10
Sodium oxalate	$Na_2C_2O_4$	0.09
Aluminum nitrate	$Al(NO_3)_3$	0.11
Sodium molybdate	Na_2MoO_4	0.01
Sodium fluoride	NaF	0.01
Sodium chloride	NaCl	0.01
Sodium hydroxide	NaOH	1.0

A simulated high-level waste was prepared by blending nine parts of alkaline sodium nitrate waste with one part of highly radioactive waste having a composition given in Table III. The activity levels in the simulated high-level waste are approximately the same as those found in the actual waste. Tracer-level and high-level experiments were performed by flash evaporation of the waste in a quartz pot calciner at temperatures of 250, 350, 450, and 600°C.

Metal Hydroxide Sludge

The sludge composition was a composite of a number of sludges analyzed at the Savannah River Plant.[39] The average SRP sludge consists of 31.6 wt % Fe_2O_3, 46.4 wt % Al_2O_3, 10.3 wt % MnO_2, 6.1 wt % U_3O_8, 3.3 wt % CaO, and 2.3 wt % NiO. The sludge was prepared by making up a HNO_3 solution of the metal elements and precipitating the metal hydroxides by neutralizing the acid solution with caustic. The sludge also contained other elements up to the following amounts: 4.1 wt % Hg, 0.1 wt % Ru, 0.02 wt % I, and 0.0033 wt % Ag. Sludge tagged with tracer was prepared by adding tracer to the acid solution just prior to caustic neutralization. Silver was added only in a few experiments involving iodine tracing. The sludge was washed twice with water to remove most of the sodium salts, resuspended in water, and fed to the calciner as a 3.3% (dry basis) oxide-water slurry. The centrifuged volume of hydrous hydroxides in the hydroxide-water slurry was 50% of the total volume.

Ruthenium Behavior

Alkaline sodium nitrate supernate (simulated West Valley waste) was pretreated with two moles of formic acid per mole of nitrate to determine the completeness of denitration. The tracer-level experiments are in essential agreement with the high-level experiments, as can be seen from Table XIII. Because of hydroxide substitution in the octahedral ruthenium complex, the ruthenium volatilities are low at all temperatures. Considerable denitration of sodium nitrate is achieved at relatively low temperatures with the use of formic acid.

Tracer-level RuO_4 volatility determinations were performed on a simulated SRP sludge recovered from an alkaline solution 6.0 *N* in sodium nitrate and 1.0 *N* in sodium nitrite after aging for one week.

Table XIII. Ruthenium volatility as a function of temperature on calcining a West Valley alkaline sodium nitrate supernate pretreated with two moles of formic acid per mole of nitrate

Temperature (°C)	^{103}Ru volatility (%)		Nitrate in residual calcine (%)	
	Tracer-level	High-level	Tracer-level	High-level
250	0.034	0.17	2.4	10.1
350	0.037	0.32	3.0	
450	0.26	0.37	1.2	11.7
600	0.055	0.22	0.6	5.9

Table XIV. Tracer-level RuO_4 volatility as a function of temperature on calcining a simulated SRP sludge recovered from an alkaline solution 6.0 *N* in $NaNO_3$ and 1.0 *N* in $NaNO_2$ after aging for one week.[a]

Temperature (°C)	RuO_4 volatility (%)
250	0.004
350	0.001
450	0.175
600	0.30

[a] Centrifuged volume of hydrous metal hydroxides was 50%. Sludge composition: 31.6 wt % Fe_2O_3, 46.4 wt % Al_2O_3, 10.3 wt % MnO_2, 6.1 wt % U_3O_8, 3.3 wt % CaO, 2.3 wt % NiO, and 0.03 wt % RuO_2. Sludge was washed twice with distilled water.

As can be seen from Table XIV, the RuO_4 volatilities were low at all temperatures, and increased slightly with increasing temperature.

Iodine Behavior

Stable iodine was added to SRP processing solutions to control the valence state of plutonium during its separation from uranium. Most of this stable iodine was added to the alkaline waste. Our studies showed that 75% of the iodine reports to the alkaline supernate, while 25% coprecipitates with the sludge. If the sludge is treated with boiling 5 *N* NaOH to remove aluminum,([38]) most of the iodine (>95%) will be found in the alkaline supernate after processing.

A simulated West Valley alkaline supernate tagged with tracer ^{131}I was rapidly evaporated to dryness in the quartz calciner held at 250, 350, 450, and 600°C. The results presented in Table XV and Fig. 6 show that the iodine volatility increases linearly with temperature. Iodine volatilities on calcining an alkaline solution are lower than those obtained on calcining an acid solution.([1])

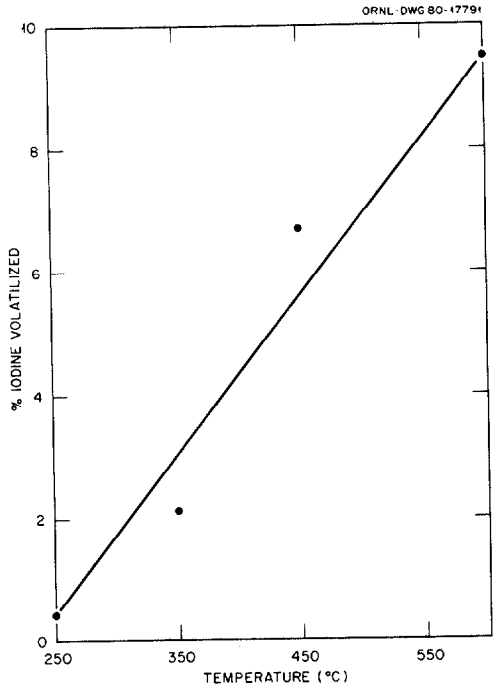

Fig. 6. Iodine volatility as a function of temperature on calcining simulated alkaline sodium nitrate supernate from West Valley, New York.

Table XV. Iodine volatility as a function of temperature during the flash evaporation of West Valley alkaline sodium nitrate supernate in a quartz pot calciner

Temperature (°C)	^{131}I volatility (%)
250	0.4
350	2.1
450	6.7
600	9.5

Iodine volatility was also determined on a simulated SRP sludge containing both mercury and silver. The results are presented in Table XVI and Fig. 7. The iodine volatility increases with increasing temperature of calcination.

Difficulties were encountered in determining ^{131}I material balances on calcining a simulated SRP sludge tagged with ^{131}I in a stainless steel spray calciner having wall temperatures of 650 to 775°C. Only 3 to 7% of the ^{131}I reported to the solid residue in the calciner. A total of 50 to 65% of the ^{131}I was recovered in rinse solutions (6 *N* HNO_3 and 1.0 *N* NaOH – 0.05 *M* sodium persulfate) used to remove iodine from the stainless steel walls. A total of 25 to 50% of the ^{131}I was still unaccounted for in the stainless steel equipment. Iodine appears to react with stainless steel at elevated temperatures.([33])

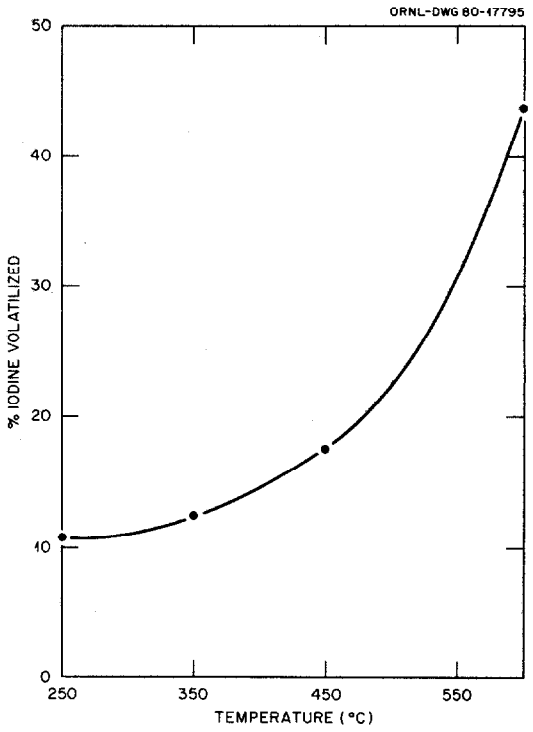

Fig. 7. Iodine volatility as a function of temperature on calcining simulated SRP sludge containing mercury and silver and tagged with ^{131}I.

Table XVI. Iodine volatility as a function of temperature on calcining a simulated SRP sludge containing mercury and silver tagged with ^{131}I.[a]

Temperature (°C)	Iodine volatility (%)
250	10.8
350	12.5
450	17.2
600	43.7

[a]Sludge composition (dry oxides): 31.6 wt % Fe_2O_3; 46.4 wt % Al_2O_3, 10.3 wt % MnO_2, 6.1 wt % U_3O_8, 3.3 wt % CaO, 2.3 wt % NiO, and up to 4.1 wt % Hg, 0.1 wt % Ru, 0.02 wt % I, and 0.0033 wt % Ag.

Technetium Behavior

Technetium is found associated with ^{137}Cs in the alkaline supernate. An analysis on a West Valley supernate showed 10.0 µg of ^{99}Tc per mCi of ^{137}Cs, which represents 92% of the theoretical amount of ^{99}Tc formed in fission. On the other hand, an analysis of an authentic SRP sludge showed <0.3% of the theoretical amount of ^{99}Tc formed in fission.

A simulated SRP alkaline sodium nitrate supernate containing 100 mg of ^{99}Tc per liter and ^{95m}Tc tracer was calcined by flash evaporation in a quartz pot calciner at 250, 350, 450, and 600°C.

The results are presented in Table XVII along with the results of ^{99}Tc volatility from a simulated high-level SRP alkaline waste pretreated with formic acid. As reported previously,[1] the volatility of ^{99}Tc is low in the presence of large amounts of salts because of the high thermal stability limits of pertechnetate compounds.

Table XVII. Volatility of ^{99}Tc as a function of temperature on calcining a simulated SRP alkaline sodium nitrate supernate containing 100 mg of ^{99}Tc per liter and ^{95m}Tc tracer, and on calcining a simulated high-level SRP alkaline supernate pretreated with formic acid.

Temperature (°C)	^{99}Tc volatility (%)	
	Tracer-level	High-level[a]
250	0.0025	<2.6
350	0.0033	<3.3
450	0.0044	
600	0.0063	<0.001

[a]Pretreated with two moles of formic acid per mole of nitrate.

The above results indicate that ^{99}Tc will concentrate in the alkaline sodium nitrate supernate. Kelley[25] notes that the alkaline SRP supernate will contain 200 megacuries (MCi) of ^{137}Cs in 100 megaliters (Ml) of solution. If it is assumed that 10 μg of ^{99}Tc are associated with each mCi of ^{137}Cs, it can be calculated that the total amount of ^{99}Tc in the SRP alkaline supernate is 2000 kg. If it is further assumed that each liter of SRP alkaline supernate contains 400 g of solids per liter and that the specific activity of ^{99}Tc is 0.0173 Ci/g of ^{99}Tc, it can be calculated that these solids contain 865 nCi of ^{99}Tc/g of solids, an amount that considerably exceeds 10 nCi/g, which is used as a guide in disposing of waste containing long-lived alpha emitters. In addition to removing ^{137}Cs, ^{90}Sr, and plutonium from SRP alkaline supernate by ion exchange processing,[40] these calculations and analyses show that it would also be desirable to remove the long-lived ^{99}Tc (half-life of 2.05×10^5 y) from the alkaline sodium nitrate supernate.

A suitable method that involves the removal of ^{99}Tc from an alkaline sodium nitrate solution by solvent extraction with lutidine (2,4 dimethylpyridine) is described in [26,27]. The distribution coefficient (K_D), which is the ratio of the Tc(VII) concentration in the organic phase divided by the Tc(VII) concentration in the aqueous phase, decreases with increasing sodium nitrate concentration in the alkaline supernate, as can be seen from Table XVIII taken from [27]. Lutidine extracts Tc(VII) almost completely even from an alkaline solution containing 2.9 *M* $NaNO_3$ and 0.1 *M* NaOH. The K_D for Tc(VII) is 102 for a simulated West Valley waste and 191 for a simulated SRP waste. Each waste contained 4 mg of ^{99}Tc/liter and ^{95m}Tc tracer.

The distribution of Tc(VII) between the organic and aqueous phases (K_D) was determined as a function of technetium loading of the organic phase (lutidine). The initial solution was a simulated SRP alkaline sodium nitrate supernatant waste containing 0.400 g of ^{99}Tc

Table XVIII. Distribution coefficient of technetium (VII) as a function of nitrate concentration in a mixture of NaOH + $NaNO_3$ at a constant ionic strength of 3.[a]

Nitrate concentration in mole/liter	K_D for Tc(VII) in lutidine
2.9	78.5
2.5	104
2.0	146
1.5	171
1.0	205
0.5	296
0.3	604
0.1	775
zero	1670
$NaNO_3$ = 6.0 *N*; Na_2So_4 = 0.35 *M*	102 (West Valley waste, see Table XII)
$NaNO_3$ = 2.2 *N*; $NaNO_3$ = 1.1 *N*; Na_2SO_4 = 0.3 *M*	191 (Savannah River waste, see Table XI)

[a]Data taken from ([27]) except the K_D values for West Valley and Savannah River wastes, which were determined experimentally.

Table XIX. Distribution coefficient (K_D) of ^{99}Tc between lutidine (2,4 dimethylpyridine) and simulated SRP alkaline sodium nitrate waste containing 0.400 g of ^{99}Tc per liter and ^{95m}Tc tracer as a function of ^{99}Tc loading in the organic phase.

Number of extraction	Distribution coefficient of ^{99}Tc (K_D)	^{99}Tc (g/liter)	
		Organic	Aqueous
2	91	0.774	0.008
4	89	1.530	0.017
6	79	2.260	0.029
8	78	2.976	0.038
10	68	3.656	0.053
12	60	4.298	0.072
15	58	5.210	0.090
16	54	5.488	0.102
20	45	6.525	0.145
22	38	6.928	0.182
24	34	7.257	0.213
26	32	7.496	0.234
28	30	7.577	0.253
29	29	7.588	0.262
30	30	7.597	0.263

per liter and ^{95m}Tc tracer. The ^{99}Tc concentration is a factor of 10 higher than the highest ^{99}Tc concentration expected in SRP waste. From the results presented in Table XIX it can be seen that the K_D for ^{99}Tc decreases slowly as the organic phase (lutidine) becomes loaded with ^{99}Tc. This K_D remains high enough to concentrate and recover ^{99}Tc in high yield with high decontamination of the waste from ^{99}Tc. A plot of the technetium distribution between the organic and aqueous phase is presented in Fig. 8.

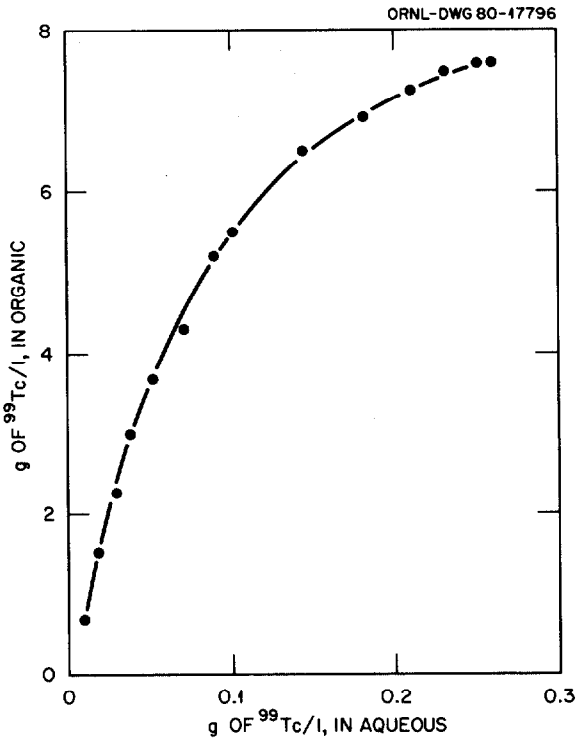

Fig. 8. Technetium distribution between organic and aqueous phase on contacting an organic lutidine (2,4 dimethylpyridine) phase with successive portions of a simulated SRP alkaline sodium nitrate supernatant waste containing 0.400 g of ^{99}Tc/liter and ^{95m}Tc tracer.

The solvent (lutidine) can be distilled and recycled back to be reused in the process. The sodium technetate can be shipped as a solid for disposal with other wastes by hydraulic fracture, or it can be incorporated into a cement and shipped to an approved site for permanent disposal.

VII. Generation of a Fine RuO_2 Aerosol

Because of its high vapor pressure,([15]) RuO_4 diffuses rapidly throughout the off-gas system. Because of its reactivity, the RuO_4 interacts with stainless steel with the formation of a black shiny deposit of RuO_2.([16]) It is not known whether the ruthenium in a practical system of stainless steel equipment is present as RuO_4, RuO_2 or a mixture of both these forms. In an all-glass system, 99.9% of the RuO_4 in an off-gas stream can be trapped in the first two water scrubbers of the train.([1]) Black RuO_2 deposits on stainless steel

equipment can be dissolved by a 1.0 *N* NaOH–0.05 *M* sodium persulfate solution to give a clear orange solution.([41]) Heavy reliance is usually placed on packed columns filled with silica gel as the sorbent material to remove RuO_4.([16,42,43]) The DF across the silica gel bed is only 8 for particulate matter and 1000 for volatile RuO_4.([44]) This system was chosen as an object of study to distinguish between RuO_4 and RuO_2 in the off-gas effluent from a silica gel column.

The equipment shown in Fig. 2 was modified by replacing the quartz calciner with a 1-liter Pyrex flask, in which gaseous RuO_4 was generated by adding periodic acid or potassium permanganate as an oxidizing agent to an 18 *N* H_2SO_4 solution containing ruthenium. Air was pulled through a dip leg in the 1-liter flask to sweep out the RuO_4. The off-gas laden with gaseous RuO_4 was passed down through a column of Davison 40 silica gel supported on a 10-cm fritted-glass filter having a medium porosity (pore size of 10 to 15 μ). The same filter shown in Fig. 2 next to the quartz calciner, which was used to trap particulate matter formed during calcination, was converted to a silica gel column by removing the glass wool packing, filling with silica gel and mounting vertically in the off-gas line. The equipment was of all-glass construction with ball joints being used for flexibility. The first four traps contained weak acid as the scrubbing medium, while the fifth trap contained a caustic solution.

As the gaseous RuO_4 reacted with the silica gel, a dark green color was noted in the upper part of the silica gel column. At this time the four acid scrubbers remained colorless. This behavior indicated that no significant absorption of RuO_4 from the off-gas stream was taking place. Soon it was noted that a tygon line connecting the fourth acid trap and the fifth caustic trap was starting to turn black. Also, significant amounts of ruthenium, indicated by a color change, were being absorbed in the fifth caustic trap. After 15 to 30 minutes, a small amount of agglomerated black particles was observed in the acid traps. It was concluded that significant quantities of a fine RuO_2 aerosol were formed by reacting RuO_4 with silica gel. This aerosol passed unscathed through the silica gel column, a fritted-glass filter, and four weak acid scrubbers. A caustic solution is a more suitable scrubbing medium than a weak acid solution for removing the RuO_2 aerosol particles from an off-gas stream. Although our previous experiments([1]) have shown that 99 to 99.9% of any RuO_4 should have been caught in the first two acid scrubbers, the amount of particulate RuO_2 trapped by acid scrubbing is considerably less.

In order to ascertain some of the physical characteristics of the fine RuO_2 aerosol, samples collected on a millipore filter were examined under a scanning electron microscope. The particles consisted primarily of agglomerated RuO_2 particles having a mean diameter of <0.5 μ. A number of particles having a mean diameter of 0.1 μ were observed in agreement with the particle size reported by Feber([17]) who noted an average diameter of 0.05 μ for an RuO_2 aerosol. X-ray diffraction analysis showed that the particles consisted mainly of RuO_2.

Tracer ^{106}Ru was added to the distilling flask, and the previous experiment was repeated in order to determine the amount of fine RuO_2 aerosol that is formed on reacting RuO_4 with silica gel. The first

trap contained an acid scrub solution, and the next three traps contained a 1.0 *N* NaOH—0.05 *M* sodium persulfate scrub solution. As can be seen from Table XX, the first acid trap caught very little of the RuO_2 aerosol, while the caustic traps were moderately efficient in trapping the RuO_2 particles. At least 3% of the total ruthenium in the distilling flask reacted with the silica gel and passed out of the bottom of the silica gel column and through the first acid trap in the form of a fine RuO_2 aerosol.

Table XX. Scrubbing of a fine RuO_2 aerosol by a 1.0 *N* NaOH—0.05 *M* sodium persulfate solution after interaction of radioactive RuO_4 with Davison silica gel (grade 40) supported on a 10-cm, fritted-glass filter of medium porosity (pore size of 10 to 15 μ)

Trap number	Percent of initial ruthenium	Type of scrubber
1	0.0037	acid
2	1.95	caustic
3	1.04	caustic
4	0.05	caustic

VIII. Conclusions and Recommendations

Denitration

Chemical denitration with formic acid leads to the formation of noncondensable gases (nitrogen or nitrous oxide), which may be eliminated through HEPA filters after liquid scrubbing to remove gaseous radioactivities. The denitration of HNO_3 and metal nitrate solutions is carried out without the evolution of toxic NO_x vapors, which have an adverse environmental effect and deleterious effects on lung function in man. Formic acid can be advantageously used to reduce the large amounts of nitrate anion that have accumulated in nuclear defense wastes without the necessity of recycling nitric acid.

Ruthenium

The intrinsic volatility of RuO_4 formed by decomposition of a highly nitrated ruthenium complex can be reduced to the vanishing point by the use of two moles of formic acid per mole of nitrate. Formic acid reacts with the nitrated octahedral complexes of ruthenium to yield lower-valence formate complexes of ruthenium that decompose with the formation of nonvolatile RuO_2 instead of the volatile RuO_4. The use of formic acid is recommended whenever it is desirable to decrease the intrinsic volatility of RuO_4 almost to zero (for example, during the calcination of high-level wastes).

Rapid thermal denitration of high-level wastes can also be carried out in a number of cases at a high temperature of 600°C with the evolution of a few percent of the ruthenium in the form of RuO_4. Even though the intrinsic RuO_4 volatility is low in this case, it is recommended that a liquid caustic scrubber be installed in front of the HEPA filters to remove any RuO_2 particulate matter formed as a result

of the interaction of RuO_4 with the stainless steel components of the off-gas system.

Finally, it is recommended that the interaction of RuO_4 with silica gel and with stainless steel at high temperatures should be investigated fully to determine how adequately the various components of the off-gas system retain the fine RuO_2 aerosol that may be formed in stainless steel systems under calcination conditions.

Iodine

A high fraction of iodine compounds is decomposed and volatilized on calcining acidic nitrate solutions. The iodine volatility is almost an order of magnitude lower on calcining alkaline wastes than it is on calcining an acid waste. Wet scrubbers are effective in removing iodine from an off-gas stream in concentrated form. It is recommended that methods be developed to withdraw an iodine concentrate from a bubble-cap plate in order to prevent the buildup and breakthrough of iodine activity in the off-gas stream.

Technetium

Generally, less than 1% of the ^{99}Tc volatilizes on calcining either acidic or basic nitrate solutions of fission products over a range of temperatures from 250 to 600°C. Most of the fission product ^{99}Tc can be found associated with ^{137}Cs in the alkaline nitrate supernate. It is recommended that pilot plant studies be initiated to recover ^{99}Tc from the alkaline nitrate supernate by solvent extraction with lutidine (2,4 dimethylpyridine).

REFERENCES

(1) S. J. Rimshaw, F. N. Case, and J. A. Tompkins, *Volatility of Ruthenium-106, Technetium-99, and Iodine-129, and the Evolution of Nitrogen Oxide Compounds During the Calcination of High-Level, Radioactive Nitric Acid Waste*, ORNL-5562 (February 1980).

(2) S. Drobnick and W. A. Hild, "Destruction of Nitric Acid in Wastes,"in *Gesellschaft für Kernforschung M.B.H., Karlsruhe, Germany, Annual and Semiannual Reports* KFK-888, p. 58 (1968); KFK-1030, p. 58 (1970); KFK-1346, p. 26 (1971); KFK-1456, p. 26 (1971); and KFK-1544, p. 30 (1972).

(3) W. Guber et al., "Lab-Scale and Pilot-Plant Experiments on the Solidification of High-Level Wastes at the Karlsruhe Nuclear Research Centre," in *Management of Radioactive Wastes from the Nuclear Fuel Cycle, Proc. OECD-IAEA Symp., March 22–26, 1976*, IAEA-SM-207/79, Vol. 1, pp. 271–81 (1976).

(4) E. G. Orebaugh, *Denitration of Savannah River Plant Waste Streams*, DP-1417 (July 1976).

(5) T. V. Healy, "The Reaction of Nitric Acid with Formaldehyde and with Formic Acid, and Its Application to the Removal of Nitric Acid from Mixtures," *J. Appl. Chem.* 8, 553 (1958).

(6) *Nitrogen Oxides-Medical and Biologic Effects of Environmental Pollutants*, National Academy of Science, Washington, D.C. (1977).

(7) D. T. Pence and T. R. Thomas, "NO_x Abatement at Nuclear Processing Plants," in *Proc. 2nd AEC Environmental protection Conf. Albuquerque, New Mexico, April 16, 1974*, WASH-1332, Vol. 1, pp. 427–443 (1974).

(8) T. R. Thomas and D. H. Munger, *An Evaluation of NO_x Abatement by NH_3 over Hydrogen Mordenite for Nuclear Fuel Reprocessing Plants*, ICP-1133 (January 1978).

(9) J. M. Fletcher et al., "Nitrato and Nitro Complexes of Nitrosyl-ruthenium," *J. Inorg. Nucl. Chem.* 1, 378–401 (1955).

(10) J. M. Fletcher et al., "Nitrato Complexes in Aqueous Nitric Acid," *J. Inorg. Nucl. Chem.* 1, 154–73 (1959).

(11) P. G. M. Brown et al., "The Significance of Certain Complexes of Ruthenium, Niobium, Zirconium, and Uranium in Plant Processes," in *Peaceful Uses of Atomic Energy, Proc. 2nd Int. Conf.*, Vol. 17, p. 188, United Nations, Geneva (1958).

(12) *Gmelin's Handbuch Der Inorganischen Chemie*, 8th ed., p. 246, System-Number 63, Ruthenium, Verlag Chemie GMBH, Weinheim/Bergstr. (1970).

(13) J. M. Fletcher, "Complexes Derived From (RuNO)III and RuIV," *J. Inorg. Nucl. Chem.* 8, 277–87 (1958).

(14) J. S. Anderson and J. D. M. McConnell, "Ruthenium (IV) Nitrates," *J. Inorg. Nucl. Chem.* 1, 371–77 (1955).

(15) R. L. Myuller and A. B. Nikol'skii "Method of Determining the Vapor Pressure of Ruthenium Tetroxide Over its Aqueous Solution by Means of Radioactive Tracers" *Radiokhimiya* 4(3), 364–70 (May-June 1962).

(16) J. D. Christian, "Process Behavior and Control of Ruthenium and Cerium," in *Controlling Air-Borne Effluents from Fuel Cycle Plants* (Proc. American Nuclear Society and American Institute of Chemical Engineers Meeting, August 5–6, 1976, Vol. 1, pp. 2-1 – 2-34 (1977).

(17) R. C. Feber, "Removal of Ruthenium," in *Prog. Nucl Energy, Ser. III*, F. R. Bruce, J. M. Fletcher, and H. H. Hyman (eds.), Vol. 2, p. 250, Pergamon, New York (1958).

(18) S. J. Rimshaw, "Ruthenium: A Special Safety Problem," *Nucl. Safety* 4(4), 117–19 (1963).

(19) J. D. Christian and D. W. Rhodes, *Ruthenium Containment During Fluid-Bed Calcination of High-Level Waste from Commercial, Nuclear Fuel, Reprocessing Plants*, ICP-1091 (January 1977).

(20) J. P. Giraud and G. LeBlaye, "Design of an Industrial Facility for the Incorporation of Fission Products into Glass and the Storage of Highly Radioactive Glass," in *Management of Radioactive Wastes from Fuel Reprocessing, Proc. OECD-IAEA Symp., November 27–December 1, 1972*, Vol. 1, pp. 813-846 (March 1973).

(21) W. T. Smith, Jr., J. W. Cobble, and G. E. Boyd, "Thermodynamic Properties of Technetium and Rhenium Compounds. I. Vapor Pressures of Technetium Heptoxide, Pertechnic Acid and Aqueous Solutions of Pertechnic Acid," *J. Am. Chem. Soc.* 75, 5773–76 (1953).

(22) E. Anders, *The Radiochemistry of Technetium*, Pamphlet NAS-NS 3021 in Chemistry, Office of Technical Services, Department of Commerce, Washington, D.C.

(23) A. N. Murin et al., "Technetium – Element 43," *Uspekhi Khimii* 33(1), 274–91 (1961).

(24) M. Wassilopulos, *On Polyoxides of Four- and Seven-Valent Technetium with Alkaline Earths*, KFK-341, p. 67 (July 1965).

(25) J. A. Kelley, W. H. Hale, J. A. Stone, and J. R. Wiley, "Solidification and Storage of Savannah River Plant Radioactive Waste." in *AIChE Symposium Series, "Radioactive Wastes from the Nuclear Fuel Cycle,"* Vol. 72, No. 154, pp. 128–31, or DP-MS-75-19 (November 1975).

(26) S. J. Rimshaw and G. F. Malling, "Solvent Extraction of Technetium and Rhenium with Pyridine and Methyl-Substituted Pyridine Derivatives from Alkaline Media," *Anal. Chem.* 33, 751–4 (May 1961).

(27) A. A. Zaitsev, I. A. Lebedev, S. V. Pirozhkov, and G. N. Yakovlev, "Extraction of Technetium (VII) by Pyridine Derivatives from Alkaline Solutions," *Radiokhimiya* 6, 445–8 (1964).

(28) O. O. Yarbro, J. C. Mailen, and M. J. Stephenson, "Retention of Gaseous Isotopes," in *Nuclear Power and Its Fuel Cycle*, Vol. 4, pp. 681–693, IAEA (1977).

(29) O. O. Yarbro, W. S. Groenier, and M. J. Stephenson, "Airborne Effluent Control for LMFBR Fuel Reprocessing Plants," in *Proc. on Controlling Airborne Effluents from Fuel Cycle Plants*, Sun Valley, Idaho, August 5–6, 1976, Vol. 1, pp. 15-1 – 15-12 (1976).

(30) E. Henrich, *Comparative Studies of Process Variables in Fuel Dissolution and in Dissolver Off-Gas Handling*, Collection of Reports on the Status of Reprocessing and Waste Treatment, KFK-2940, pp. 163–81 (November 1979).

(31)F. Baumgärtner et al., *Status of the Technology of Handling the Off-Gases of a Reprocessing Plant and Modes of Operational Optimization*, KFK-2615, p. 73 (November 1977).

(32) Yu. N. Degtyarev and G. A. Beloslyudova, "The Determination of ^{131}I," *Radiokhimiya* 7(6), 729–32 (1965).

(33) C. E. Lamb, C. L. Fitzgerald, and V. C. A. Vaughen, *Behavior of Fission Product Iodine in the Head-End Reprocessing of HTGR Fuel*, Iodine-129 Studies (Series I), ORNL/TM-6642 (July 1979).

(34) *Gmelin's Handbuch Der Inorganischen Chemie*, 8th ed., p. 245, System-Number 44, Thorium, Verlag Chemie GMBH, Weinheim/Bergstr. (1955).

(35) *Alternatives for Long-Term Management of Defense High-Level Radioactive Waste*, Idaho Chemical Processing Plant, Report ERDA 77-43, Table 4-1, pp. 4-2 (September 1977).

(36) *Gmelin's Handbuch Der Inorganischen Chemie*, 8th ed., p. 156, System-Number 35, Aluminum, Part B, The Compounds of Aluminum, Verlag Chemie, GMBH, Berlin, Germany, 1934.

(37) Staff of Battelle Northwest Pacific Laboratory, *Alternative Process for Managing Existing Commercial High-Level Radioactive Wastes*, NUREG-0043 (April 1976).

(38) G. W. Becker, *Defense Waste Processing Facility*, DPSTD-77-13 (January 1979).

(39) M. J. Plodinec, *Viscosity of Glasses Containing Simulated Savannah River Plant Waste*, DP-1507, p. 9 (August 1978).

(40) J. R. Wiley, *Decontamination of Savannah River Plant Waste Supernate*, DP-1436 (August 1976).

(41) *Gmelin's Handbuch Der Inorganischen Chemie*, 8th ed., pp. 144–153, System-Number 63, Ruthenium, Verlag Chemie GMBH, Weinheim/Bergstr. (1970).

(42) J. D. Christian and D. T. Pence, *Critical Assessment of Methods for Treating Airborne Effluents from High-Level, Waste, Solidification Processes*, PNL-2486 (June 1977).

(43) R. E. Schindler, *Removal of Particulate Solids from the Off-Gas of the WCF and NWCF*, ICP-1157 (June 1978).

(44) R. A. Brown, D. A. Knecht, and T. R. Thomas, *Reference Facility Description for the Recovery of Iodine, Carbon, and Krypton*, ICP-1126, p. 6 (April 1978).

DISCUSSION

KABAT: Did you identify the chemical form of the iodine that was released from the solution in the Purex process?

RIMSHAW: No, we just started with a 4N nitric acid solution and all data were obtained with tracer iodine. We did not identify the chemical form. It was whatever it would be in 4N nitric acid.

KABAT: What about organic iodides?

RIMSHAW: I would guess, just looking at our data, that you would not have much chance for organic iodides. Since formic acid reduces, you would have most iodine in the iodide form in that solution. Some iodine and iodate would be formed in nitric acid but the formic acid would tend to keep it all as iodide. It would be my guess that it would tend toward the iodide form in the reducing

medium. But I guess iodine would evolve from the salts by thermal decomposition. The higher temperature makes me think it would be analogous to a thermal denitration except that this process should be considered as a thermal deiodization.

ROUYER: Do you have indications of the performance of the silica gel column for ruthenium?

RIMSHAW: We deliberately reacted silica gel with RuO_4 in the vapor form. We did not know what was going to come out and we were very surprised when the ruthenium went all the way through our acid traps and got caught in the last caustic trap. So, we started to look at the reaction more closely. From previous experiments we knew that RuO_4 in the vapor form was efficiently scrubbed by weak acid medium. So we suspected that the ruthenium was present as particulate RuO_2. Then, we ran an x-ray defraction pattern on a sample collected on a Millipore filter and found that it was RuO_2. Does that answer your question?

ROUYER: At which temperature?

RIMSHAW: This was from room temperature up to about 100°. We distilled the ruthenium tetroxide at 60-80°. We had a heating jacket around the silica gel column. We kept it warm so that the RuO_4 entered the silica gel column at about 100°, I would say.

SRIDHAR: I think you have shown that with predenitration with formic acid you can reduce the volatility of ruthenium. At the same time, the volatility of iodine increases. You showed a separate stream of iodine being treated quite independently. Could you clarify what stream you are talking about?

RIMSHAW: We are talking about the Purex waste, from which most of the iodine has been removed. The residual iodine is only 0.1 to 1% of the total amount in the fuel rods. However, there was a mandate to look at this problem. Even though we are only dealing with a tenth of a percent, iodine behavior during calcination is of interest. I do not know if I am answering your question, but we are not dealing with the main stream of iodine at this point.

SRIDHAR: That is what I wanted to know. I was confused by your saying on one hand that you are looking at the chemical predenitration with formic acid that reduces the volatility of ruthenium but at the same time pointing out that it also increases the volatility of iodine. Are you referring to the dissolver solution?

RIMSHAW: We are not dealing with the dissolver solution at this point. We are dealing with the waste after fuel rod dissolution. In fact, we corroborated the German results. We got over 99% of our iodine to distill out during waste preparation; so we took the residual waste and added iodine and tracer back in to see how it would behave on calcination.

CHEMICAL BEHAVIOUR OF RADIOIODINE UNDER LOSS OF COOLANT ACCIDENT CONDITIONS

M.J. Kabat
Ontario Hydro
Safety Services Department
Toronto, Ontario

Abstract

An experimental study on radioiodine behaviour and its release and control under LOCA conditions is being carried out at Ontario Hydro. The reaction of I_2 vapour with H_2O (25° - $85^{\circ}C$) and steam (100° - $120^{\circ}C$) was experimentally evaluated, using a species selective sampler to determine the concentrations of airborne radioiodine species. The formation and release of chemical species were strongly dependent on water temperature. More than 90% of iodine was released as HOI at $> 60^{\circ}C$, with relatively small amounts of organic species formed under the above conditions. A significant portion of radioiodine also remained airborne after mixing I_2 vapour with air and steam and subsequently condensed at 25° - $80^{\circ}C$. Hypoiodous acid was the major species formed in all experiments. Desorption and composition of iodine species released from the condensate was also evaluated. Desorption of > 1% in the first few hours was measured and HOI was again found to be the major component. Airborne HOI was found to be relatively stable under normal conditions, while it rapidly decomposed when heated to $> 250^{\circ}C$ or exposed to high intensity UV light. Mass spectrometric analysis of species evolved from aqueous radioiodine solutions showed distinct mass peaks at 143 and 161, corresponding to IO^- and $IO^- \cdot H_2O$ respectively. This strongly supports the presence of HOI as a stable airborne iodine species.

I. Introduction

A considerable amount of data is available in the literature on the qualitative and quantitative aspects of radioiodine release from reactor accidents. However, the chemical behaviour of iodine at very low concentrations has not been fully understood and the majority of previous reactor accident analysis were based on the assumption that only elemental iodine and its gaseous organic compounds could be formed and released from a damaged reactor core. However, the existence of hypoidous acid, the missing member of the hypohalous group, was theoretically predicted and, in the last decade, considerable effort has been made to obtain experimental confirmation of its existence. However, only indirect, radiometric methods have been used for its measurement because it occurs only at very low concentrations, detection of which was very difficult with existing direct physico-chemical methods (mass, molecular structure, etc.). Nevertheless this low concentration of airborne radioiodine potentially could still present serious environmental hazards in an emergency situation. Improved knowledge of iodine is essential for performing an analysis of radiological hazards from reactor accidents. The objective of this experimental investigation was to provide the basic data for this purpose.

II. Generation of Gaseous I_2 and HOI

A suitable method for generation of elemental iodine (with $^{131}I_2$) vapour, containing minimum amounts of HOI and organic iodine compounds, was needed for the experimental investigation of I_2 reactions with water and steam and for qualitative and quantitative evaluation of reaction products.

Pure HOI was needed for the determination of its airborne stability, its partition with water and LiOH solutions and for future investigations on its surface deposition and for optimization of its control in gaseous releases.

Generation of I_2 Vapour

The method used in our experiments for I_2 vapour generation is based on the red-ox reaction:

$$5I^- + IO_3^- + 6H^+ \rightleftarrows 3I_2 + 3H_2O \qquad [1]$$

In highly acidic solutions of $> 10^{-3}$M concentrations its hydrolysis to HOI is negligible. In our experiments approximately 50 ml of 10^{-3}M KI solution, containing 20-50 μCi of $Na^{131}I$, was mixed with equivalent amounts of KIO_3 and H_2SO_4 to obtain pH = 1. Zero air was bubbled through the solution at the rate 2-10 ml/min., stripping the I_2 vapour which was subsequently diluted with air or other carrier gas.

Typical composition of iodine species in the stream was:

99.4% I_2
0.5 (0.2-0.7)% HOI
0.1 (0.05-0.2)% org. I

The portion of HOI slightly increased with depletion of iodine from the solution. After about 3 hours use of the generator the HOI portion increased to 0.5-1%.

Distilled water, analytical grade chemicals and fresh solutions had to be used for I_2 generation in order to maintain organic compounds content below 0.2%.

Generation of Gaseous HOI

Hypoiodous acid HOI is formed from iodine solutions either by its hydrolysis:

$$I_2 + H_2O \rightleftarrows HOI + H^+ + I^- \qquad [2]$$

or by red-ox reaction:

$$2I_2 + IO_3^- + 6H^+ + 2H_2O \rightleftarrows 5H_2OI^+ \qquad [3]$$

$$H_2OI^+ + H_2O \rightleftarrows HOI + H^3O^+ \qquad [4]$$

The method of the generation of HOI, with a low content of both I_2 and organic compounds, which involved the reactions [3] and [4] was used in our experimental investigations on HOI airborne stability and its water/air partitions. Detail description of the HOI generator is given in publication (1). At elevated temperatures (50-70°C) gaseous HOI (at concentrations up to 100 ppb) was released from the solution with air which also contained:

$\leq$ 5% I_2 (easily removed with Cu screens)

$\leq$ 1% organic iodine compounds

The evaluation of airborne HOI yield from iodine hydrolysis, reaction [2], under loss of coolant accident conditions was the basic purpose of this project. Results will be given and discussed in sections IV and V.

III. Measurement of Airborne Iodine Species

Elemental iodine and organic iodine compounds can exist at high airborne concentrations, therefore, their chemical or physico-chemical determination is not difficult. However, HOI can be generated only at very low airborne concentrations (presently the maximum obtainable concentration is approximately 100 ppb) which have been only radiometrically detectable.

Radiometric Determination of Iodine Species

A method of selective absorption of airborne I_2, HOI and CH_3I, described in publication (1) was used in our experiments. Elemental iodine is absorbed on Cu screens, HOI collected with a specific absorbent (silver impregnated carbon) and organic iodine compounds with TEDA impregnated charcoal. The typical absorption profile of the above species in the selective sampler components at 25°C, 70% RH and 10 cm/sec. face velocity, is illustrated in Figure 1.

The diagram shows that all elemental iodine is collected by 3-4 Cu screens, which coincidentally absorb less than 2% HOI. None of CH_3I is absorbed on the Cu screens. Hypoiodous acid is then quantitatively absorbed in less than 50 mm of the specific absorbent, also retaining 2-4% of organic iodine compounds which are finally collected with TEDA impregnated charcoal.

In the absence of other analytical methods for direct determination of HOI, the above highly selective absorption method was considered to be adequate for the purpose of this experimental study.

Mass Spectrometry of Gaseous Iodine Species

The formation and behaviour of HOI generated in the laboratory, also identified in field samples, correspond to properties theoretically derived in publication (2) and several chemical publications. However, its direct identification was not performed because it is only available at very low concentration.

Preliminary measurements were made using a highly sensitive TAGA TM 3000 mass spectrometry system, described in publication (3) to determine the mass number of the iodine species. Several spectra were obtained which clearly indicate the presence of molecules with mass number 143 (IO^-) and 161 (hydrated IO^-). Description of the experiment and discussion of the results follow.

Testing Procedure. A gaseous sample, containing specific iodine forms, was mixed with zero air (carrier gas), the molecules were chemically ionized using O_2^- as the reagent ion and analyzed with a quadrupole mass spectrometer. Elemental iodine vapour in dry air was injected into the carrier gas stream (zero air) with a syringe at a controlled rate. Hypoidous acid was generated from KI + KIO_3 solutions, as described in publication (1) and also carried with zero air into the mass spectrometer.

Elemental iodine solutions in distilled water were also bubbled with air and the sample analyzed for iodine species.

Discussion of Results

The mass spectrum analysis results are presented in Figures 2-11.

The "zero air" background spectrum in Figure 2 does not contain any peaks above the noise level at the mass numbers (m/z) 143, 161, 175 and 254.

Figure 3 presents large peaks of I^- (m/z = 127) and I_2^- (m/z = 254) formed after adding I_2 vapour into the carrier gas (zero air) stream.

Figure 4 indicates efficient removal of I_2 from the sample with a copper trap.

Figure 5 illustrates the mass spectrum of I_2 vapour in zero air at higher aperture potentials. The ratio of I^- (127) to I_2^- (254) increased due to fragmentation of I_2^- to I^- resulting from the higher internal energy of I_2^-.

Figure 6 shows that a little amount of HOI seen as IO^- (143) and its hydrated form (161) can be stripped with air from water solution of iodine at approximately 10^{-3}M concentration. A clear peak at the m/z = 175, corresponding to IO_3^- is also present in this spectrum.

It is evident from Figure 7 that the relative amount of HOI significantly increased after diluting the iodine solution to approximately 10^{-5}M.

Figure 8 demonstrates that the non-elemental iodine species, formed in our HOI generator, are identical with species formed from hydrolysis of elemental iodine solutions.

The hydrated HOI is practically eliminated and HOI generation rate reduced with increasing pH, as follows from Figure 9. However, the generation rate of HOI again increased with increasing temperature.

Removal of elemental iodine from the sample stream with copper is illustrated in Figure 10. The ratio of the peaks at mass numbers 127 and 143 indicates that the Cu trap removed elemental iodine more efficiently than it removed hypoiodous acid.

Figure 11 demonstrates good efficiency of the specific HOI absorbent for removal of both HOI forms.

The above results strongly indicate that the volatile non-elemental species, formed from iodine hydrolysis and also in our HOI generator are two forms (basic and hydrated molecule) of hypoiodous acid. Their chemical behaviour (temperature and pH dependence, absorption properties) is as expected from the theoretical analysis in publication (2). However, the results are not considered to be sufficiently conclusive. Insufficient time (less than 2 days) was available for performing the mass spectrometry analysis, high humidity in the samples (from bubbler) caused some experimental difficulties and the possibility of HOI also being formed in the process of chemical ionization could not be adequately investigated. However, from the preliminary measurements it is apparent that the mass spectrometry method has a good potential to clarify the existence of HOI and could also be used to thoroughly investigate its properties.

IV. Reactions of I_2 Vapour With H_2O

Reactions of elemental iodine with water were theoretically evaluated in publication (2). It is evident from the analysis, our previous experimental work and difficulties experienced in other laboratories that low concentration iodine chemistry is a very difficult area.

From the theoretical analysis it was concluded that:

1. Iodine hydrolysis depends:
   - on temperature of iodine solution
   - inversely on iodine concentration in H_2O (significant formation of HOI at concentrations of $< 10^{-5}$M).
2. Besides elemental iodine, HOI is the only highly volatile inorganic iodine compound present in water solutions of iodine.

The actual conditions, under which iodine would be released from defective fuel under LOCA conditions, could not be specified. Therefore, the following assumptions were made:

1. Gap release of volatile fission products into primary coolant and emergency cooling water occurs in the initial stage of the accident. This release should not exceed 3% of volatile fission products inventory and the coolant temperature should not significantly exceed 100°C.

2. Melt down release stage begins when the water coolant boils off the reactor core and fuel melting temperatures, exceeding 2000°C, may be approached. Most of the fission product release will occur early in the melting period. Air + steam (eventually containing H_2) sweep the fission products from the core into the containment atmosphere. Practically all the inventory of the gaseous fission products can be released in the case of complete core melt down.

In Table 1, publication (2) total amount of fission product iodine isotopes in Pickering NGS was calculated to be approximately 8 kg after 1 year of full power operation. Gap release from all fuel would cause the iodine concentration in the primary coolant to be less than 10^{-6}M, which would be additionally diluted with emergency cooling water. It can be therefore assumed that significant portion of released iodine would be hydrolysed to HOI under the conditions of gap release (if no reducing agent is added to the coolant).

No assumption on the behaviour of iodine from the melt down release was made because no relevant information was available on I_2 steam reaction.

Results of our experimental investigations on iodine behaviour under the above conditions are further presented and discused.

Iodine Release Conditions

The reaction of I_2 vapour (in air) with water within the temperature range of 20-85°C was investigated. Three aspects of the reaction were investigated:

1. Absorption of I_2 from carrier gas, bubbled through water. This experiment simulated the conditions of gaseous iodine "gap" release from defective fuel into coolant, which is immediately leaking into the containment.

2. Desorption of gaseous iodine forms (I_2, HOI, org. I) from water with forced (bubbling) stripping gas, to simulate open drainage or agitated reservoirs open to the containment atmosphere.

3. Desorption of gaseous iodine forms from water solutions, to simulate water/air partitioning of iodine from coolant on containment floors and open reservoirs.

Absorption of I_2 Vapour in Water and LiOH Solution

Equipment and Procedure. The experimental assembly is illustrated in Figure 12.

Elemental iodine vapour, generated in G, was stripped with air from A1, and mixed with air stream A2 to obtain the required flow through the bubbler B, which was filled with distilled water and heated with thermostatically controlled bath WB. Dry air A3, added downsteam of B, eliminated moisture condensation on Cu screens, used to collect elemental iodine. Hypoiodous acid and organic iodine species were subsequently absorbed in a column containing HOI absorbent AC and impregnated charcoal TA. Loss of sample was eliminated by installing pump P at the end to maintain negative pressure in the assembly.

Discussion of Results. The absorption of I_2 vapour in water was evaluated in three independent runs, with airborne concentrations of 0.1-0.5 ppm, at three temperatures in the bubbler (room temperature, 50°C and 85°C) each for 1 hour period. The results, given in Table 1, can be summarized as follows:

1. A significant portion of iodine released from defective fuel could be immediately transferred through the emergency coolant into the containment atmosphere under reactor accident conditions.

2. Penetration of I_2 through water significantly decreases with increasing temperature.

3. However, the amount of released HOI increases with increasing water temperature. Its content increases from approximately 16% at room temperature to 47% at 50°C and 95% at > 60°C.

4. The portion of organic compounds is low and also slightly increases with increasing water temperature.

5. It can be assumed that the 85°C runs are the optimal simulation of iodine reactions with coolant during the initial phases of LOCA.

The absorption of I_2 vapour in water solution of LiOH, pH ≈ 10.3, was also measured under the same conditions. The results, listed in Table 2 show that:

1. Penetration of elemental iodine vapour through LiOH solution was significantly lower than its penetration through water.

2. The rate of HOI release was similar to its release from water at temperature up to ≃ 50°C, however, at 85°C it was significantly reduced, probably due to its accelerated red-ox transfer to nonvolatile IO_3^- (iodate).

Stripping of Volatile Species From Iodine Solutions With Air

The assembly in Figure 12, with the exception of the generator G and air supply A1, was used for the evaluation of iodine species liberation from water solutions with air.

Air from A2 was bubbled at 70 ml/min. through 250 ml of iodine solution, maintained at 60°C. Liberated airborne iodine was analyzed for the content of I_2, HOI and organic iodine compounds.

Discussion of Results. Results are listed in Table 3 which show strong dependence of I_2/HOI ratio on iodine concentration and high portion of HOI released from iodine solution at < 10^{-5}M concentrations. The experimental results are in good agreement with the theoretical analysis results from publication (2).

The table also shows that the fraction of iodine, stripped from the solutions as HOI, was practically independent of the concentration of iodine in the solution. This means that the airborne HOI concentration is directly proportional to the molarity of the solution. However, the fraction of airborne I_2 increased with approximately the square of iodine concentration in the solution.

Diffusion of Airborne Iodine Species From Water Solution of Iodine

A simple assembly, illustrated in Figure 13, was used for the evaluation of gaseous iodine species diffusion from steady iodine solutions.

Iodine solutions (IS), 100 ml from previous experiments described in Absorption of I_2 Vapour in Water and LiOH Solution, were transferred into a flask F (500 ml volume) and laboratory air passed, at 100 ml/min. flow, above the level of the solution. Release of iodine species from both iodine in water and iodine in LiOH solution (pH ≃ 10.3) was evaluated.

Discussion of Results. Results are listed in Table 4. It is evident also from this table that HOI is the major airborne iodine species, formed in the primary coolant and emergency cooling water at elevated temperature (LOCA conditions) and subsequently released into the containment atmosphere.

The measured time dependence of the rate of HOI desorption from both H_2O and LiOH solution at 60°C is illustrated in Figure 14. The desorption rate was evaluated for the first five hours after terminating the absorption experiments described in Absorption of I_2 Vapour in Water and LiOH Solution. From the graph it was estimated that approximately 2-3% of radioiodines from the heat transport water (pH = 10.3) and 3-5% from emergency cooling water, open to the containment atmosphere, would be transferred to airborne forms within the first day, assuming approximately 60°C temperature inside the containment and no chemical spray or additives are used to inhibit the release from solution.

Reaction of I_2 Vapour With Steam

The experimental assembly built specifically for this purpose is illustrated in Figure 15.

The whole setup, except the steam generator SG, was made of Pyrex and Vycor glass and components connected with ground glass joints.

Elemental iodine, stripped from the generator G with air from A1, was diluted with air from A2 (at the constant flow of 100 ml/min.) and mixed with steam from the steam generator SG. The temperature of the iodine + steam + air (ISA) mixture was maintained at approximately either 90° or 120°C for 2-3 minutes. The mixture was condensed in the cooler WC and the condensate collected in CC and maintained at constant temperature with the water bath WB. Airborne species of iodine were drawn from the condensate collector CC into a selective sampler and analyzed for the content of I_2, HOI and organic iodine compounds. Iodine dissolved in the condensate was also measured and the percentage of airborne iodine species was then calculated.

Discussion of Results. The results are given in Table 5.

Hypoiodous acid was found to be the major airborne species in all experiments (75-90%). Its airborne portion increased with higher steam content (runs 9-11) and particularly at higher ISA temperature (runs 7-8) but less HOI is released from larger volume of the condensate (runs 9-11) and at lower temperatures (runs 1-4), where apparently more HOI remains dissolved in the condensate.

The portion of airborne elemental iodine was found to be within 1.6-21.7%. Higher airborne fractions were found in experiments where the steam air mixture was maintained at lower RH values (runs 1-6) and at lower temperatures (runs 5, 6, 12) with no reheating applied. The proportion of nonreacted I_2 vapour remaining airborne was inversely dependent on the condensate volume (runs 9-11) and increased with increasing condensate temperatures (runs 2-6). A similar behaviour was observed with HOI.

The rate of formation of organic iodine compounds increased with larger flow of steam and when the steam air mixture was reheated. However, the maximum measured portion of I transferred to organic compounds was 0.47%, with all other results below 0.2%. The maximum

measured airborne portion of organic compounds was 18.4% with most results below 10% of the total of airborne iodine passing through the condensate collector.

Desorption of Iodine Species From The Condensate

The procedure and equipment described in paragraph Diffusion of Airborne Iodine Species From Water Solution of Iodine was also used for the evaluation of iodine species desorption from the condensate samples. The measured desorption rates and the HOI/I_2 ratio were similar (as expected) to the values of desorption from water, listed in Table 4, except that slightly higher proportion of organic iodine species was desorbed from the condensate samples.

V. Water-Gas Partitioning of HOI

The solubility of hypoiodous acid controls its partitioning between liquid and gas. The partition factor PF is simply its equilibrium liquid to gas concentration ratio.

$$PF = \frac{\text{conc. (liq.)}}{\text{conc. (gas)}}$$

where the concentration is given in units of HOI weight per unit of gas and liquid volume.

The rate of approach to equilibrium is a first order process (diffusion controlled) only when the dissolved gas cannot chemically react with liquid and gaseous components of the system and when both components are in a steady, non-turbulent state.

However, previous results indicate that HOI has significant chemical reactivity, which give rise to a range of PF values under different physical conditions during LOCA. To evaluate the possible effect of simultaneous chemical reactions, the partition factors were evaluated for "static partitioning" (where both liquid and gaseous components are in steady, non-turbulent state) and "dynamic partitioning" (where turbulence exists in both gas and liquid phases).

Static Partitioning

The assembly, illustrated in Figure 13, was also used for evaluating HOI "static" partition between liquid and gaseous phases. The results are listed in Table 6.

During run 1, hypoiodous acid in nitrogen gas was filled into 4 L glass container, containing 100 ml of distilled water. After storing the container for 16-20 hours in the dark at room temperature, the gaseous components were purged with N_2 through an iodine sampler and the amount of HOI in gaseous form was evaluated. The amount of HOI dissolved in water was also measured and the PF calculated.

In run 2 the exchange process was reversed. Distilled water (100 ml) with dissolved HOI, was transferred into the container and N_2 was purged at the rate of 100 ml/min (causing only little turbulence in the covering gas) through the container into an iodine sampler. Four subsequent 1 hour measurements were taken under the same conditions.

In run 3 the water-air partition of HOI was measured under the conditions applied in run 1.

Discussion of Results. Partition factors obtained from the above measurements were consistently within the 330-450 range at 25°C for both water-N_2 and water-air systems, with the exception of the last result in run 2, which was possibly affected by chemical changes in the solution after four hours of continuous operation. However, the results indicate that HOI is relatively stable under mild physical and chemical conditions. Reasonable agreement between the results of runs 1 and 2 indicate that the gas-liquid equilibrium was obtained in less than 1 hour.

Dynamic Partitioning

The assembly, illustrated in Figure 12, was used for the evaluation of dynamic partitioning of HOI between gas and water. Hypoiodous acid, in air or nitrogen carrier gas, was bubbled through distilled water or LiOH solution (pH ≃ 10.3) for 60 min. and both iodine dissolved in water and airborne iodine collected with a species selective sampler downstream of the bubbler were measured.

Discussion of Results. Partition factors, listed in Table 7 show good agreement with PF values measured under static conditions (Table 6). The results indicate some dependence of PF on water temperature. The higher PF measured in LiOH solution confirms previous findings that alkaline condition accelerate the transfer of HOI to nonvolatile products, possibly IO_3^-.

VI. Stability of Airborne HOI

A few measurements were taken to obtain preliminary estimate on:

1. The long-term stability of airborne HOI under normal environmental conditions;

2. The sensitivity of HOI to high temperature and UV light.

Long-Term Stability of Airborne HOI

Airborne HOI from the generator was mixed with dry air to reduce the sample humidity below 50% RH. Glass containers of 4 L volume were filled with the sample and stored at room temperature, either in the dark or exposed to daylight. Airborne HOI was then quantitatively purged with air from the container into a species sampler. The container was also measured for any remaining iodine.

Discussion of Results.

1. Two glass containers were filled with HOI. One of them was exposed to direct sunlight for approximately 10 hours and the second one was stored in a dark box. After 24 hour storage time more than 90% of the HOI decomposed in the container exposed to sunlight and less than 15% HOI decomposed in the nonexposed container.

2. Approximately 85% HOI remained airborne in similar container stored in the dark at room temperature for 7 days.

Sensitivity of HOI to Heat and UV Light

Hypoidous acid, carried with nitrogen from a generator, was mixed with dry air and, after removing I_2 with Cu screens, carried into a glass chamber where it was exposed to heat (propane torch or electric heating coil) or UV light (400 W UV lamps at approximately 10 cm distance) for time periods of 0.3 to 10 seconds. Airborne iodine was then collected from the stream with the specific iodine sampler and analyzed for HOI decomposition products.

Discussion of Results. From the results in Table 8 it is evident that rapid decomposition of HOI occurs at temperatures exceeding 250°C and also from its exposure to high intensity UV light.

The rate of HOI decomposition was relatively slow at 160°C. This is consistent with the observations from mixing I_2 vapour with H_2O (< 100°C) and with steam at temperatures slightly exceeding 100°C, where HOI formation was not reduced with increasing temperature.

The insignificant effect of temperature up to 160°C also verifies that HOI decomposition in UV light was caused by photons rather than by elevated temperature in the exposure chamber.

The decomposition product was mainly collected on Cu screens, therefore, we assumed it was elemental iodine vapour.

VII. Summary of Results

Airborne Iodine Measurements

Specific sampling of iodine species, followed by radiometric evaluation of the sampler components was sufficiently selective and sensitive for investigating the behaviour of airborne iodine under LOCA conditions.

From the preliminary mass spectrometry analysis of gaseous iodine species, released from iodine solutions, it was evident that HOI was present in gaseous samples entering the quadrupol system. It remains to be confirmed that HOI was not quantitatively formed in the process of chemical ionization.

Reactions of Iodine Vapour With H_2O

1. Investigations on the reaction of I_2 vapour with water and LiOH solutions (pH ≃ 10.3) at temperatures of 25-85°C (simulating gap release of I_2 from defective fuel into the heat transport water and emergency cooling water) were summarized as follows:

   - The penetration of iodine through water bubbler was found to be 3-8% of its upstream concentration. The rate of penetration and the proportion of resulting chemical species was strongly dependent on water temperature. The highest penetration of > 8%, with highest portion of I_2 vapour (> 80%) was measured at room temperature. At ≥ 60°C the penetration was ≥ 3% with > 90% of iodine present as HOI.

   - In LiOH solutions iodine penetration decreased to 1.4-2%. The penetrating forms contained > 90% of HOI at ≥ 50°C.

   - Less than 0.1% of introduced iodine was transferred to organic airborne species under the above conditions.

2. The ratio of airborne iodine species, released from turbulent solutions, was strongly dependent on iodine concentrations. Desorption rate of 1-2% in the first hour was found at 50°C, with > 50% HOI at ≤ 10^{-5}M and > 90% HOI at ≤ 3 x 10^{-6}M iodine concentration. The concentration of airborne HOI was approximately proportional to, and airborne I_2 increased with approximately the second power of iodine concentration within 3 x 10^{-6} to 3 x 10^{-5}M.

3. Hypoiodous acid is also the major species desorbed from steady, nonturbulent iodine solutions at elevated temperatures. The HOI/I_2 ratio strongly depends on temperature. Desorption rates of 0.8-1.35% per hour were measured from iodine solutions in water within the range of 25-85°C.

   It was estimated that 3-5% of radioiodines dissolved in water (pH7) and 2-3% of radioiodine from LiOH solution (pH ≃ 10.3) would be transferred to airborne forms within the first day at approximately 60°C in the containment.

4. The portion of radioiodine remaining airborne after I_2 vapour with air and steam and condensed at 25-80°C temperatures was found to be 0.6-3.6% depending on steam content and its temperature. Hypoiodous acid was the major species (75-90% content) formed in all experiments. Both the rate of airborne iodine desorption from the condensate and the HOI/I_2 ratio were similar to the rates measured from water solutions.

Water-Gas Partitioning of HOI

Water-air (or N_2) partition factors for HOI were found to be in the ranges of 330-450 at 25°C and 250-340 at 60°C. The partition factor range for HOI bubbled through LiOH solution (pH ≃ 10.3) was found to be 850-950 at 25°C.

Stability of Airborne HOI

Decomposition of airborne HOI is affected by elevated temperature and light. Under normal conditions HOI is relatively stable. About 15% of HOI decomposed while stored in the dark for a one week period. Rapid decomposition (within few seconds) of airborne HOI occurred when it was exposed to temperature ≥ 250°C or to high intensity UV light.

VII. References

1. Kabat, M.J., "Selective sampling of hypoiodous acid"; paper presented at the 14th AEC Air Cleaning Conference, Sun Valley, Idaho; pp. 490-506; (August 1976).

2. Kabat, M.J.; "Testing and evaluation of absorbers for gaseous penetrative forms of radioiodine"; paper presented at the 13th AEC Air Cleaning Conference, San Francisco; pp. 765-800; (August 1974).

3. Thomson, B.A., Davidson, W.R., Lovett, A.M.; "Applications of a versatile technique for trace analysis - atmospheric pressure negative chemical ionization"; paper presented at the Second Conference on Negative Chemical Ionization Mass Spectrometry, Chapel Hill, North Carolina; (March 1979).

Table 1

Penetration of I_2 Vapour through Water Bubbler and Formation of other Iodine Species

Temperature °C	Species	Penetration (% of upstream I_2 concentration) Run 1 %	Run 2 %	Run 3 %	Average of runs 1-3 %	Species composition (downstream) %
25 ± 5	I_2	9.4	6.5	4.6	6.8	83.6
	HOI	1.1	1.7	1.1	1.3	16.0
	org I	0.03	0.05	0.02	0.03	0.4
	Total	10.53	8.25	5.72	8.13	100
50 ± 5	I_2	2.2	3.0	0.5	1.9	51.9
	HOI	1.5	1.6	1.9	1.7	46.5
	org I	0.1	0.06	0.02	0.06	1.6
	Total	3.8	4.66	2.42	3.66	100
60 ± 5	I_2	0.07	0.1	-	0.09	3.1
	HOI	2.77	2.72	-	2.75	94.2
	org I	0.1	0.06	-	0.08	2.7
	Total	2.94	2.88	-	2.92	100
85 ± 10	I_2	0.05	0.15	0.14	0.11	3.2
	HOI	3.2	3.0	3.6	3.3	94.8
	org I	0.04	0.06	0.1	0.07	2.0
	Total	3.29	3.21	3.84	3.48	100

Table 2

Penetration of I_2 Vapour through LiOH Solution and Formation of other Species

Temperature °C	Species	Penetration (% of upstream I_2 concentration) Run 1 %	Run 2 %	Run 3 %	Average %	Species composition (downstream) %
25 ± 5	I_2	1.0	-	-	-	52.4
	HOI	0.88	-	-	-	46.1
	org I	0.03	-	-	-	1.5
	Total	1.91	-	-	-	100
50 ± 5	I_2	0.07	0.02	0.02	0.04	2.6
	HOI	1.38	1.53	1.45	1.45	93.0
	org I	0.09	0.03	0.1	0.07	0.4
	Total	1.54	1.58	1.57	1.56	100
60 ± 5	I_2	0.02				1.0
	HOI	1.87				97.4
	org I	0.03				1.6
	Total	1.92				100
85 ± 10	I_2	0.03				2.2
	HOI	1.27				92.0
	org I	0.08				5.8
	Total	1.38				100

Table 3

The Rate of Iodine Transfer from its Water Solution to Bubbling Air

Iodine Solution		Airborne Iodine Desorbed with Air				
Concentration M	Temperature °C	The Rate of desorption %/hr.	Composition of Airborne Species -% I_2	HOI	org I	Concentration ratio HOI/I_2
3×10^{-6}	50 ± 5	1.34	2.6	96.5	0.9	37
8×10^{-6}	50 ± 5	1.05	19.4	80.5	0.5	4
1.6×10^{-5}	50 ± 5	2.09	45.6	54.2	0.2	1.2
3×10^{-5}	50 ± 5	6.75	88.1	11.8	<0.1	0.1

Table 4

The Rate of Iodine Diffusion from its Solutions to Air

Soluent	Concentration M	Temperature °C	Airborne Iodine Diffused from its Solution: The Rate of Desorption %/hr.	Composition of Airborne Species-% I_2	HOI	org I	Concentration ratio HOI/I_2
water	1×10^{-6}	25 ± 5	1.37	90.5	8.8	0.7	0.1
	2.5×10^{-6}	80 ± 10	0.96	1.0	99.0	--	99
LiOH solution	6×10^{-7}	60 ± 5	0.79	5.0	95.0	--	19

Table 5

Reaction of I_2 Vapour with Steam

Run No.	I_2 - air flow ml/min.	Condensate temperature °C	Condensate volume ml/hr.	Airborne Iodine Species from the Condensate Collector: Fraction of introduced Iodine %	Composition - % I_2	HOI	org I
1*	150	25	98	0.82	14.6	79.3	6.1
2	150	25	88	0.56	12.5	80.4	7.1
3	150	50	90	0.89	18.0	78.7	3.3
4	125	50	100	1.61	21.7	75.2	3.1
5	125	80	100	2.72	15.1	82.4	2.5
6	110	80	100	3.58	21.2	76.3	2.5
7*	110	80	80	2.57	3.9	88.7	7.4
8*	110	80	91	2.53	1.6	90:1	8.3
9	110	80	250	0.65	3.1	78.5	18.4
10	110	80	260	1.24	1.6	83.9	14.5
11	110	80	208	1.21	10.7	79.4	9.9
12	110	80	185	1.71	11.7	76.6	11.7
13*	110	80	182	2.65	6.8	75.5	17.7

*During the runs 1, 7, 8 and 13 the ISA temperature before condensation was maintained at ≈ 120°C

Table 6

"Static" Partitioning of HOI between Water and Gas

Run No	HOI transfer regime	Temperature °C	Measured PF
1	$N_2 \rightarrow H_2O$	25	430
2	$H_2O \rightarrow N_2$	25	418 443 340 560
3	air $\rightarrow H_2O$	25	330

Table 7

"Dynamic" Partitioning of HOI between Gas and Water

Run No	HOI Transfer regime	Temperature °C	Measured PF
1	$N_2 \rightarrow H_2O$	25	540 710 710
2	air $\rightarrow H_2O$	25	480 400 550 350
3	air $\rightarrow H_2O$	60	250 320 250 340
4	air $\rightarrow$ LiOH solution (pH = 10.3)	25	850 925 930 967

Table 8

The Effect of Heat and UV Exposure on HOI Decomposition Rate

Exposure conditions			Remaining airborne iodine forms			
Source	Approx. temper. °C	Approx. time Sec.	Particulate %	I_2 %	HOI %	org I %
flame	> 1000	~ 2	NM	98.0	1.3	0.7
	> 1000	~ 1	6.1	75.8	17.9	0.2
	> 1000	~ 0.3	7.0	75.0	17.6	0.4
electr. heating coil	160	~ 10	2.5	5.3	91.6	0.6
	250	~ 10	6.7	81.8	11.5	< 0.1
UV light	< 100	~ 3	1.8	23.3	74.6	0.3
		~ 10	NM	47.2	51.5	1.3

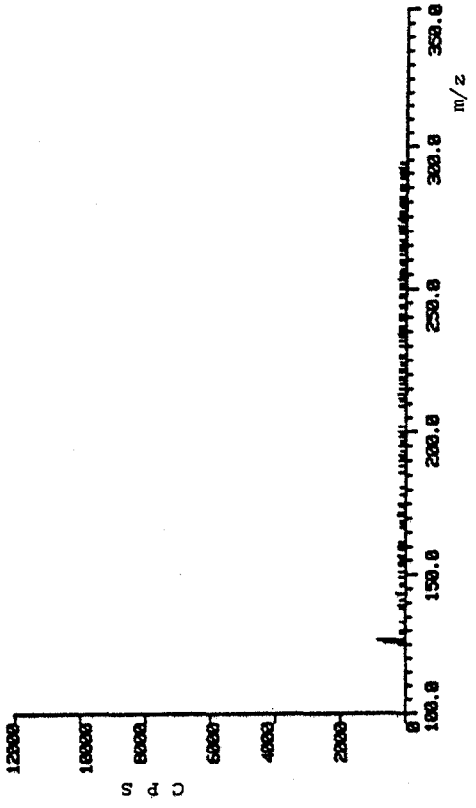

Fig. 2 "Zero air" background spectrum

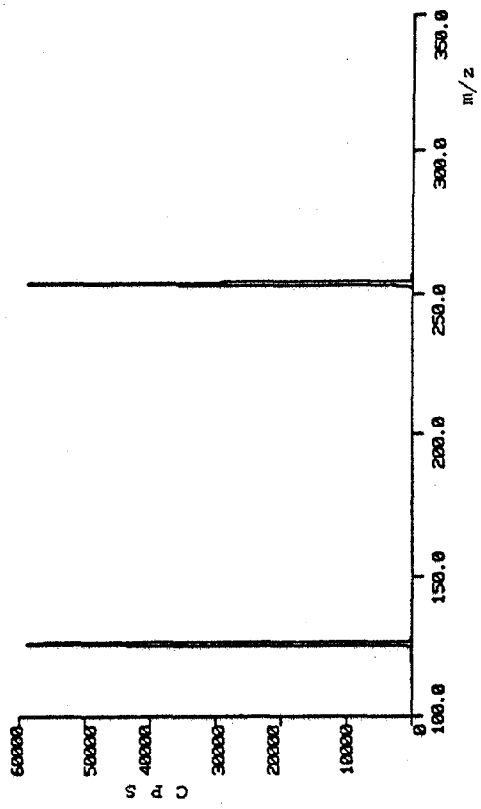

Fig. 3 Spectrum of I_2 vapour in zero air

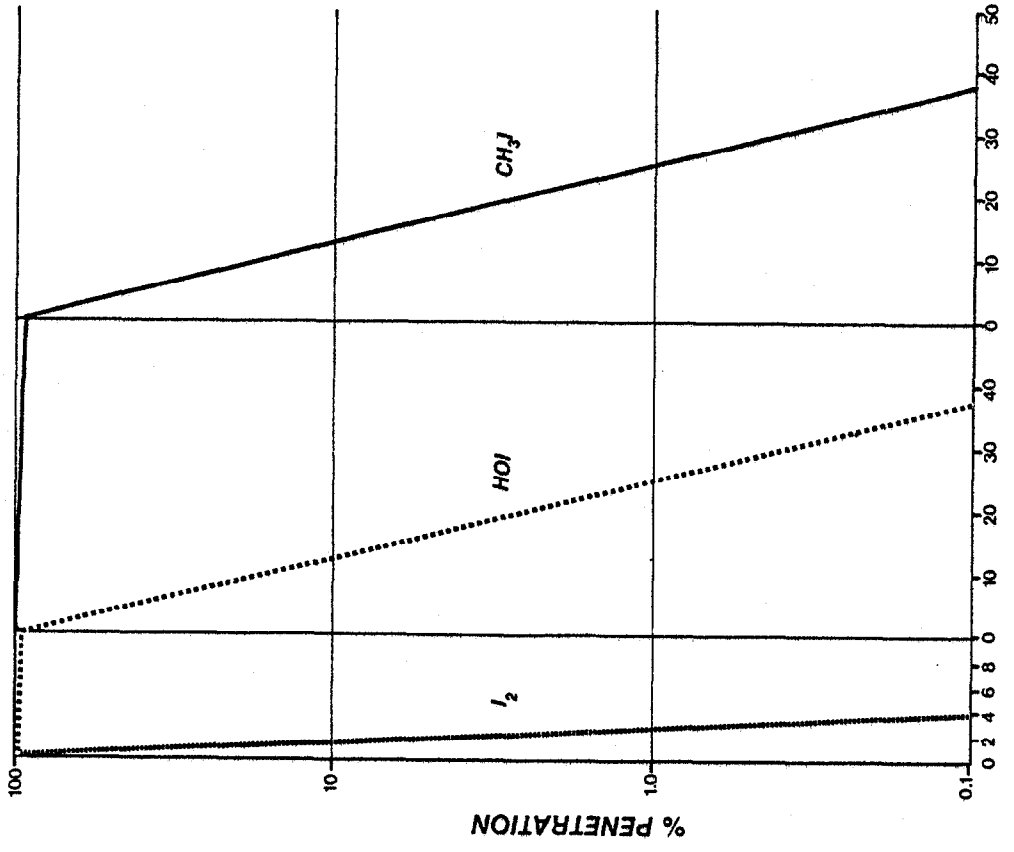

Fig. 1 Typical profile of I_2, HOI and CH_3I penetration through a Selective Iodine Species Sampler (25° C, 60 % RH)

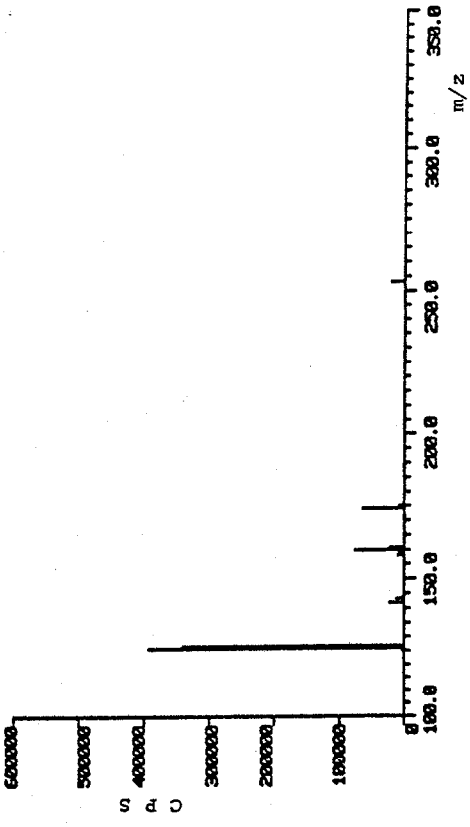

Fig. 6 Spectrum of iodine species, liberated with air from 10^{-3} M iodine solution

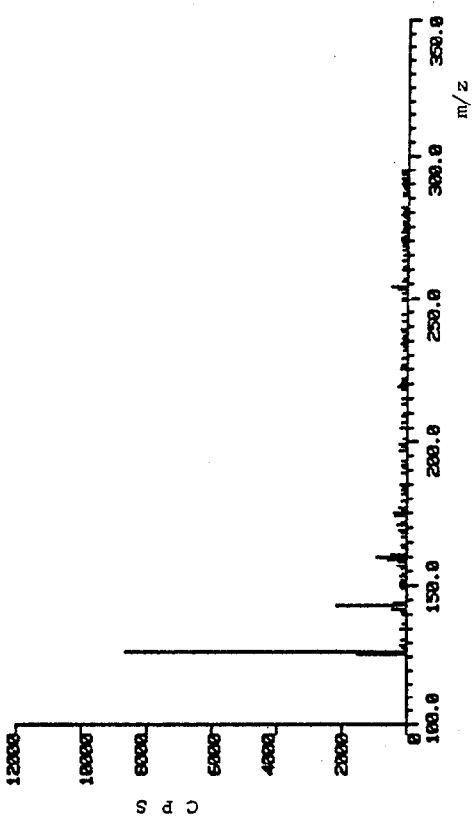

Fig. 7 Spectrum of iodine species, liberated with air from 10^{-5} M iodine solution

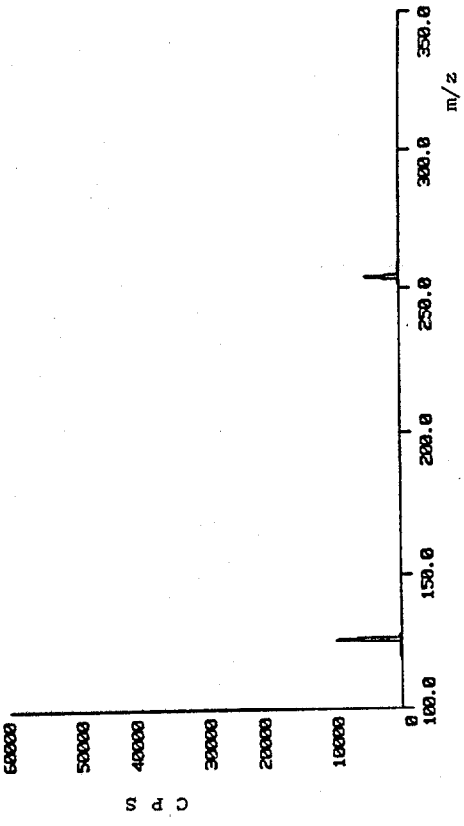

Fig. 4 Removal of I_2 vapour with Cu trap

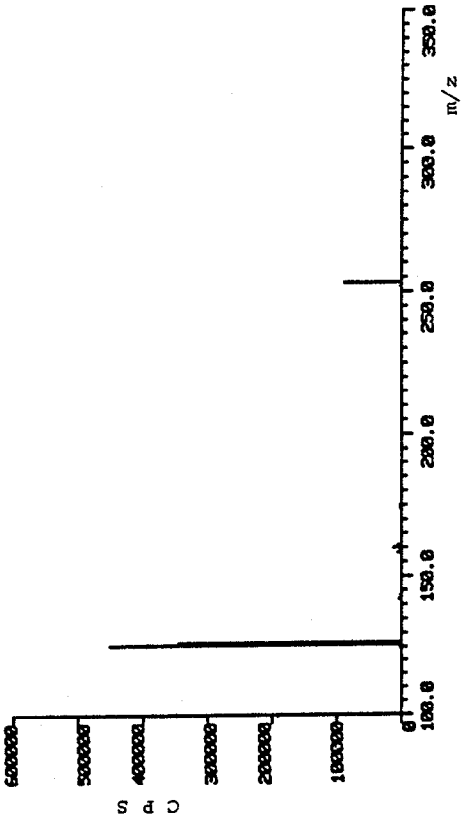

Fig. 5 Elemental iodine vapour in zero air (the setting of the apperture potential L 1 - 42.000)

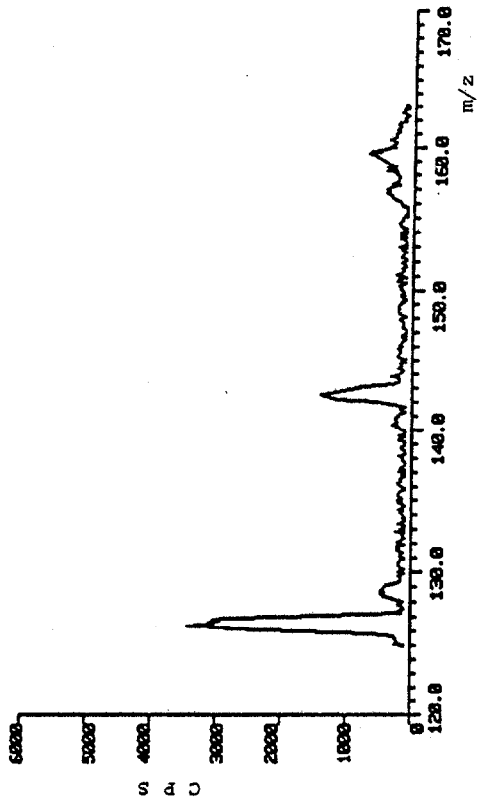

Fig. 10 Removal of I_2 with Cu trap from a mixture of iodine species generated at pH = 6

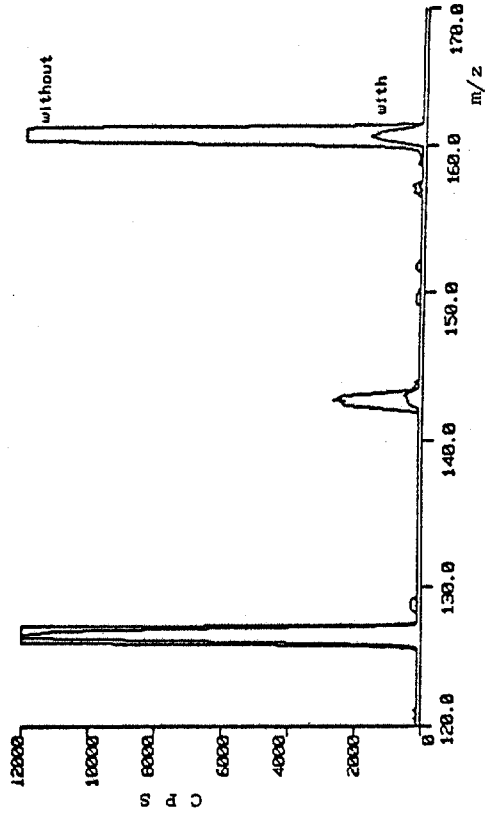

Fig. 11 Removal of HOI with the specific HOI absorbent

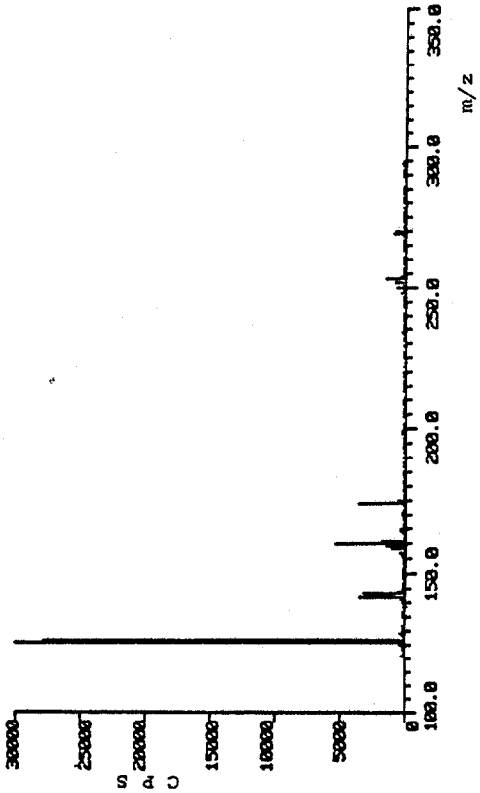

Fig. 8 Spectrum of iodine species, liberated with air from HOI generator (at pH = 2.3)

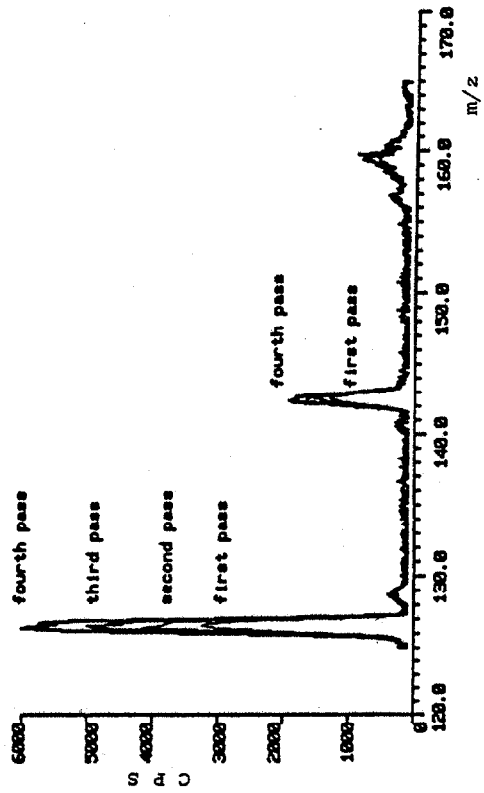

Fig. 9 Increase in I^- and IO^- upon heating the iodine generator (at pH = 6) to 45° C.

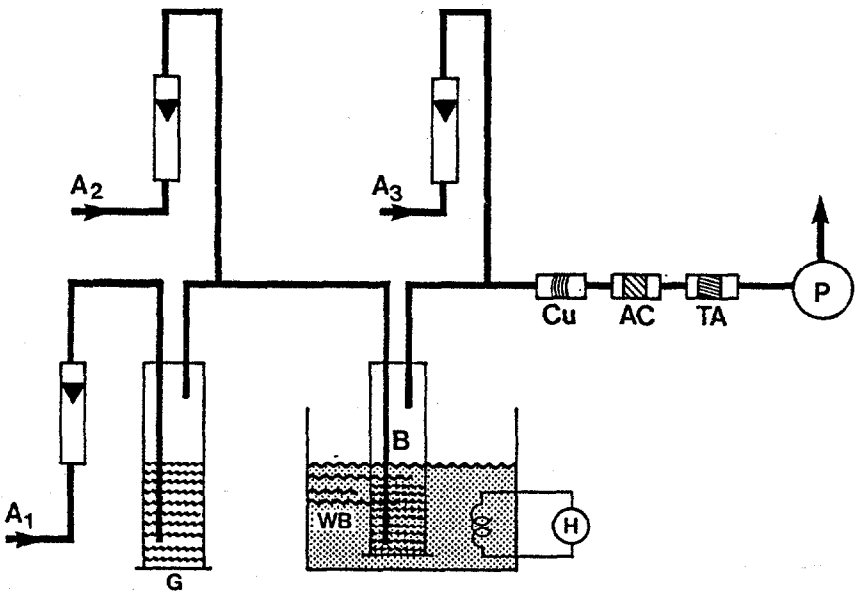

Fig. 12 Evaluation of I_2 vapour reaction with water and LiOH solution

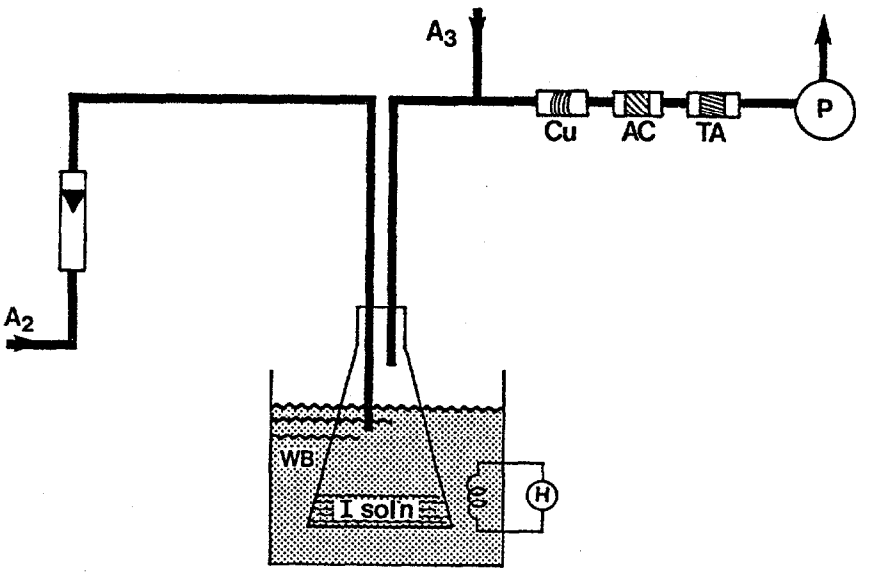

Fig. 13 Evaluation of iodine species desorption from iodine solution

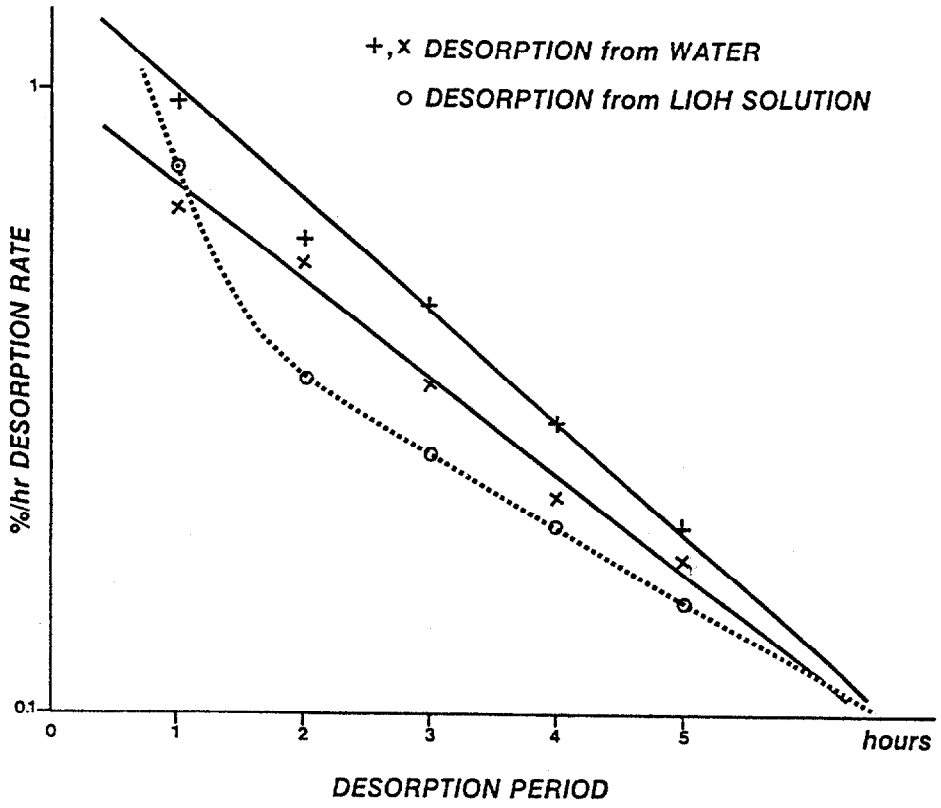

Fig. 14 Time dependence of HOI desorption by diffusion from water and LiOH solution (pH = 10.3) at 60° C.

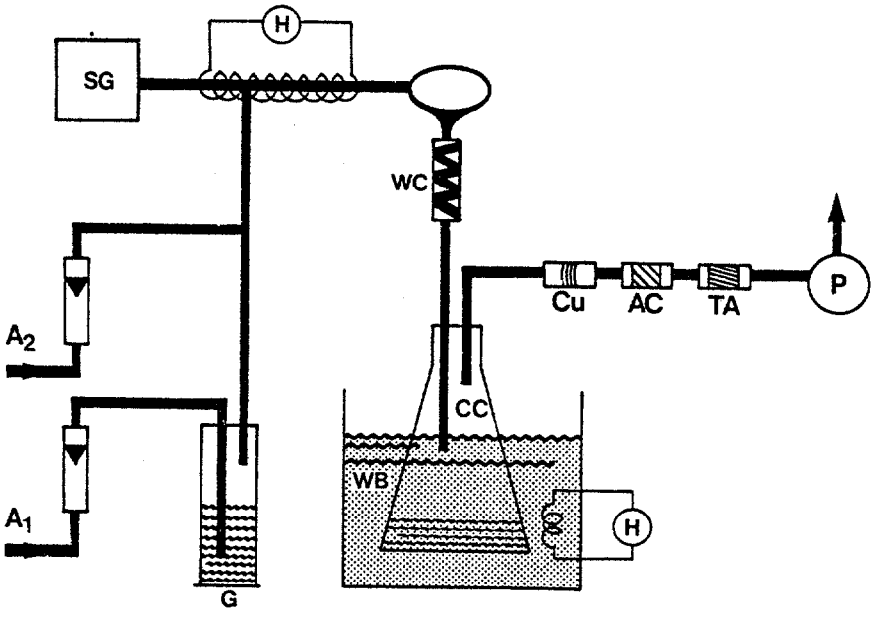

Fig. 15 Evaluation of I_2 vapour reaction with steam

DISCUSSION

v. AMMON: Is hydrogen iodide being generated after you bubble iodine in water?

KABAT: It was experimentally confirmed that HI had only insignificant volatility from its aqueous solution. A negligible amount of gaseous radioiodine was collected from the stream of inert gas, bubbled through a solution of pure HI, containing ^{131}I isotope, at 60°C.

v. AMMON: I am not insisting that it was confused with HI. I was just wondering whether HI can't be formed and evolved.

KABAT: Yes, HI is formed in diluted iodine solutions as a hydrolysis product, simultaneously with HOI.

ANON.: In one of your mass spectrums, there is also one peak for IO_3. Can you infer anything from this finding about the volatility of the acid.

KABAT: I believe that IO_3^- was formed in the mass spectrometer from chemical ionization of the mixture of air carrier gas with elemental iodine vapor, released from its 10^{-3} M solution, rather than as a byproduct of the aqueous reaction. Very low volatility of HIO_3 was confirmed from our previous experiments.

ANON.: As far as these mass spectrometer measurements are concerned, do you see any chance to carry them out in real effluent gases from nuclear power plants?

KABAT: I feel that iodine concentrations in the effluent gas, under normal reactor conditions, would be too low for this purpose. In our experiments approximately 100 ppb of HOI was introduced into the mass spectrometer. This is about the maximum concentration of gaseous HOI which can be evolved under controlled laboratory conditions at present.

NUCLEAR WASTE VITRIFICATION EFFLUENT

R. W. Goles, F. P. Brauer, D. C. Hamilton and J. E. Fager
Battelle, Pacific Northwest Laboratory
Richland, Washington 99352

Abstract

Important gaseous and airborne off-gas emissions associated with the solidification of high level liquid waste have been characterized. Effluents specifically sampled for in this off-gas monitoring study include: the gaseous chemical species of ^{3}H, ^{14}C, ^{85}Kr, ^{129}I and NO_x; the semivolatile forms of ^{79}Se, ^{99}Tc, ^{106}Ru, $^{125,126}Sb$, ^{125m}Te and $^{134,135,137}Cs$; and all radionuclides contained in particulate matter.

The sampling and laboratory techniques employed and the off-gas analytical results obtained in this study are described herein. In addition, the magnitudes of vitrification-produced gaseous emissions are compared, whenever possible, to those associated with the complete fuel reprocessing cycle.

I. Introduction

In order to fully assess the potential impact of future waste solidification facilities upon the environment, a sampling network was established to characterize emissions of gaseous and particulate matter generated by the Nuclear Waste Vitrification Project.

The Nuclear Waste Vitrification Project (NWVP) conducted at the Pacific Northwest Laboratory (PNL) was initiated as part of the Department of Energy's Commercial High Level Waste Immobilization program. The objective of NWVP was to provide a demonstration of the vitrification of high-level liquid waste (HLLW) generated from typical spent power reactor fuel. This involved the dissolution of spent PWR-enriched uranium fuel, the separation of uranium and plutonium isotopes from the resultant dissolver solution, and finally the vitrification of all unextracted fission product activity present in the liquid waste stream as a borosilicate glass. A detailed description of NWVP is given elsewhere.[1] This paper deals with the sampling and analysis of off-gas emissions generated by this project with particular emphasis placed upon the composition of vitrification exhaust emissions.

II. Off-Gas Sampling

Two sampling stations with essentially identical monitoring capabilities were established in order to sample both the undiluted vitrification process off-gas as well as the less concentrated stack gas exhaust. This allowed both weak and strong emissions to be conveniently measured with commercially available instrumentation.

Sampling of the stack gas was accomplished through use of a multiport sampling tube that transected the 8-ft height of the exhaust plenum that ran beneath the floor of the sampling stack house. A two-stage centrifugal pump located in the stack house continuously pulled stack gas from the multiport sampling tube through a sampling manifold

and then returned it to the exhaust plenum. All experiments conducted in the stack house extracted stack gas from the sampling manifold described above.

Sampling of the undiluted off-gas process stream (POG-88) was conducted at the first accessible location outside of the hot cell. This was accomplished by installing a tapered 3/4" stainless steel pipe along the central axis of the 3" off-gas process line. Beyond the sample inlet, there was a large orifice ball-valve, a particulate filter, and then a transition to a 3/4" stainless steel tube. The tubing was routed through the ceiling to the room directly above which contained the main sampling manifold and an interactive variable flow isokinetic pumping system. The sampled off-gas was then returned to the process off-gas line. Figure 1 contains a process line schematic illustrating both sampling site locations.

Each of these sampling sites was equipped with a mass flow probe. This permitted any effluent species measured at the stack to be related directly back to its concentration in the off-gas process line, POG-88, and vice versa providing no other process line sources were present.

III. Sampling Network

The sampling systems developed for this monitoring program were designed to characterize the concentrations of selected effluents escaping the process hot cell. In some instances, various chemical forms of a given element or radioisotope were selectively sampled for in order to extract as much information concerning the process as was possible. A complete list of all gaseous and airborne effluent species for which sampling was conducted appears in Table I.

The sampling systems deployed during this monitoring campaign were of two distinct types--those involving sample collection and those providing direct detection. Samplers falling into the sample collection category are primarily integrating devices that trap a particular effluent species over a fixed period of time and must be returned to the laboratory for analysis. Direct detection devices are real or quasi-real time sampling devices that continuously provide measurement data related to particular effluent species or sampling conditions. Collection of this real-time data was accomplished with a commercial data logger that provided periodic printed and punched records of all data generated by electronic sampling and measurement equipment. During important fuel cycle stages, the status of all real-time, sampling and measurement equipment was interrogated by the data logger at 5-min intervals. Longer sampling intervals were utilized during quiet non-active periods. A description of the sampling methods and systems employed for the collection and measurement of the effluent species listed in Table I are described below.

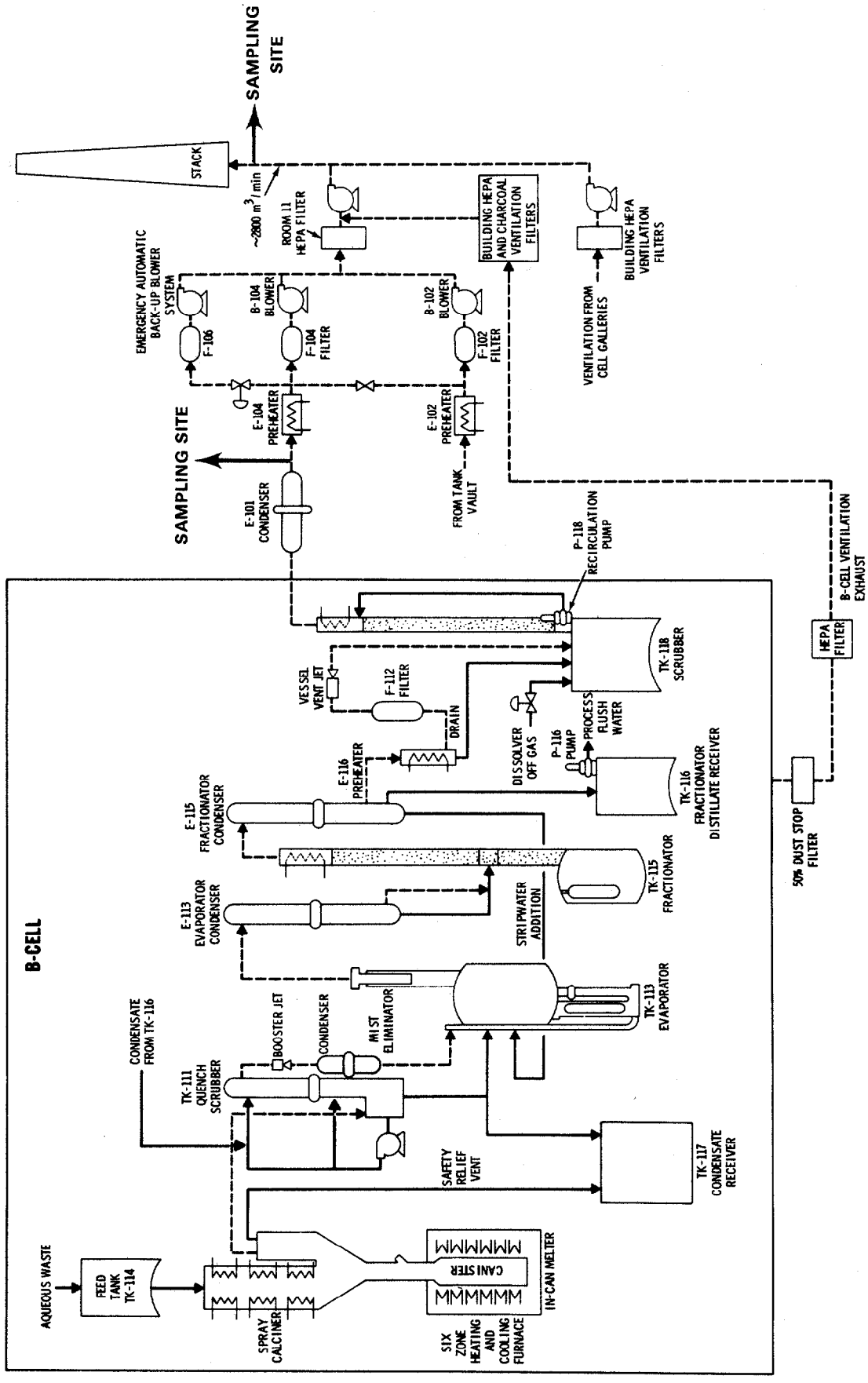

FIGURE 1. Vitrification Effluent Control System and Off-Gas Sampling Sites

TABLE I. Important Process Effluents

1. GASEOUS EFFLUENTS

^{3}H
^{14}C
^{85}Kr
^{129}I
NO_x

2. SEMIVOLATILE EFFLUENTS

^{79}Se
^{99}Tc
^{106}Ru
^{125}Sb, ^{126}Sb
^{125m}Te
^{134}Cs, ^{135}Cs, ^{137}Cs

3. PARTICULATE EFFLUENTS

Fission Products
Activation Products
Heavy Elements

^{3}H and ^{14}C

Of the radioactive elements that can be expected to be volatilized during the calcination process, ^{3}H and ^{14}C form by far the greatest number of chemically different volatile species. Consequently, a chemically-specific sampling system was developed to differentially collect all major volatile forms of ^{3}H and ^{14}C including tritiated forms of water, hydrogen and organics and ^{14}C containing carbon monoxide, carbon dioxide and organics. A schematic of this sampling system is illustrated in Figure 2. The underlying basis of this differential sampling system is that of controlled oxidation. By employing various catalysts and trapping agents in the proper order, one can selectively remove each of the previously mentioned chemical compounds from a sampling air stream in a sequential manner. This is accomplished by initially desiccating the sampled air to remove all isotopic forms of water. The dried air then passes through a caustic bed that removes all carbon dioxide. The sampled air next passes through a mixed oxide, room temperature catalyst, Hopcalite (Mine Safety Appliances Company), that oxidizes carbon monoxide. The catalytically-formed CO_2 is then collected by a caustic trapping agent. A room temperature Pd catalyst is subsequently employed to oxidize the hydrogen component of the air stream, and a desiccant immediately collects the oxidation product. Finally, all organic constituents are combusted with a 600°C Pt converter, and the oxidation products, water and carbon dioxide, are removed as previously described. Molecular sieve material with an effective pore size of 3Å was used as the primary desiccating material in these studies, while the commercially available product, Ascarite (Arthur H. Thomas Company), was used to collect carbon dioxide. To insure quantitative removal of the sought after trace chemical compounds, a carrier gas containing stable isotopic forms of H_2, CO and CH_4 was bled into the sampled gas stream prior to any contact with chemically-specific traps.

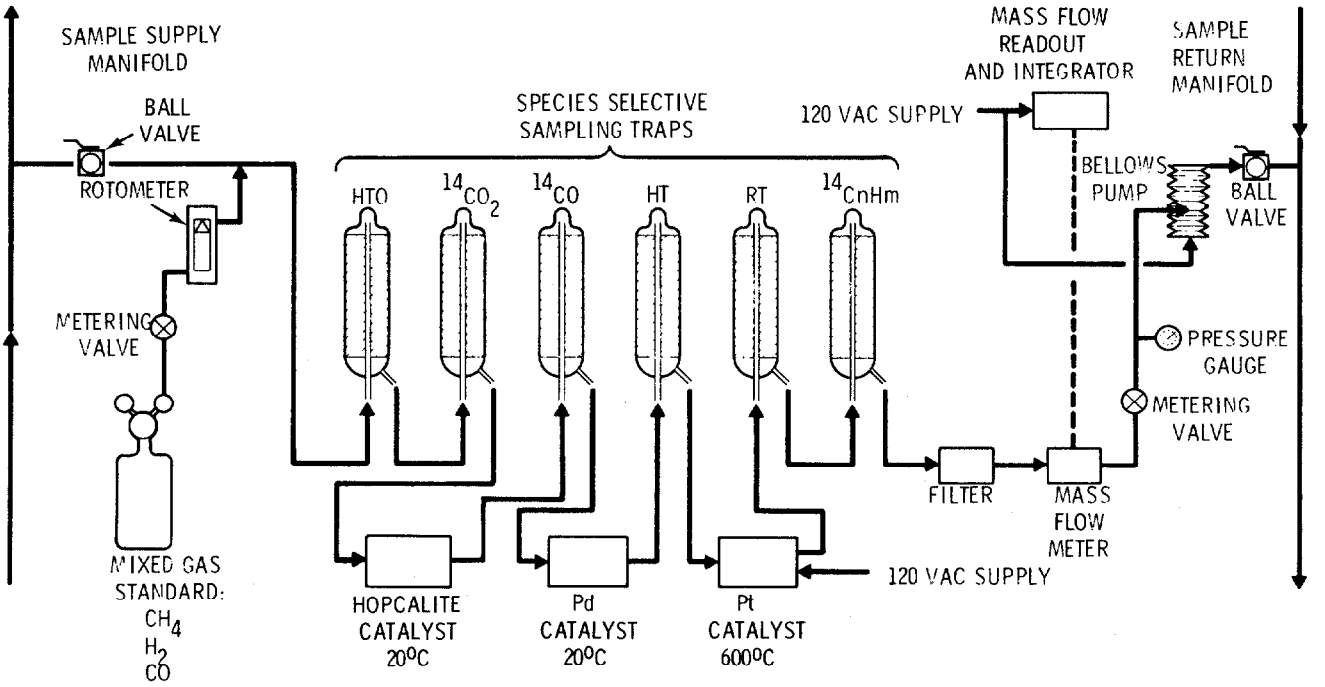

FIGURE 2. Differential ^{3}H-^{14}C Sampling System

^{85}Kr

Although not a vitrification-produced effluent, the presence of ^{85}Kr in the NWVP off-gas exhaust was, nevertheless, determined by γ-spectrometry at the stack house sampling location. A Ge(Li) detector, housed in a lead cave, was used with a high-geometry, 6-liter, pressurized (60 psia), well-type spectroscopy gas cell to detect the 514 keV γ-ray associated with the decay of ^{85}Kr. The advantage of this analytical approach over conventional β^- detection methods stems from the high degree of specificity associated with the discrete nature of the γ-ray detected. Other gaseous β^- emitters certain to be present in large concentrations along with ^{85}Kr, such as ^{14}C, ^{3}H and ^{129}I, have absolutely no impact upon the detection sensitivity or experimental uncertainties associated with this γ-analysis system. All possible analytical interferences due to positron emitters and/or the presence of gaseous ^{106}Ru were eliminated through use of absolute filters and silica gel, respectively. A diagram of this γ-ray analytical system appears in Figure 3.

The Kr γ-analytical system was calibrated in concentration units; that is, the 514 keV γ-ray counting rate of this system was related directly to the concentration of ^{85}Kr in the spectroscopy cell. Since this cell was pressurized, pressure and temperature information had to be simultaneously recorded with counting rate in order to establish ^{85}Kr concentrations under standard conditions. An absolute pressure transducer and a copper constantan thermocouple provided continuous data with regard to pressure and temperature, respectively.

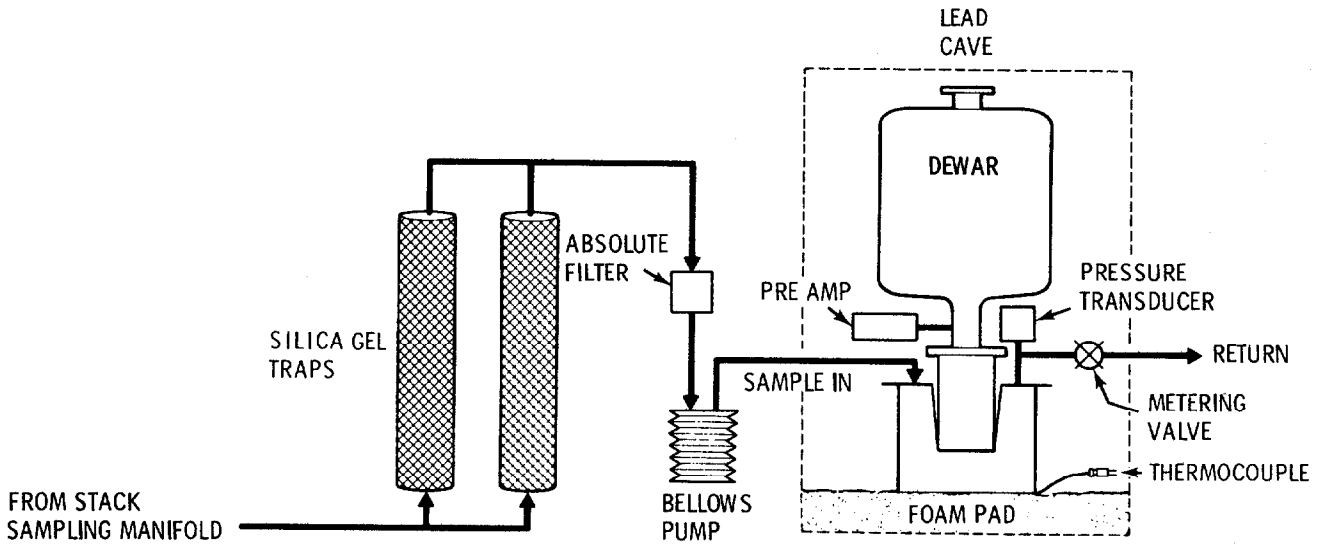

FIGURE 3. ^{85}Kr Gamma Ray Spectroscopic Analytical System

^{129}I

Iodine was sampled both in the undiluted process off-gas stream and at the stack. A packed column, counter-current flow, caustic scrubber was used along with three heated beds of silver-exchanged mordenite to quantitatively remove all iodine from the sampled undiluted process off-gas. This sampling subsystem is illustrated in Figure 4. The scrubber was operated continuously at a flow rate of 10 ℓ/min only during the actual vitrification process. A mass flow meter/integrator system measured the total volume of process off-gas stream sampled.

At the stack, a differential sampling system was constructed to characterize the stack gas concentrations of ^{129}I. The basis of this sampler is a series arrangement of two sorption beds consisting of an anion exchange resin followed by a layer of charcoal. When used in this order, the resin bed acts to remove all inorganic iodine. The remaining organic forms, if any, are subsequently removed from the sampled gas stream by the charcoal. A silver-exchanged zeolite was periodically used as an absolute back up to this sampler in order to check for breakthrough. All sampling beds were maintained at room temperature and were of sufficient thickness at the sampling flow rate of 10 ℓ/min to insure maximum trapping efficiencies. Flow rate and total sampled volume were measured with a mass flow meter and electronic integrator system. This type of sampling system was employed throughout the entire duration of NWVP.

NO_x

Nitrogen oxide measurements were made on a real-time basis at the stack monitoring site. A commercial nitrogen oxide monitor was utilized to establish stack gas concentrations of both NO and NO_x ($NO + NO_2$). This instrument employed the well established chemiluminescent reaction of NO and ozone to determine NO concentrations. By converting NO_2 to NO, utilizing a high-temperature converter, NO_x

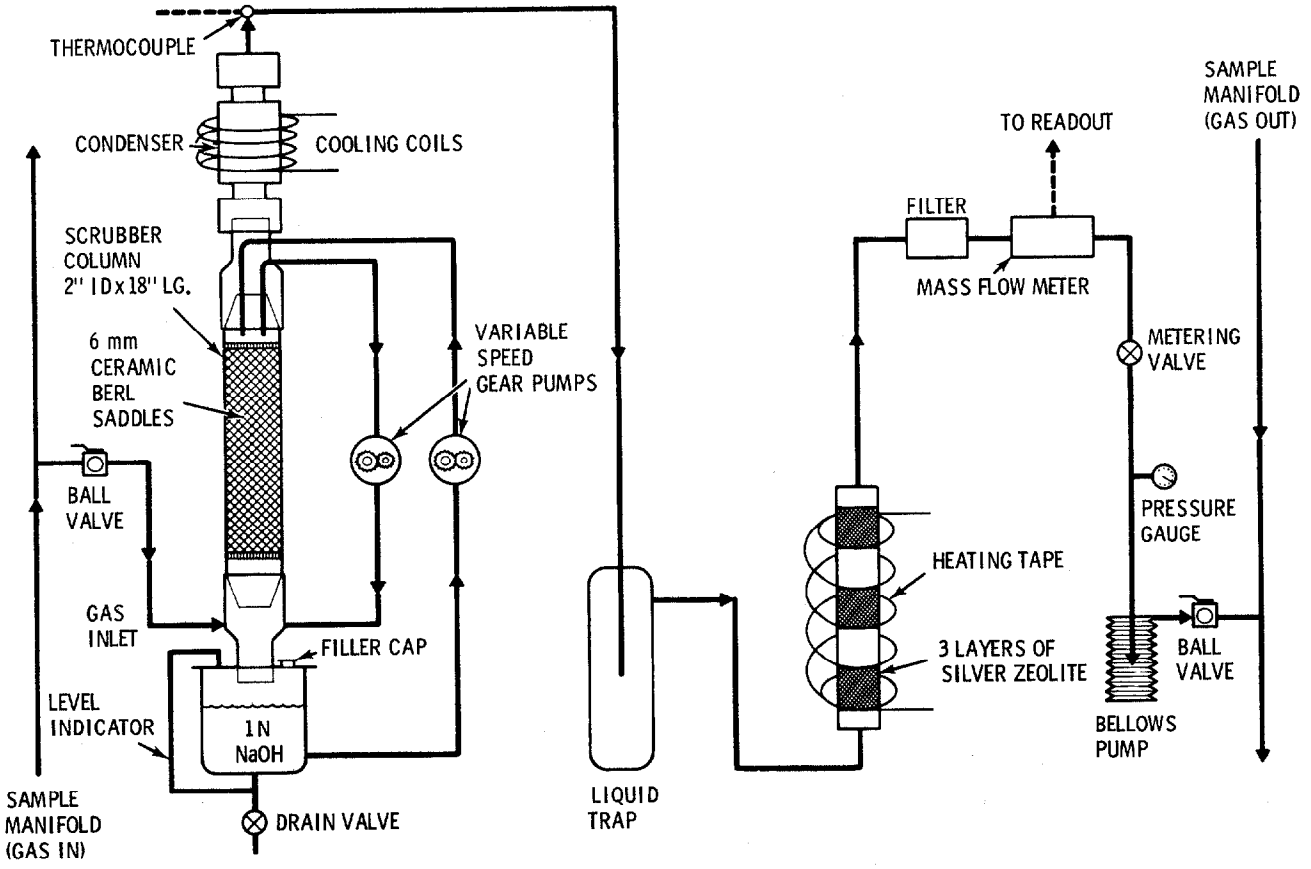

FIGURE 4. Caustic Scrubbing System

concentrations were similarly established. Being a single channel instrument, detection of either NO or NO_x was determined by a selector switch. During important fuel cycle operations, concentrations of both NO and NO_x were established sequentially at 30-sec intervals by manual operation of this selector switch; other-wise only NO_x values were measured. All measurements made by this instrument were transferred to and recorded by the data logger at preset reporting intervals.

Semivolatiles

The semivolatile isotopes listed in Table I all possess acidic gaseous chemical forms allowing these species to be removed from the process off-gas by caustic scrubbing techniques. A highly efficient, packed column, counter-current flow, 1M NaOH scrubber system, shown in Figure 4, was used to sample for these isotopes. Experimental scrubbing efficiencies of greater than 95% for both CO_2 and I_2 have been achieved with this system. Flow and total sampled volume were determined by a mass flow/integrating totalizer system.

In addition to the scrubbing system described above, two Ge(Li) γ-ray detectors were used in conjunction with high geometry gas cells to examine the filtered vitrification process off-gas for all γ-emitting semivolatiles. These two spectroscopic systems were identical except that one included a Ru trap that protected one

spectroscopy cell from possible contamination with ^{106}Ru. These systems were similar in construction to that of the ^{85}Kr monitor illustrated in Figure 3.

Particulates

Particles were collected in a more or less conventional manner. However, special attention was devoted to insuring collection of a truly representative sample. Sampling was conducted with a 3/4" tapered and polished stainless steel pipe located along the axis of the 3" process line, POG-88. The sampled gas and all entrained particles moved along this uniform diameter pipe directly to a commercially available filter of known collection efficiency. This filter was located as close as physically possible to the process line and along a common central axis defined by the collection tube and the process line itself, thereby insuring a straight, short trajectory to the filter. Because erratic changes were expected to occur in the process line flow rate, a truly active control network was designed to match the sampling rate to the instantaneous process off-gas velocity, thereby insuring continuous isokinetic sampling conditions. Details concerning the construction of this system are given elsewhere.(2)

IV. Analysis and Results

Some of the components of the sampling network described in the previous section generate samples that require further laboratory manipulation before analytical results can be extracted. This section briefly describes the laboratory methods used to analyze the various types of samples taken during NWVP. A more detailed discussion of laboratory analytical methodology employed in this study is given in Reference 2. All reported results, unless otherwise specified, are expressed in terms of stack concentrations independent of whether they were measured at the stack or not.

Tritium

The three sampled forms of tritum (tritiated water, hydrogen, and organics) were all collected in the chemical form of water on a molecular sieve desiccant. The water was extracted from this desiccant by vacuum distillation at 560°C. In the case of the hydrogen and organic tritium traps where the quantity of collected water is small, water containing no tritium was used to remove any sample memory left on the desiccant.(3) This method allows the total sample to be extracted from the desiccating material.

After extraction of the water samples, aliquots were taken and mixed with a liquid scintillator and counted using liquid scintillation techniques. For overnight counts, the sensitivity of this analytical system was such as to yield a minimum detectable(4) tritium concentration of 1 pCi/m^3.

The results obtained from NWVP tritium sample analyses are summarized in Table II and Figure 5. The data appearing in Table II represents tritium emissions measured during periods when only a single off-gas source term was present. Due to suspected poisoning of the room temperature Pd catalyst, the tritiated hydrogen and organic

TABLE II. ^{3}H-^{14}C Stack Emission Concentrations

Isotope	Chemical Form	pCi/m^3/(% error) Pre NWVP	Dissolution	Vitrification
^{3}H	Water	80/(5)	41,000/(5)	1,000/(5)
	Hydrogen } Organics }	36/(10)	200/(5)	35/(20)
^{14}C	Carbon Dioxide	3/(10)	814/(5)	110/(5)
	Carbon Monoxide	Bkg/(10)	20/(5)	20/(5)
	Organics	Bkg/(10)	Bkg/(10)	23/(5)

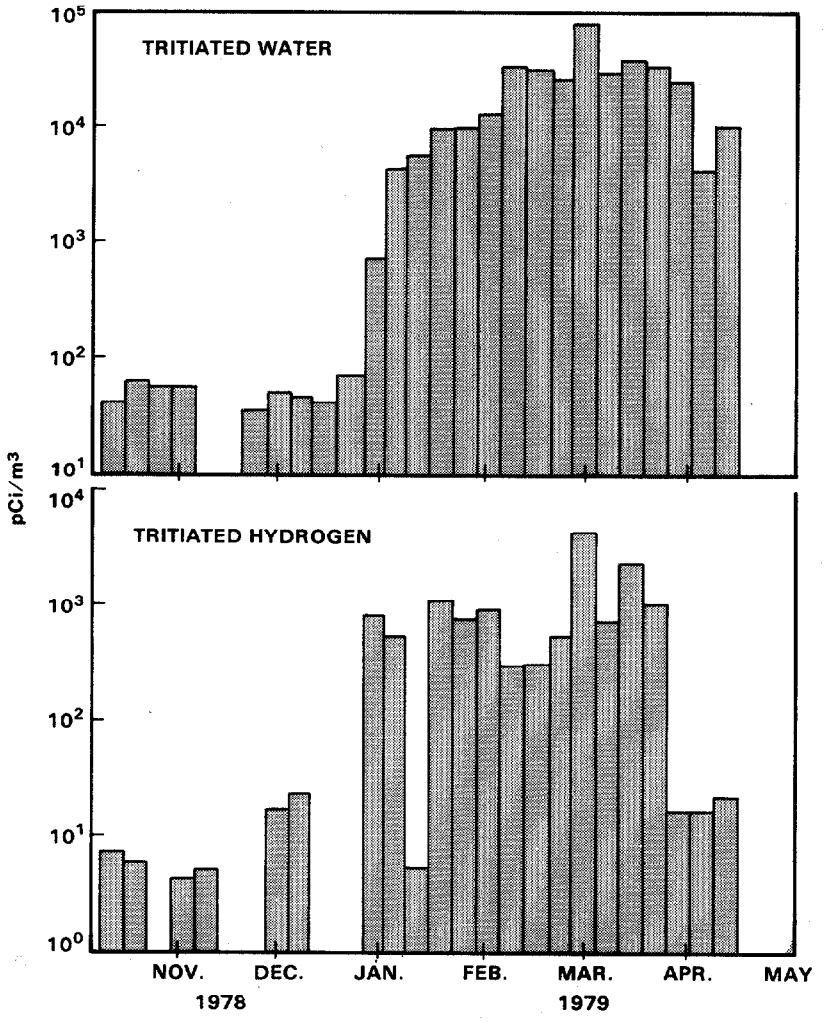

FIGURE 5. NWVP Tritium Stack Emissions

fractions have been combined in this table as combustible tritium. The pre-NWVP values listed in Table II represent measurements taken before the project hot cell work had begun.

Figure 5 presents weekly averaged emissions of tritiated water and hydrogen measured throughout the duration of NWVP, using an independent sampling system. Clearly, the major gaseous chemical form of

tritium that escaped the NWVP process was that of water. This was true not only for the entire process as a whole, but was also the case during the discrete steps of dissolution and vitrification. The ratio of tritium emitted during vitrification to that emitted during the entire NWVP project was calculated from the data and was found to be of the order of 10^{-3}.

Carbon-14

All forms of sampled ^{14}C, carbon dioxide, carbon monoxide and organics, were collected in the chemical form of CO_2 on a caustic bed of Ascarite. Chemically, Ascarite is NaOH suspended on an asbestos substrate. The collected CO_2 sample was extracted by dissolving it in water and precipitating the resultant $CO_3^{=}$ ion with Ba^{++}.

The extracted samples of ^{14}C were then analyzed using liquid scintillation techniques. In this method, a liquid scintillation compatible CO_2 absorber, a basic amine, was utilized in a bubbler that formed part of a closed-loop recirculation system. The sample, in the form of $BaCO_3$, was introduced into the closed system and acidified to convert the sample to CO_2. The CO_2 was continuously recycled through the basic amine until absorption was complete. The absorbed sample was then mixed with a toluene-based scintillator and counted with a liquid scintillation detection system. The minimum ^{14}C detection limit[4] associated with this analytical system is nominally 0.5 pCi/m^3 for 1000-min counting intervals.

The results obtained from the analysis of these samples are summarized in Table II. These data represent ^{14}C effluent concentrations averaged over the entire duration of the particular process being studied. Again a single chemical form, CO_2, was found to be responsible for most of the NWVP emissions of ^{14}C. Unlike tritium, routine sampling of major gaseous forms of ^{14}C was not conducted during NWVP.

Krypton-85

Because ^{85}Kr is a major gaseous effluent associated with the nuclear fuel cycle, this isotope was monitored continuously throughout NWVP. The analysis of γ-ray counting data was accomplished using two different approaches. The most direct involved a single channel analyzer/count-rate meter combination. In this system the single channel analyzer measures γ-ray activity in the 514 keV response region of the Ge(Li) detector. It passes this frequency information on to a count-rate meter that converts it to an analog output that is directly related to the 514 keV γ-ray counting rate, and consequently to the ^{85}Kr concentration in the spectroscopy gas cell. This analog output, accompanied by cell pressure and temperature data, was interrogated and recorded at preset intervals by the data logger. In addition, a continuous record of this analog signal, or 514 keV, γ-ray counting rate, was generated with a strip chart recorder.

Because the accuracy of determining ^{85}Kr activity via the real-time, count-rate meter approach is limited by gain shifts, spectral interferences, and by the nominal 30-sec time constant associated with the electronics, the Ge(Li) detector output was also integrated over

selectable time intervals utilizing a Canberra multichannel analysis system. Gamma-ray spectra of the stack gas were collected in a recycle mode by this analysis system over a 0-1 MeV energy range. Analysis of the γ-spectra generated by this system occurred automatically at the end of each counting period. During this analysis time, a peak search was conducted that yielded information on the energies and net counting rates of all significant γ-rays appearing in the spectrum being analyzed. In addition, gross counting rates occurring in important prespecified γ-ray energy intervals were also determined in order to establish background levels during passive intervals and/or to insure collection of all pertinent data when counting rates were too low to be determined by the automated search routines. All spectral analytical results were recorded magnetically on a cassette and printed out on a data terminal.

Gamma-ray stack gas monitoring was conducted continuously throughout NWVP. Not surprisingly, all detectable emissions of ^{85}Kr occurred during the dissolution step of the fuel reprocessing cycle. The temporal ^{85}Kr emission characteristics resulting from a typical dissolution campaign are illustrated in Figure 6. The discrete process steps associated with chopping and dissolving, with dissolver solution heating and with leaching the hulls are clearly illustrated in this figure.

With the use of stack flow measurements, also recorded continuously throughout NWVP, the above ^{85}Kr data was integrated over time to obtain daily stack emissions which are illustrated in Figure 7. In addition, the total emission values for the various fuel assemblies processed were also calculated from this data. Since no attempt was made to control ^{85}Kr emissions during NWVP, these values should be consistent with theoretical values derived from the amount and exposure

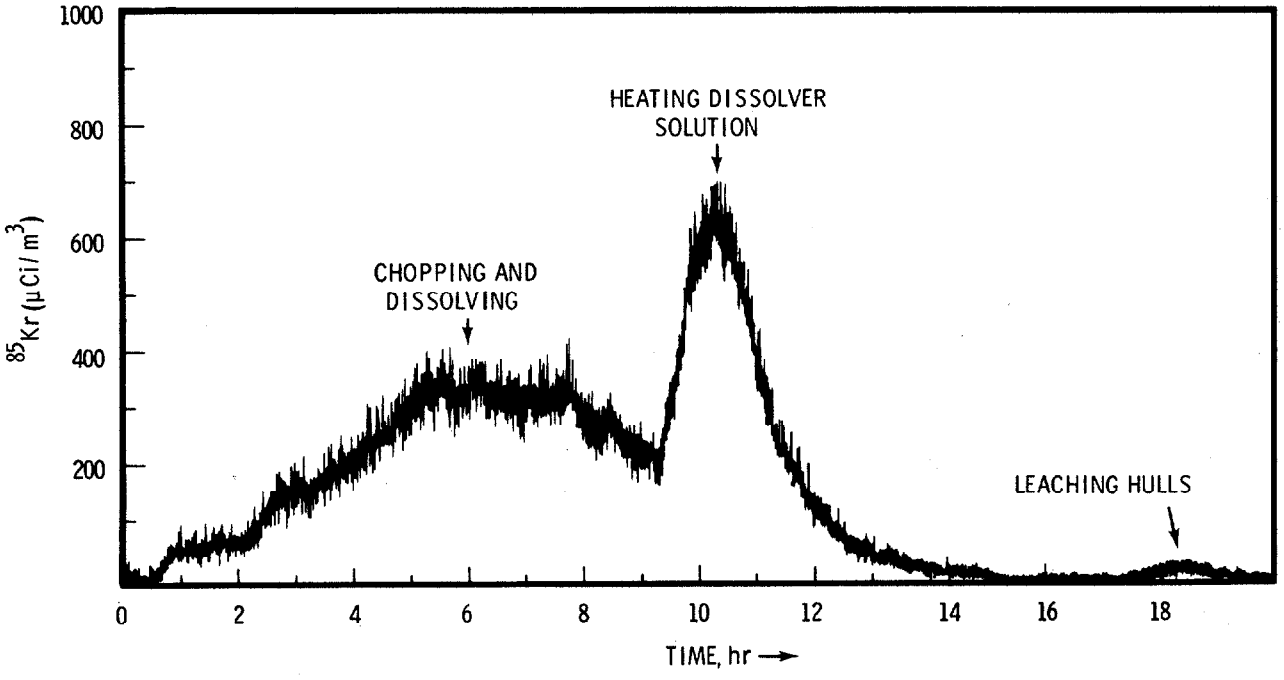

FIGURE 6. Strip Chart Record of ^{85}Kr Emissions Associated With a Typical Dissolution Campaign

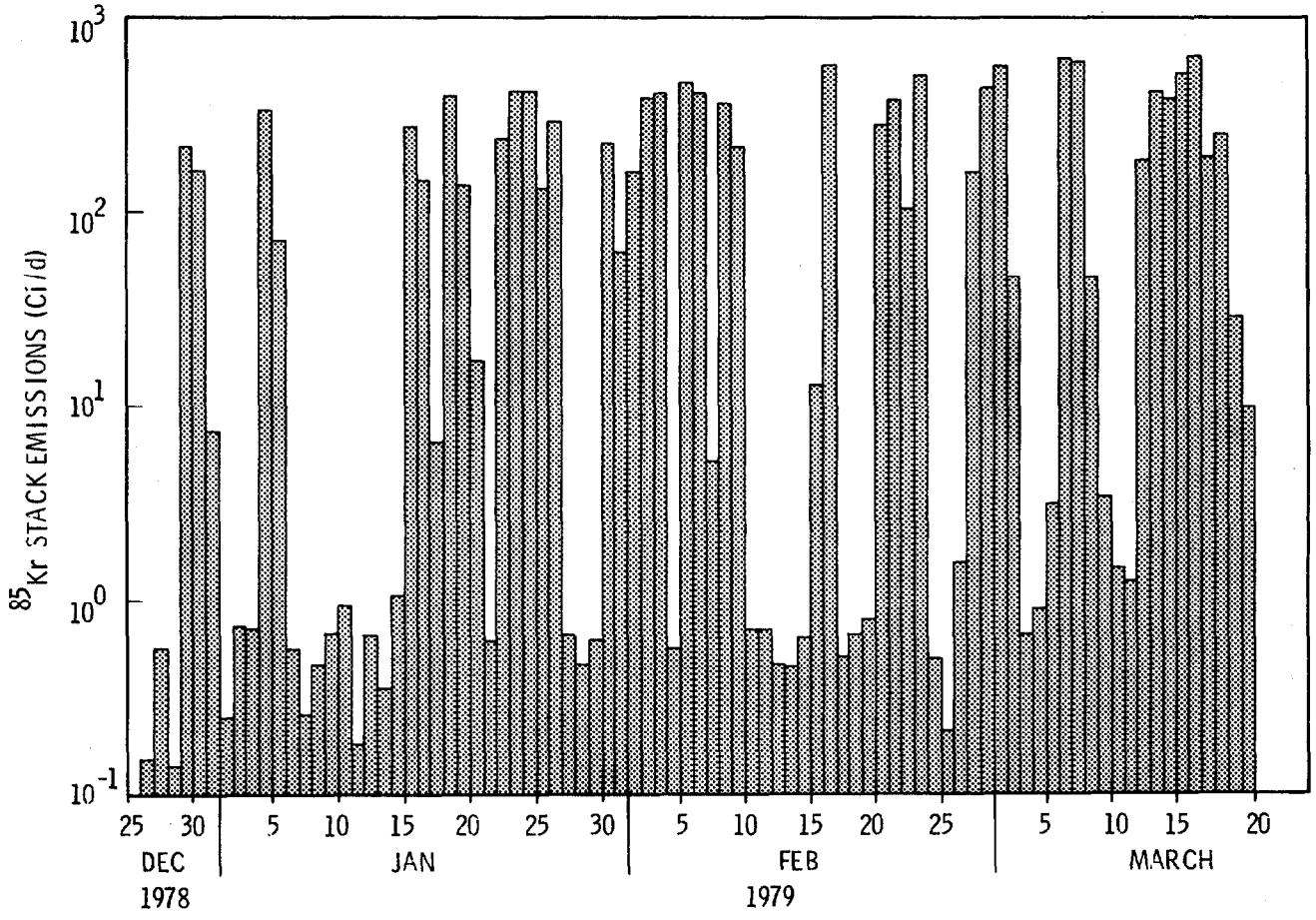

FIGURE 7. Daily NWVP ^{85}Kr Stack Emissions

history of the fuel utilized in this project. These values appear in Table III. The theoretical results presented in this table were generated from the computer code "ORIGEN" where input parameters were established from dissolver solution analysis. Clearly, the agreement between the ^{85}Kr data and theory illustrated in this table establishes internal consistency between γ-ray ^{85}Kr data and dissolver solution composition and strongly supports the accuracy and adequacy of γ-ray analysis of ^{85}Kr emissions.

^{129}I

Iodine samples were collected on and in a variety of substrates including resins, charcoals, silver-exchange sieves, and caustic solutions. The basis of analysis for all these samples involved basically γ-ray spectrometry. Resins, charcoals and silver-exchanged sieves were counted in a fixed geometry between two opposed Ge(Li) detectors operated in a summing mode. The 39.5 keV γ-ray served as a measure of the quantity of ^{129}I present in these samples. Aliquots of the caustic solutions used in the packed column scrubber were counted in Ge well detectors. In all cases the samples were compared to reference materials obtained from the National Bureau of Standards that were prepared to resemble the samples as closely as possible.

TABLE III. Measured Fission Products Versus Theoretical Predictions

	^{137}Cs Results			^{85}Kr Results		
	G/MTU			Ci/MTU		
Assembly	Exper	Theory	%Diff	Exper	Theory	%Diff
A-15	717	714	0.4	4940	4960	-0.4
A-16	743	714	4.1	4901	4960	-1.2
A-27	760	714	6.4	5117	4960	3.2
B-01	997	998	-0.1	7063	7420	-4.8
B-24	1011	998	1.3	7234	7420	-2.5
B-25	979	998	-1.9	6913	7420	-6.8

In addition, the iodine in selected samples was extracted from the trapping substrates, loaded into ampules and irradiated in a nuclear reactor. The neutron-activated samples were again counted utilizing γ-ray spectrometry to establish total ^{129}I content in low-level samples.

During vitrification, samples were obtained from the undiluted process off-gas stream, POG-88, as well as from the stack. Both sets of data are internally consistent and agree within experimental errors as is illustrated in Table IV. The division of ^{129}I activity between resin and charcoal suggests that organically-bound iodine is as important as the inorganic forms as an effluent. However, the silver-exchange sieve material used for iodine emission abatement throughout NWVP may be contributing to these numbers in an undetermined way.

Species independent measurements of stack gas iodine were averaged over nominal weekly periods throughout NWVP. This relative data appears in Figure 8. A poisoned silver-exchanged iodine trap was responsible for the large emission excursion occuring at the outset of NWVP. Replacement of this bed clearly eliminated this problem for the duration of the project. The sample result obtained during vitrification is denoted by diagonal cross hatching. The quantity of ^{129}I emitted during vitrification to that emitted by the entire NWVP project was calculated to be of the order of 10^{-3}, although, Figure 8 suggests that other sources may have strongly contributed to this value.

TABLE IV. ^{129}I Vitrification Emissions

Sampling Site	Sampler Type	Concentration	Total POG-88	Total Stack	Error %
POG-88	Scrubber	1.0 nCi/m^3	1.0 nCi/m^3	(0.86 pCi/m^3)*	5
Stack	Resin	0.4 pCi/m^3			
Stack	Charcoal	0.6 pCi/m^3	(1.2 nCi/m^3)*	1 pCi/m^3	25
Stack	AG Sieve	<50 fCi/m^3			

*Calculated from flow rate data.

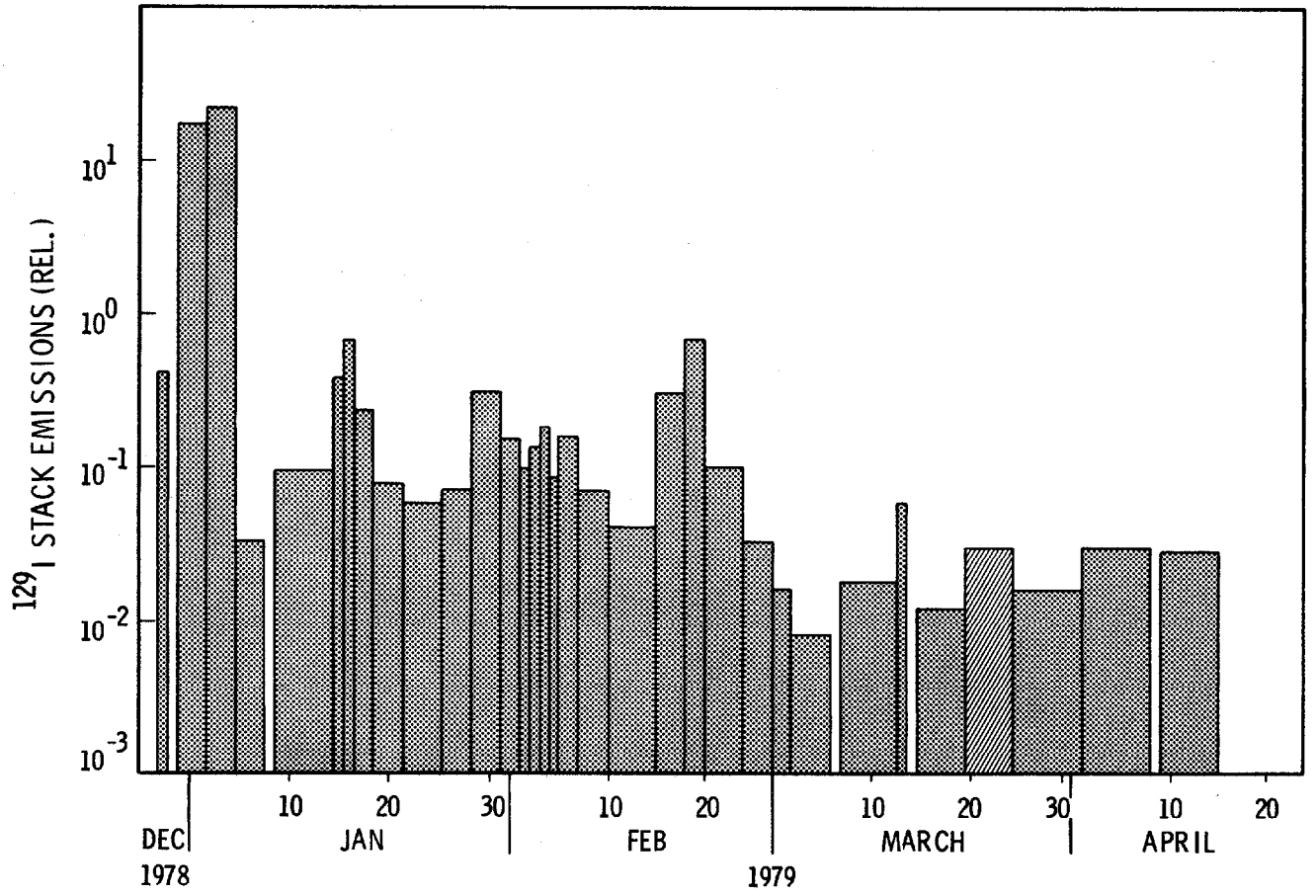

FIGURE 8. NWVP ^{129}I Stack Emissions

NO_x

Nitrogen oxides were measured at the stack sampling location with a commercially available NO-NO_x monitor. Previtrification background levels for NO and NO_x were, nominally, 0.3 ppm and 0.5 ppm, respectively. During active vitrification the main stack exhaust exhibited a tenfold increase in nitrogen oxide emissions. Average values for NO and NO_x measured at the stack during this period were 3 ppm, and 5 ppm, respectively. The peak value observed for NO_x during vitrification was 8 ppm. With the completion of spray calcining, the levels for NO and NO_x dropped to 0.5 ppm and 1.5 ppm, respectively. A time history of NWVP-NO_x emissions is presented graphically in Figure 9 where vitrification data is denoted by diagonal cross hatching. The integrated amount of NO_x emitted during vitrification to the total emitted by the NWVP project is of the order of 10^{-1}.

Semivolatiles

Direct γ-ray spectrometry of the process off-gas stream and of the scrubber solutions was used to determine the concentration of gaseous γ-ray-emitting semivolatiles present during vitrification. All γ-emitting semivolatile isotopes listed in Table I were below the detection limit of the analytical systems employed. However, an

average total γ-ray activity per unit volume of the process off-gas stream was estimated from the data generated. These results are summarized in Table V.

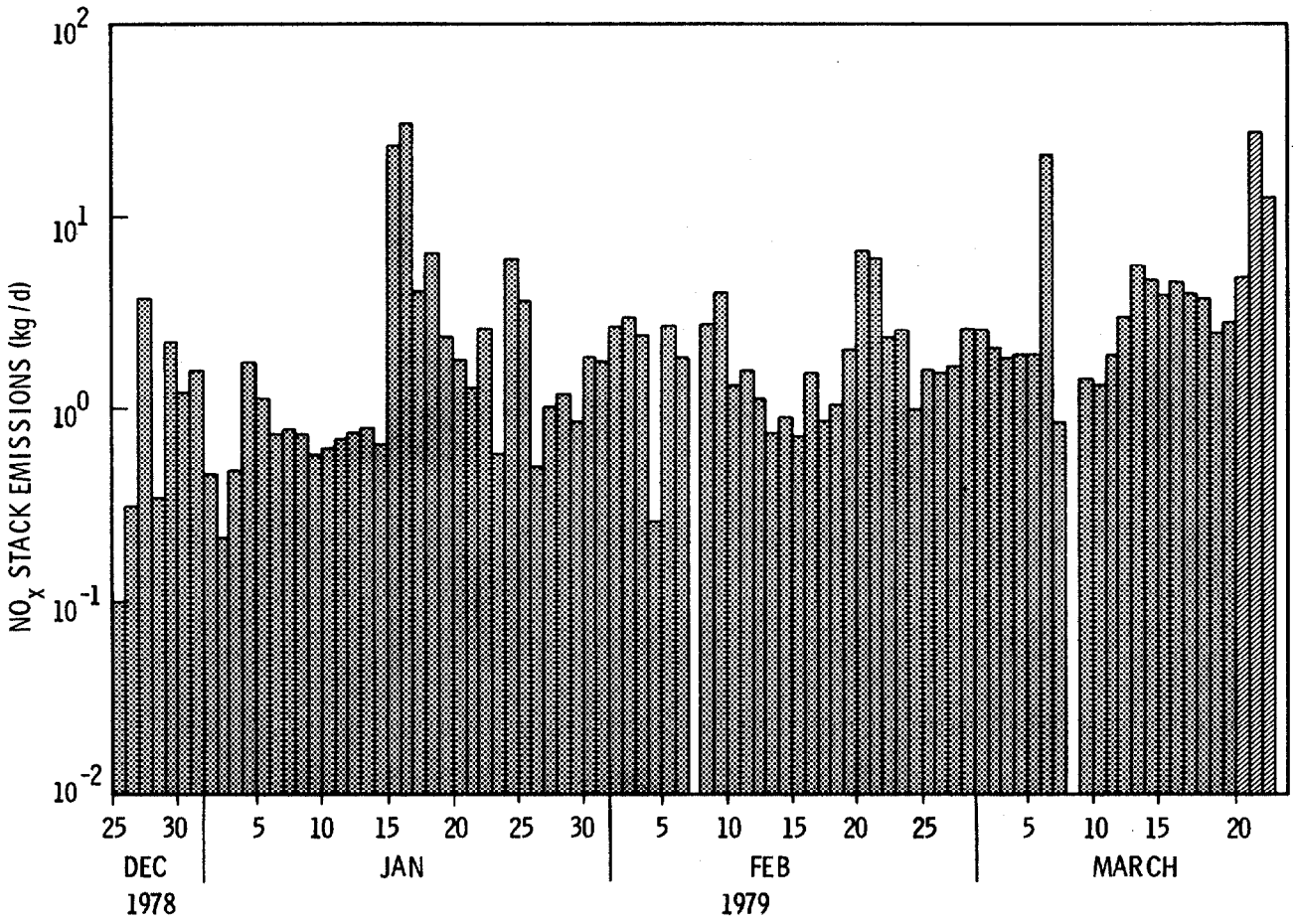

FIGURE 9. Daily NWVP NO_x Stack Emissions

TABLE V. Semivolatile Emissions

Isotope	Detection Method	Process Line Concentration	Error (%)
^{79}Se	β-Counting	<20 fCi/m^3	
^{99}Tc	β-Counting	1.8 pCi/m^3	20
^{106}Ru	γAnalysis	<200 nCi/m^3	
^{125}Sb	γAnalysis	<50 nCi/m^3	
^{126}Sb	γAnalysis	<3 nCi/m^3	
^{125m}Te	γAnalysis	<0.1 nCi/m^3	
^{134}Cs	γAnalysis	<6 nCi/m^3	
^{137}Cs	γAnalysis	<100 nCi/m^3	
All	γAnalysis	$\sim 10^5$ γ's/sec m^3	

The non γ-emitting semivolatile isotopes were chemically separated from the caustic scrubber solution and analyzed using low-level β^- counting techniques. The results of these analyses also appear in Table V. No attempt was made to measure ^{135}Cs since ^{134}Cs and ^{137}Cs served as excellent measures of the degree of process-induced volatility for all Cs isotopes. Semivolatile sampling was conducted only during the process of vitrification.

Particulates

Particulates were isokinetically collected utilizing a 0.4 μm Nuclepore polycarbonate membrane filter only during the vitrification process. This particulate sample was analyzed for both radionuclide content and size distribution. The radionuclide analysis was conducted utilizing γ- and x-ray spectrometric techniques. The results of this analysis are summarized in Table VI. Comparison of the results appearing in Table VI with calculated isotopic ratios expected in vitrification feed indicates preferential escape of both ^{106}Ru and ^{125m}Te.

Particle size analysis was accomplished utilizing scanning electron microscopic (SEM) techniques. Thirty-eight SEM-generated pictures ($2x10^4$ X magnification) were evaluated with a Zeiss particle size analyzer. The resultant normalized histogram of that data appears in Figure 10. This size frequency distribution was analyzed empirically and by fitting the data to a log normal distribution. The results of this analysis are summarized in Table VII.

The fit of the data to a log normal distribution is illustrated in Figure 11. Since particles generated by the vitrification process must travel a tortuous route through sintered filters, evaporators, condensers, heaters, and scrubbers before reaching the sampling point, a good fit to the data would be fortuitous. However, the analytical description of this distribution provides a convenient parametric means for handling and evaluating the data.

TABLE VI. Radionuclide Content of Particulate Matter

Isotope	Concentration (nCi/m^3)	Error %
^{106}Ru	44.0	10
^{125}Sb	0.52	10
^{125m}Te	1.7	15
^{134}Cs	7.8	10
^{137}Cs	52.0	10
^{144}Ce	0.82	10
^{154}Eu	0.28	30
^{155}Eu	0.18	15
^{241}Am	0.19	20

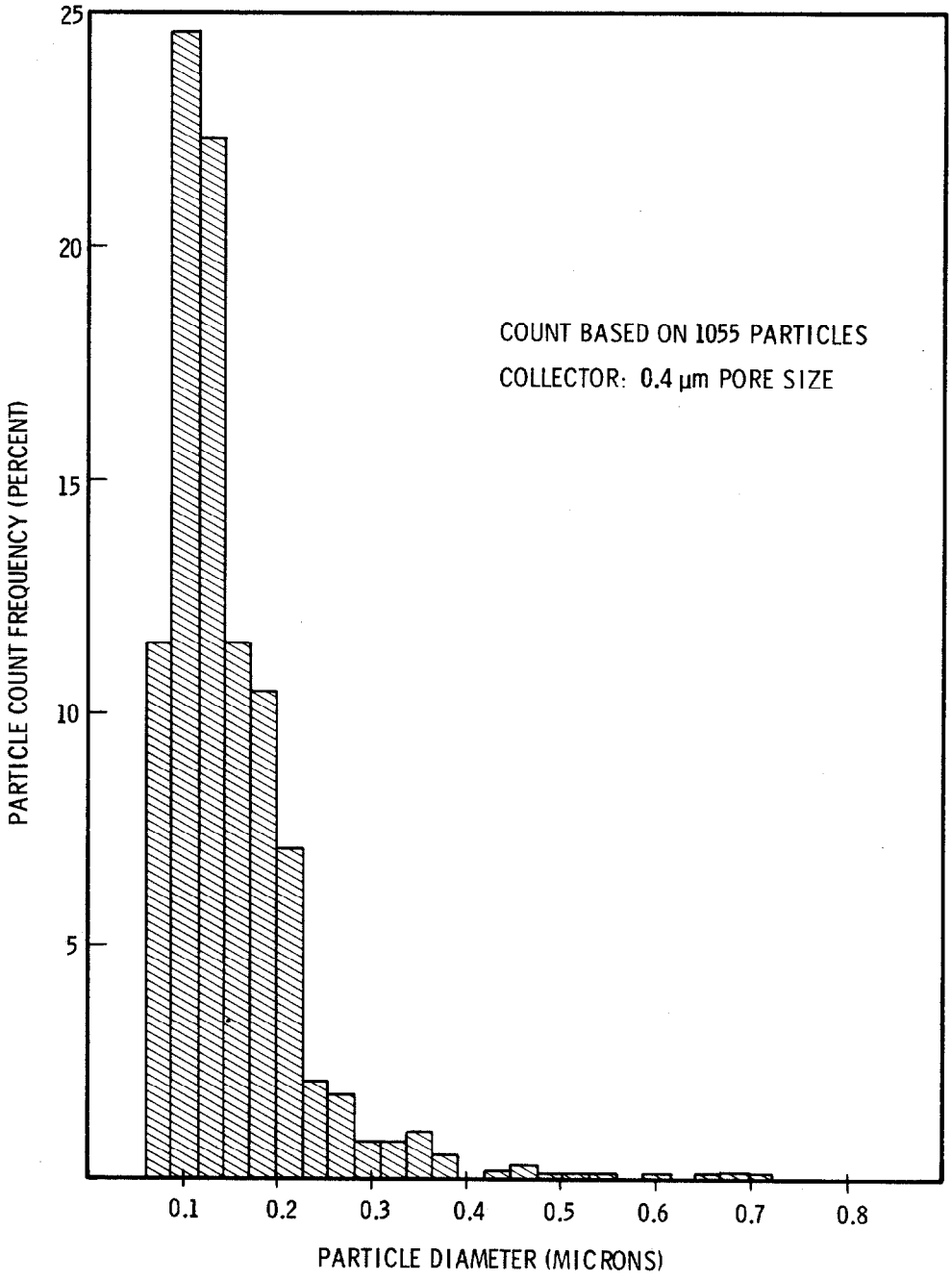

FIGURE 10. Particle Count Frequency Versus Particle Size Interval

TABLE VII. Particulate Size Distribution Analysis

Parameter*	Empirical	Log Normal
Geometric Mean Diameter	0.13 μm	0.10 μm
Geometric Standard Deviation	1.51	2.01
Correlation Coefficent	--	0.975
Mass Mean Diameter	--	0.55 μm
Particle Concentration	168/cm^3	--
Particle Mass Concentration**	84.7 pg/cm^3	--

*All parameters relate to undiluted process off-gas before final HEPA filtration.
**Assumed calcine density--3g/cm^3.

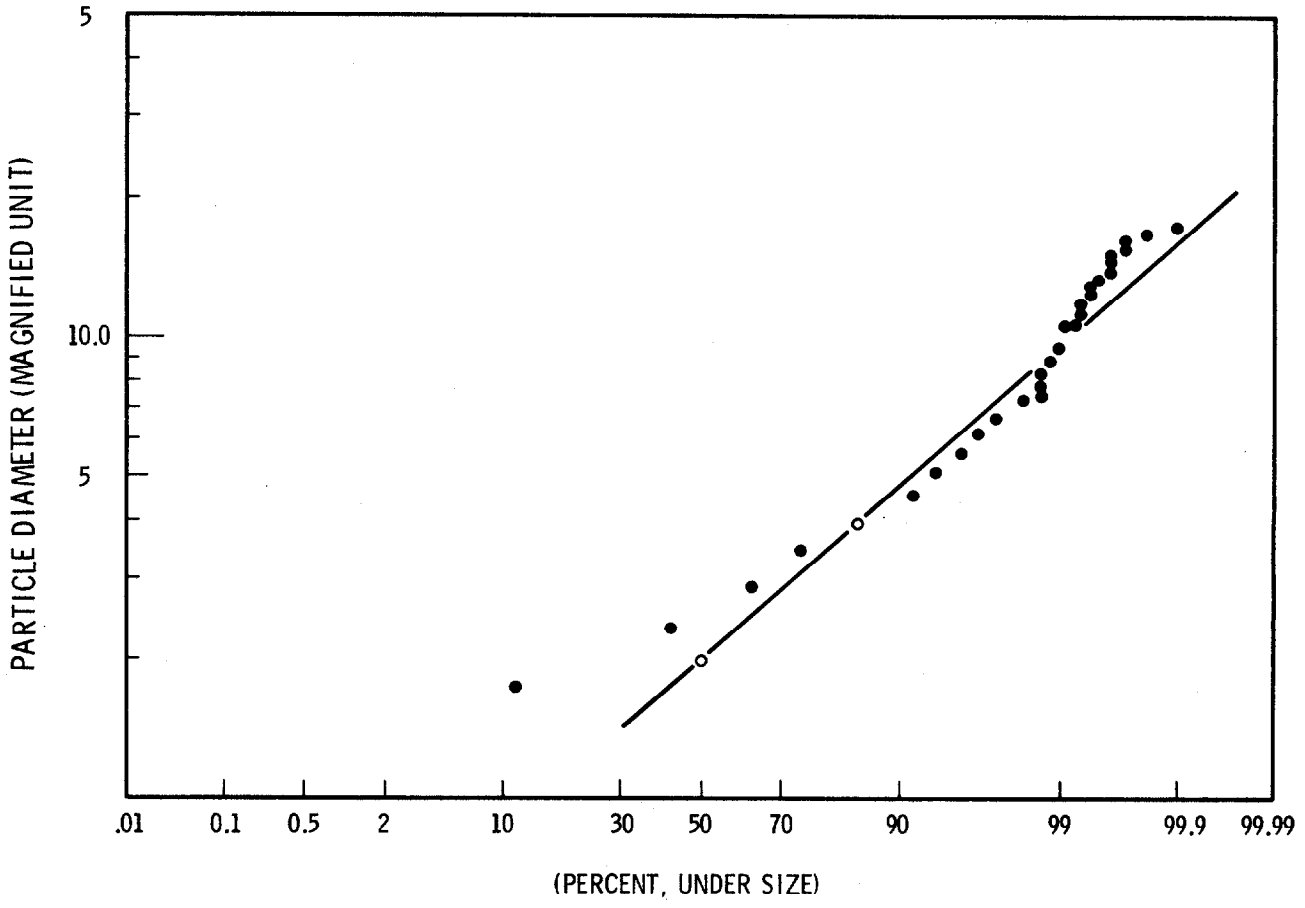

FIGURE 11. Log Normal Fit To Empirical Particle Distribution Data

The total efficiency of the Nuclepore filter employed as related to particle size was calculated using standard models and experimental data. Figure 12 summarizes the results of this efficiency calculation. Values for the total efficiency appearing in this figure serve only as a measure of confidence for the particle count at a specific size.

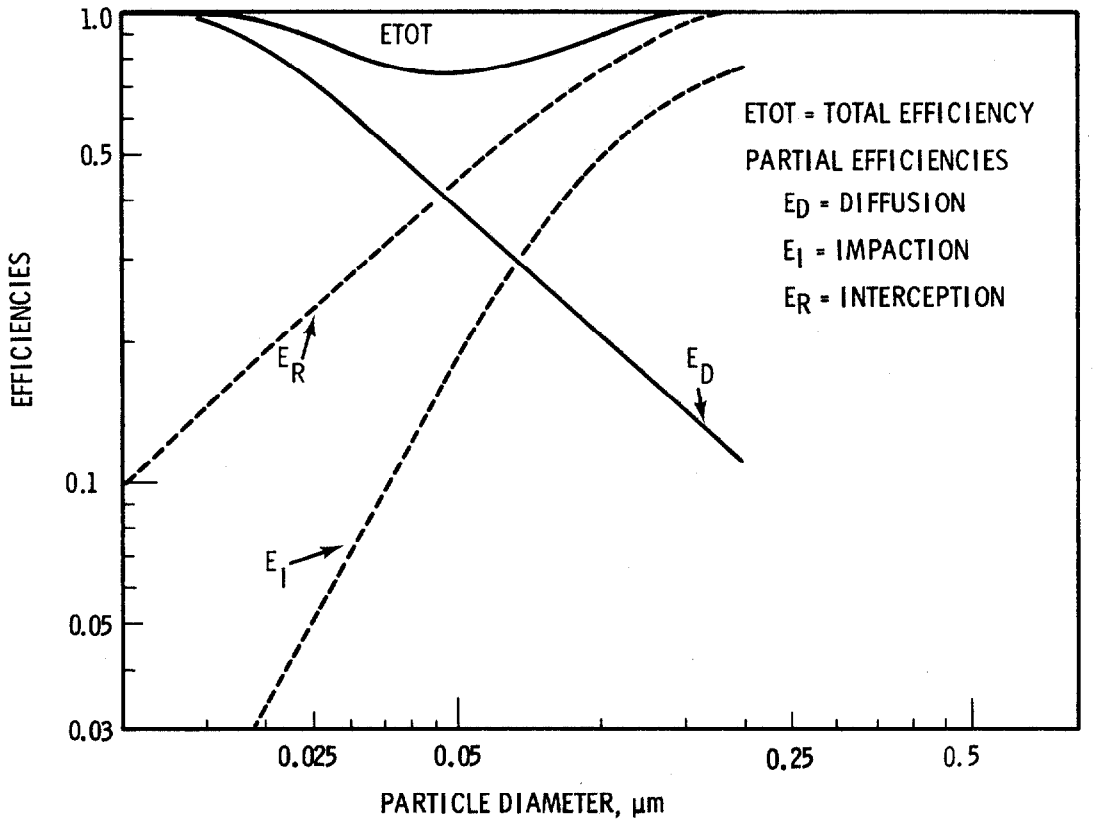

FIGURE 12. Some Empirical Partical Collection Efficiencies for a 0.4 μm Nuclepore Membrane Filter

ACKNOWLEDGMENT

This work was sponsored by the Department of Energy and performed under DOE Contract No. DE-AC06-76RLO 1830. The authors also wish to acknowledge the assistance of C. A. Shields, J. H. Kay and S. C. Simpson with experimental measurements and J. W. Courtney who supplied some of the samples used in this investigation.

REFERENCES

1. Wheelwright, E. S., W. J. Bjorklund, L. M. Browne, G. H. Bryan, L. K. Holton, E. R. Irish and D. H. Siemens. 1979. Technical Summary: Nuclear Waste Vitrification Project. PNL-3038. Pacific Northwest Laboratory, Richland, WA.

2. Goles, R. W., D. C. Hamilton, F. P. Brauer, H. G. Rieck, Jr., D. M. Robertson, R. L. Gordon, J. H. Kaye. 1979. Characterization of Gaseous and Particulate Effluents from the Nuclear Waste Vitrification Project. PNL-3181. Pacific Norhtwest Laboratory, Richland, WA.

3. Ostlund, H. G., and A. S. Mason. 1974. "Atmospheric HT and HTO." Tellus, 26:91.

4. Currie, L. A. 1968. "Limits for Quantitative Dectection and Quantitative Determination." Anal. Chem., 40:586.

DISCUSSION

LAMBERGER: I was curious about the distribution of the tritium with respect to how much of it stays in the fuel, how much is released and what fraction of what is released is HT, HTO, or tritiated methane.

BRAUER: We made no analysis of the amount that stayed with the dissolver. We did not do a tritium analysis on the dissolver residue. The process was designed to encourage the tritium, as well as the iodine, to leave the dissolver. Indeed, we did measure the iodine and found that 99% of the iodine had left the dissolver. The tritium would be scrubbed out by the water scrubbers in the offgas stream and, as the graph showed, the percentage of HT was considerably lower, less than 10% of the total tritium effluent from the plant. Because of the nature of the offgas stream, I would think that most of the effluent from the dissolver had to be HTO. We had some problems with our sampler differentiating between organic and HT forms of tritium. I guess we are uncertain of our results on that point.

LAMBERGER: When you say 10%, is that HT plus tritated methanes or triate organics?

BRAUER: It would be the summation of HT plus tritiated organics.

LAMBERGER: And the 90% of the tritium would be in the oxide form?

BRAUER: Yes. The actual graph is in the paper.

HENRICH: We measured the distribution of tritium during dissolution. With the typical pressurized water reactor fuel, we found 63% in the leached hulls and the rest was in the form of HTO in the fuel solution. About 0.4% was HT.

BRAUER: Yes, that is consistent with what we found. We did not find as much HT as we thought we might.

BEHAVIOR OF SELECTED CONTAMINANTS IN LIQUID-FED CERAMIC MELTER WASTE-VITRIFICATION OFF GAS

K. H. Oma
T. A. Nelson

Abstract

Vitrifying (immobilizing) high-level radioactive waste into a borosilicate glass is one method being developed for converting the wastes to a stable form for disposal. One promising process approach makes use of the liquid-fed, joule-heated ceramic melter. In this process, simulated high-level liquid wastes are fed directly to the melter, eliminating the calcining step used in previous concepts to dry the wastes before introducing them into the melter.

A good understanding of the types, forms and quantities of wastes passing from the process to the off-gas treatment system is necessary in order to determine off-gas cleanup requirements for this kind of waste vitrification. Tests have been performed during direct liquid-feeding of simulated high-level defense waste to a ceramic melter to characterize and quantify the gases, semivolatiles, and solids in the off-gas stream. The effluent sampling apparatus consisted of a wet scrubbing system, a plating sampler assembly, a gas chromatograph, and a classical scattering aerosol spectrometer. Tracer elements present in the nonradioactive, simulated waste feed were strontium, ruthenium, antimony, tellurium, and cesium.

Temperatures in a liquid-fed ceramic melter range as high as 1200°C in the molten glass. At these temperatures, the tracer isotopes of primary concern are ruthenium and cesium. During steady-state operation, ruthenium losses to the off-gas system averaged less than 0.16 wt%--while cesium losses were higher, ranging from 0.91 wt% to 24 wt% and averaging 13 wt%.

Chloride and sodium were the two major volatile species present in the off gas. Effluent particulates contained 44 wt% chloride and 27.6 wt% sodium. High chloride levels pose potential corrosion problems for the melter lid and the effluent system.

Due to the high chloride and sodium volatility observed, entrainment losses from the melter to the effluent treatment system account for only 10% to 30% of the total losses. Particulate decontamination factors from feed to off gas in the melter system ranged from 5×10^2 to greater than 10^3 without any filtration or treatment. Particle diameter ranged from below the 0.32-μm detection limit to 3.2 μm, with the maximum mass distribution peak occurring at 0.4 to 0.6 μm.

Introduction

The Pacific Northwest Laboratory (PNL), operated for the U.S. Department of Energy by Battelle Memorial Institute, is conducting studies to develop processes for converting liquid radioactive wastes into stable, solid forms--one of which is glass. A major component of the glass-making process developed by PNL is the powder-fed, joule-heated ceramic melter. Originally, several of these melters were developed to process calcine produced by spray calcination of liquid waste. However, more recently a liquid-fed ceramic melter (LFCM) has been developed that will eliminate the requirement for a calciner in the vitrification process.

A major portion of the vitrification process is the effluent treatment system. Full knowledge of melter effluents produced during the idling and

liquid-feeding modes is required to develop an adequate treatment system. When not processing waste, the LFCM is allowed to "idle" at a temperature above the solidification point for glass.

The research effort described in this report was conducted to characterize gaseous, volatile and particulate effluents produced by a full-scale LFCM both during liquid-feeding of a generic defense waste and when idling.

Process Description and Sampling Equipment Description

Liquid-Fed Ceramic Melter

The LFCM is a joule-heated ceramic melter system designed to convert simulated liquid waste into a stable glass product (Figure 1). The primary process component consists of a high-density chromia/alumina refractory-lined vessel in which borosilicate glass is maintained in a molten state by passing an alternating electrical current between two submerged electrodes; the molten glass serves as the conductive path. The upper portion of the melter's containment box consists of a lid surrounding a vapor space (plenum) through which simulated liquid waste and glass-forming additives called "frit" enter the melter. The typical melt temperature is 1050° to 1200°C and the typical plenum temperature during liquid-feeding is 200°C. Effluents are removed under vacuum through a 10.16-cm (4-in.) nominal-diameter stainless-steel pipe to an off-gas treatment system that consists of an ejector-venturi, condenser, and packed scrubber (Figure 2).

The nominal glass-conversion rating for the LFCM is 80 L/h--a rate equivalent to a production rate of 29 kg/h or a melting flux of 28 kg/h-m^2. A complete equipment description of the LFCM has been prepared by Buelt and Chapman.[1]

Effluent Sampling System

The effluent sampling system designed for characterizing LFCM off gases and entrained particles consists of four main components (Figure 3):

1) volatile plating sampler
2) gas-scrubbing system
3) gas-sample ports and an inline sample cylinder
4) classical scattering aerosol spectrometer (CSAS).

Plating behavior of volatilized glass components was studied using a plating sampler that consisted of two 25-mm-dia by 147-mm-long quartz glass tubes supported end-to-end above the melt. The tube surfaces were roughened by sandblasting. Scale and spatterings on the tubes were analyzed by an induction-coupled plasma (ICP) spectrometer. The plenum temperature profile was monitored and recorded during the experiment.

Waste glass components, as well as radionuclide substitutes leaving the melter due to volatilization and entrainment, were recovered using a gas-scrubbing system. The system consisted of a 15.4-mm (1/4-in.) heat-traced stainless steel sample line, water-cooled condenser, a trap to collect condensate, a 500-ml scrubber containing 0.2M nitric acid (HNO_3), a second 500-ml scrubber containing 1.0M sodium hydroxide (NaOH), a liquid trap, rotameter, vacuum pump and a flow totalizer. The condensate and scrub solutions were analyzed by ICP for all elements except cesium (which was by atomic adsorption) and Cl^-, NO_3^- and SO_4^{2-} (which were by ion chromatographic and specific ion electrode techniques).

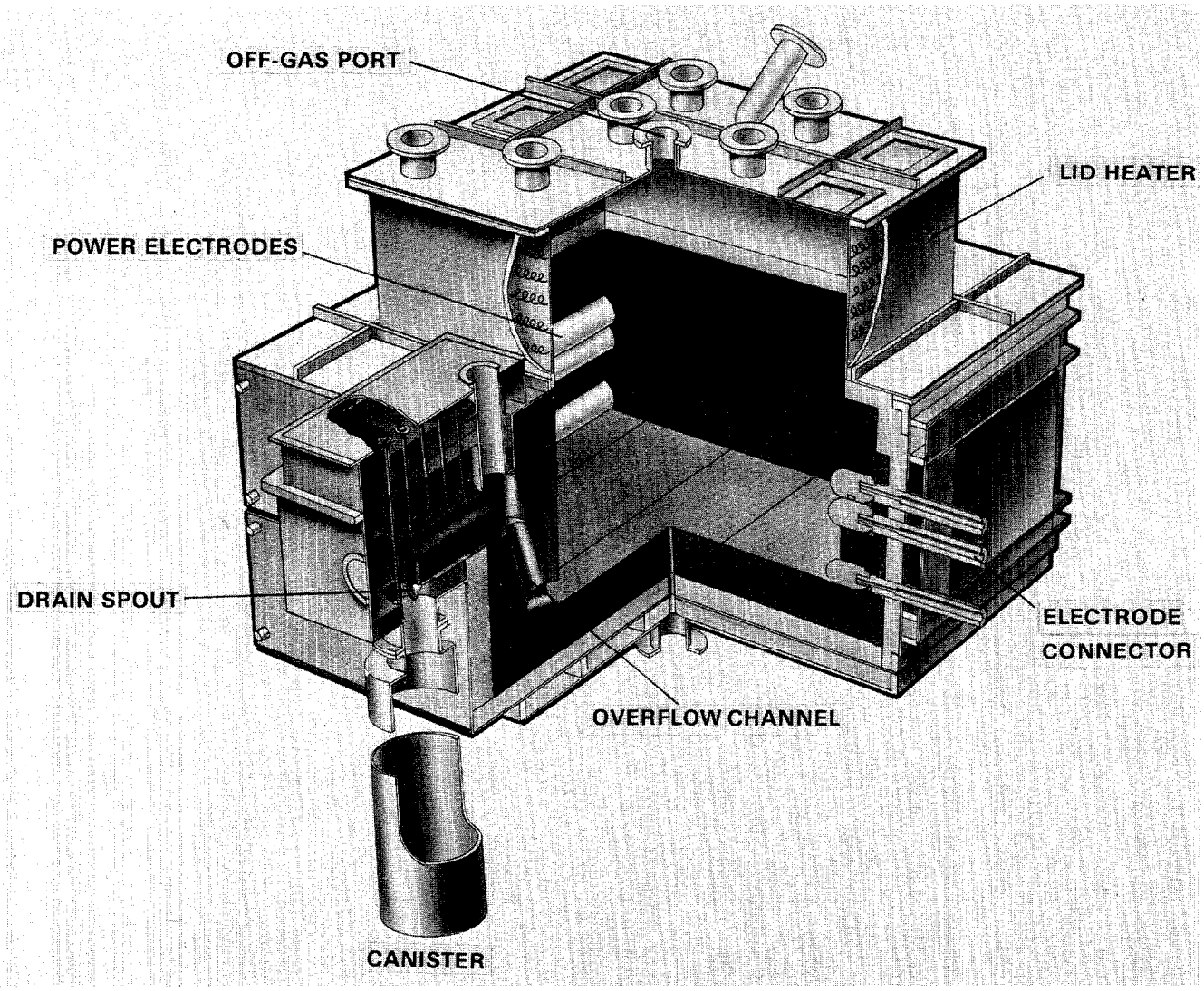

FIGURE 1
LIQUID-FED CERAMIC MELTER

Noncondensable effluents were analyzed using a gas chromatograph and a mass spectrometer for CO_2, CO, O_2 and N_2. Gas chromatograph samples were taken with a 20-cc syringe injected through teflon septums at sample points #1, #2, and #3 (Figure 3). Mass spectrometry samples were taken with a 75-cc stainless steel in-line sample cylinder placed in the gas-sample line below GC sample point #1.

The mass loadings and size distributions of solids leaving the melter were studied using a CSAS. These parameters are important for design of a process off-gas system.

The CSAS system is composed of:

- an isokinetic sample port
- a Particle Measuring Systems, Inc. (PMSI) Model CSASP-100 He-Ne laser probe
- a PMSI model PDS-200 particle data system
- a Nova 3 Mini Computer for data acquisition and analysis.

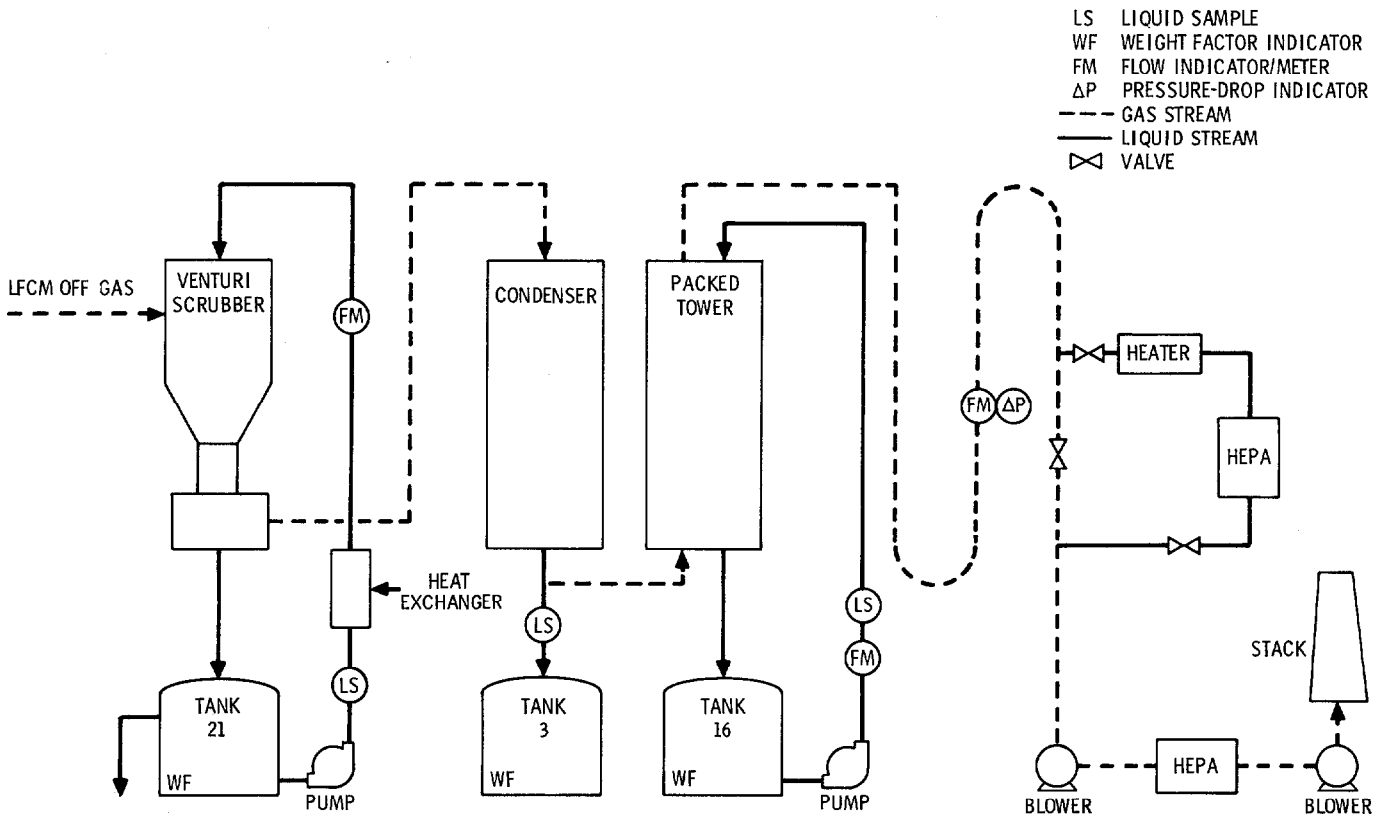

FIGURE 2
LFCM OFF-GAS TREATMENT SYSTEM

The isokinetic sample port is a 2.54-cm (1-in.)-dia stainless steel tube centered in the off-gas line (Figure 3).

The PMSI model CSASP-100 He-Ne laser probe is designed to detect up to 30 size channels simultaneously in a 0.3- to 20-μm particle-size range using a high-resolution, element-refraction imaging system in its collecting optics.

The probe is calibrated using monodispersed latex spheres, so the particles counted during sampling are assumed to be spheres. The size of the particle is determined by the pulse height (intensity) of the scattered light. This differs from other size-distribution measuring devices (such as cascade impactors) that separate particles based on their aerodynamic size.

The PMSI particle data system Model PDS-200 is a data acquisition and recording system designed for use with the standard PMSI particle spectrometer probe. The PDS-200 allows for on-line monitoring of particle characterization and ease of CSASP-100 probe calibration and has capabilities to output data to the Data General Nova 3 computer for data acquisition and graphic interpretation.

The Data General Nova 3 computer is used to process data from the PDS-200 through data-conversion and data-analysis programs. During spectrometer operation, data are automatically transferred to the Nova 3 for disc storage. The data-acquisition system outputs sets of data that are stored on the disc. Data analysis programs are used to normalize and average the data sets. Then the gas-sample flow rates are input and the program calculates masses and mass percentages as a

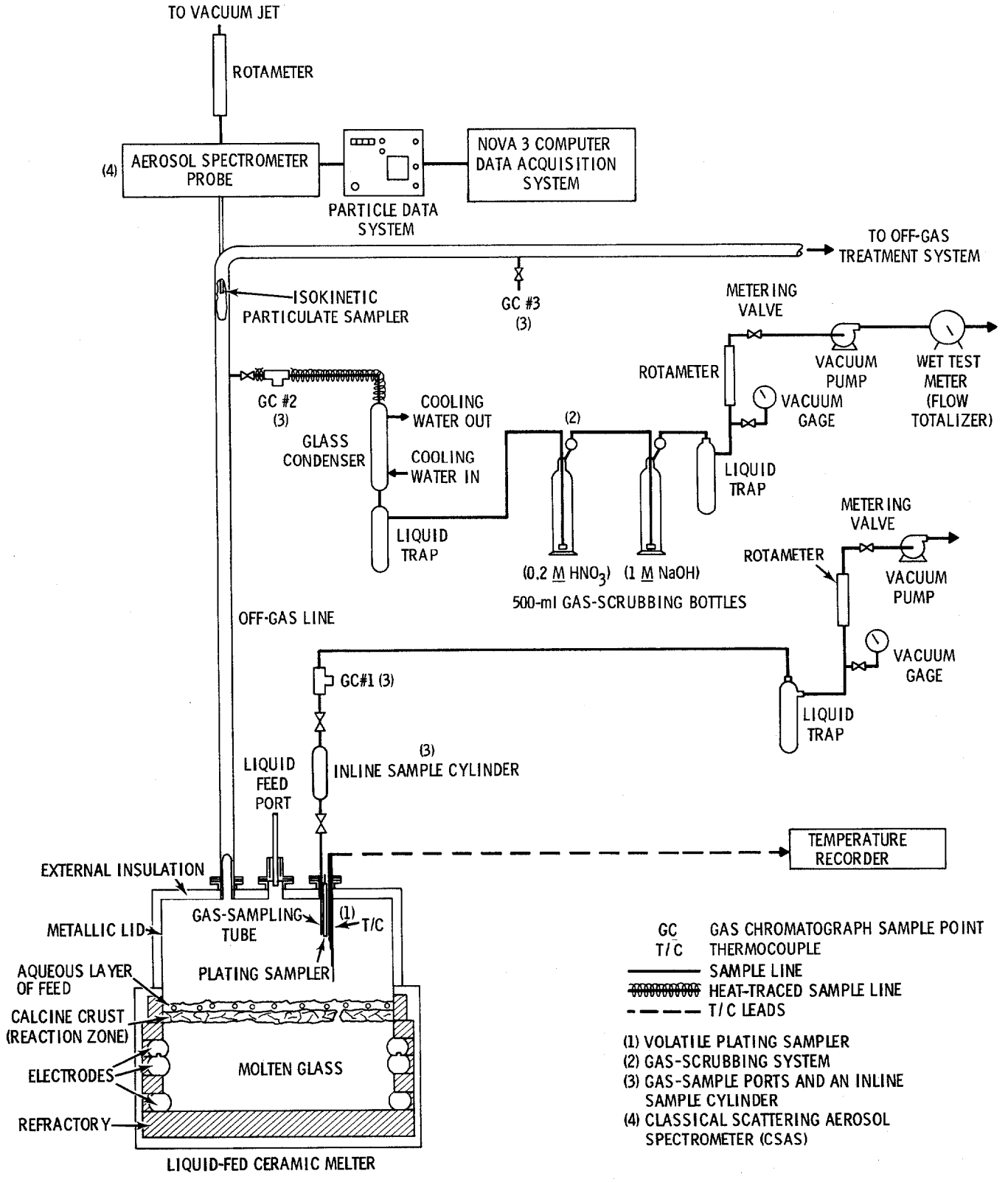

FIGURE 3
EFFLUENT SAMPLING SYSTEM

function of particle size, after which the program plots all of the particle count and mass distribution data.

A gas sample was drawn through the CSAS at a mean rate of 9.84 m/s by a steam jet with the flow controlled by a metering valve on a rotameter. The sample flow was started 30 min prior to collecting data, thus allowing the system temperature to reach an equilibrium. The CSAS was operated for 60 to 120 s per data set.

Melter and Sampling System Operating Summary

The liquid feed composition (elemental basis) is shown in Table I. The feed was a mixture of 72 wt% glass former and 28 wt% anticipated Savannah River Plant waste sludge as the waste oxides (SRP TDS-211 waste/frit composition as defined by Savannah River Plant). Nonradioactive trace isotopes of strontium (Sr), ruthenium (Ru), antimony (Sb), tellurium (Te), and cesium (Cs) were added to the feed. All trace elements except Sr are considered to be semivolatile. Bentonite was added (2 wt%) as a suspending agent, along with 1 to 2 wt% cornstarch.

Table II gives a summary of run conditions for time periods during which the gas-scrubbing system was operated. The scrub system was operated at three different times during steady-state, once during startup and once during foaming. During steady-state, the percent of melt surface flooded ranged from 80% to 100% and the plenum temperature ranged from 94° to 273°C. The plenum temperature was lowest during periods of complete flooding. Melter inleakage was quite high due to leaks in the lid and was typically greater than 80% of the total flow. A detailed description of the melter operation is provided by Brouns et al.[2]

Table I. Liquid Feed Composition

Component*	Average Composition, g/L	Deviation**
Li	4.14	0.36
B	9.10	0.89
Na	38.01	3.04
Al	8.94	0.85
Si	70.92	5.48
Ca	12.64	1.19
Mn	6.31	2.29
Fe	32.15	2.68
Ni	3.40	0.32
Cl-	4.58	0.37
Sr	0.110	0.012
Ru	0.816	0.079
Sb	0.234	0.023
Te	0.206	0.022
Cs	0.169	0.021

* The compositions are given in elemental form but are present as hydroxides, oxides carbonates, nitrates and sulfates.

** Standard deviation for 25 samples taken during liquid-feeding.

Table II. Run Conditions During Sampling-System Operation

Melter Operational Mode	Average LFCM Feedrate, L/h	LFCM Melt Surface Flooded, %*	Average Plenum Temperature, °C	Melter Air In-Leakage, sLm (scfm)**	Total Off-Gas Flow, sLm (scfm)**
Startup	60	0	100-920	9,450 (334)	10,530 (372)
Steady State	67	90	273	12,030 (434)	13,230 (467)
	60	100	94	4,300 (152)	5,370 (190)
	60	80	149	6,100 (215)	7,170 (253)
Foaming	--	0	100-970	---	---
Average	62	---	---	7,470 (281)	9,075 (320)

* Melt surface flooded describes the percentage of the melt surface covered by liquid.

** Calculated flow based on condensate volume and liquid feed rate. Assumes 862 g H_2O per L feed and scrub-sample dew-point of 25°C.

Results

Noncondensable Off gas

The average noncondensable off gas analysis from the three gas chromatograph sample ports and the in-line sample cylinder is shown in Table III. Average concentrations of all gas samples taken during steady-state liquid feeding, foaming,* and idling are shown. No concentration trends were observed between the different sample locations or between the gas chromatograph and mass spectrometer sample analysis. The CO_2 concentration is the highest during foaming, and the O_2 concentration is higher than the air reference during foaming. This indicates that CO_2 and O_2 are being evolved from the melt during foaming. During idling both the O_2 and CO_2 levels are lower than the reference air, indicating that the melt is absorbing or somehow reacting with these components. This supports a current theory of foaming by L. D. Pye, who suggests three mechanisms for foam generation.[3] The first mechanism involves an O_2 solubility change in the melt due to a temperature change. As the melt is cooled to bring about an idling state, the melt solubility of O_2 increases and the melt absorbs O_2. It appears that CO_2 may also be absorbed in this manner. Then, as the melt is heated to begin feeding the melter, the oxidation state of some of the metals in the melt (principally Fe and Mn) is lowered and O_2 is released ($Fe_2O_3 \xrightarrow{\text{heat}} 2FeO + 1/2\ O_2$) causing foaming (foaming due to temperature changes is called "reboil"). The second mechanism is related to the first and involves the decomposition of carbon-containing compounds ($CaCO_3$ and cornstarch) and residual nitrates in the crust. When the melt starts foaming due to the first mechanism, some of the dried crust is engulfed. As the crust is heated, the carbon is oxidized to CO_2 and the nitrates are converted to

* Foaming is the release of dissolved or evolved gases from molten glass. Although most melts generate gases, this particular composition creates bubbles that are not easily ruptured, so that as the gases are released the number of bubbles increases. Foaming is not desirable because it can reduce the melter capacity, affect the process stability, and in extreme cases may cause equipment damage or shutdown.

Table III. Average Noncondensible Off-Gas Composition During Liquid-Feeding

	Gaseous Component, vol%				
	CO_2	O_2	N_2	CO	Ar
Steady-State Liquid-Feeding (no foam)	0.104	23.6	75.4	0.001	0.96
Foaming	0.222	23.1	75.7	---	0.96
Idling	0.021	19.5	79.5	---	0.96
Air	0.061	21.0	78.1	---	0.96
Average Standard Deviation*	0.07	2.1	2.1	0.01	---

* up to 7 samples taken during each condition

NO_x. These gases bubble up through the melt and increase the foaming. Foaming due to this mechanism can also occur independent of the first mechanism (reboil). The third mechanism involves generation of gases as the calcine changes state from a solid to a liquid. The liquid (molten glass) may have a lower O_2 solubility than the solid, so that as the calcine melts, O_2 may be released.

Volatilized and Entrained Constituents

Volatilized and entrained glass components, including radionuclide substitutes, were recovered using the gas-scrubbing system previously described and shown in Figure 3. Scrub solutions were analyzed for all elements, then the results were corrected by subtracting out the initial elemental concentrations present in the fresh scrub solutions. Elemental quantities present in the trap and both scrubbing bottles were totaled and converted to an off-gas concentration basis (µg/std. L off gas). Off-gas concentrations of major glass components and radionuclide substitutes, as well as steady-state decontamination factors, are presented in Table IV. Concentrations of ion species are presented in Table V. The most prominent glass component is sodium with lesser quantities of iron, boron and lithium. Sodium metal has the lowest boiling point (883°C), followed by lithium (1317°C), and both elements have relatively low-boiling chlorides and hydroxides (<1400°C); thus, higher volatilities for these elements would be expected. Elemental boron is not volatile (M.P. 2300°C); however, boric oxide (B_2O_3), the form used in the feed makeup, and boric acid are more volatile. In a water-vapor atmosphere, B_2O_3 is known to be unstable and loses weight when heated above 250°C[4]. The higher the air flow and the more vigorous the boiling (typical of the LFCM during operation), the greater the B_2O_3 vaporization. The highest off-gas concentration of most elements was during steady-state operation, with lesser amounts evident during foaming and start-up.

Of the trace elements, Cs has the lowest average DF (Table IV). The Cs volatility appeared to be dependent upon run parameters; however, a mechanism has not been identified. Cesium, being in the same alkali metal family as Na and Li, has the lowest boiling point (690°C) and in turn was observed to have the lowest DF. Sodium and Li have higher boiling points and show higher DFs, respectively. The

Table IV. Elemental Off-Gas Concentrations and Steady-State Decontamination Factors*

Element	Off-gas Concentration,** µg/std. L Off Gas, Melter Operation Mode: Startup	Steady-State†	Foaming	Average DF During Steady-State
Major Glass Elements				
Li	0.12	1.32	0.36	940
B	2.80	7.82	8.97	190
Na	5.97	58.8	19.8	150
Al	0.17	0.08	0.13	11,000
Si	0.41	1.03	1.79	18,000
Ca	0.72	0.25	0.46	19,000
Mn	0.06	0.03	0.05	35,000
Fe	0.58	2.10	0.05	2,300
Ni	0.12	0.47	0.16	1,100
TOTAL	10.95	71.90	31.77	---
Radionuclide Substitutes				
Sr	0.138	0.010	0.004	7,400
Ru	0.023	0.160	0.049	810
Sb	0.002	0.031	0.039	1,700
Te	0.06	0.110	<0.06	3,000
Cs	0.257	2.734	0.420	44
TOTAL	0.257	3.045	0.512	---

* The decontamination factor (DF) is the ratio of mass entering the melter with the feed to the mass leaving with the off gas.

** Combined quantity from trap, 0.2M HNO_3 scrubber, and 1.0M NaOH scrubber except for Na and Si, which are combined quantities from trap and 0.2M HNO_3 scrubber only. Caustic scrub solution invalidates Na analysis and tends to leach Si from the glass scrubber. Elemental concentrations of reference samples are subtracted from the scrub analysis.

† Average of three sample periods.

cesium DF ranged from 4.2 to 110, which corresponds to weight losses of 0.91 to 24 wt%.* The average loss to the off-gas system of the semivolatile trace elements during steady-state is as follows: Ru = 0.16 wt%, Sb = 0.11 wt%, Te = 0.44 wt%, and Cs = 13 wt%. These are based on the average losses over the entire steady-state sample period as opposed to the average DF of each sample period. There were periods during the run when all species exhibited higher DFs. No mechanism for this behavior has been identified. The ruthenium DF was high, ranging from 530 to 1000 and averaging 810. Ruthenium tetraoxide (RuO_4) is a liquid

* This volatility is substantially higher than previously observed by J.L. Buelt, Research Scientist, PNL. He observed Cs volatility losses of 0.4 to 1.4 wt% when feeding simulated power-reactor waste.

Table V. Chloride, Nitrate and Sulfate Off-Gas Concentrations

Operational Mode	Number of Samples	Ion Concentrations,* µg/std. L Off Gas					
		Cl^-		NO_3^-		SO_4^{2-}	
		Trap	Total	Trap	Total	Trap	Total
Startup	1	6.55	14.9	18.6	(b)	0.81	**
Steady-State	2	94.8	282	2.79	(b)	10.2	**
Foaming	1	58.76	(†)	50.28	(b)	0.76	**

* Total concentrations are sum of concentration trap and 0.2M HNO_3 scrubber.
** NO_3^- analysis of HNO_3 scrub not performed. High NO_3^- concentration in the scrub interfered with SO_4^{2-} analysis.
† HNO_3^- scrub not analyzed.

at 25.5°C and has been the cause of high Ru volatility under oxidizing conditions. The defense waste is neutralized, thus minimizing the potential for Ru oxidation.

The most prominent ion species collected by the scrub system are chloride (Cl^-) followed by nitrate (NO_3^-), then sulfate (SO_4^{2-}). The Na-to-Cl mole ratio during steady-state operation was 1.0 to 3.1, which indicates that most of the Cl^- exists in some form besides NaCl. In a LFCM production unit, the melter lid and off-gas components must be fabricated from materials resistant to corrosion induced by Cl^-, NO_3^-, and SO_4^{2-}.

Plating and Particulate Constitutents

Plating behavior of volatilized glass components was studied using a plating sampler previously described and shown in Figure 3. The sampler was suspended from the melter lid for 15.75 h during steady-state melter operation.

Due to a period of melter foaming and continual spattering of the liquid feed, the plating sampler collected feed and glass along with volatilized species. The data is not reported because it is not possible to differentiate between the volatilized and spattered materials.

Table VI presents the analysis results of a particulate sample taken from the off-gas line. The particulate sample composition ratios do not resemble those of the feed because each oxide has a different volatility. All the major glass components are less abundant--especially the oxides of aluminum and manganese. Approximately 75 wt% of the sample was not accounted for and is believed to be Na and Cl. The sample was too small to allow analysis for either Na or Cl.

A second particulate sample taken from the plenum sample-system line was analyzed and found to contain 27.6 wt% Na and 44 wt% Cl (a 1:1.03 mole ratio). Of the trace elements, Ru and Cs are the most abundant--their concentrations respectively being 2.5 and 50 times those of the feed oxides. The Sb and Sr remained relatively constant in all the samples and no Te was detected in any of them.

Table VI. Particulate Sample Compositions

Feed Component		Off-Gas Line Particulate Sample**	
Oxide Form	Composition,* wt%	Composition, wt%	Fraction of Glass Composition
Major Glass Components			
Li_2O	2.66	1.45	0.67
B_2O_3	8.75	2.41	0.28
Na_2O	15.30	-	-
Al_2O_3	4.26	0.71	0.17
SiO_2	45.32	12.30	0.27
CaO	5.28	1.83	0.35
MnO_2	2.98	0.10	0.03
Fe_2O_3	13.73	4.94	0.36
NiO	1.57	0.39	0.25
Radionuclide Substitutes			
SrO	0.0098	0.0158	1.6
RuO_2	0.0809	0.206	2.5
Sb_2O_3	0.0215	0.0194	0.90
TeO_2	<0.025	<0.025	---
Cs_2O	0.135	0.68	50
TOTAL	100%	25.1%	

* Based on actual elemental analysis and assumes oxide form as shown (normalized to 100%)

** Sodium analysis not valid, since sample was fused in Na for ICP analysis. Solid sample taken from sample-system line contained 27.6 wt% Na and 44 wt% Cl.

Particle Loading and Size Distribution

Entrained particles in the off-gas line were analyzed by using a CSAS. A sample stream was drawn isokinetically from the off-gas line and passed through the CSAS probe. The CSAS measures, analyzes and reports particle-size distribution data in four overlapping size ranges that cover the total particle-diameter range of 0.32 to 20 μm. The mini-computer removes overlap during data reduction and integration.

Figures 4 and 5 are graphs of the average data from four particle sample periods during idling, normalized to 900-s sample intervals. Figure 4 shows the particle count versus particle size. The graph shows that 95% of the particles are less than 1.5 μm in dia and the count peaks at a size range smaller than the instrument limitation of 0.32 μm. There are, however, particles up to the size of 5.5 μm. Figure 5 shows the mass distribution for the same runs as Figure 4. The maximum mass-loading occurs at between 0.6 to 0.7 μm.

Figures 6 and 7 are graphs made from the averaged data of two sample periods during liquid-feeding, normalized to 60 s. More than 99.9% of the particle count

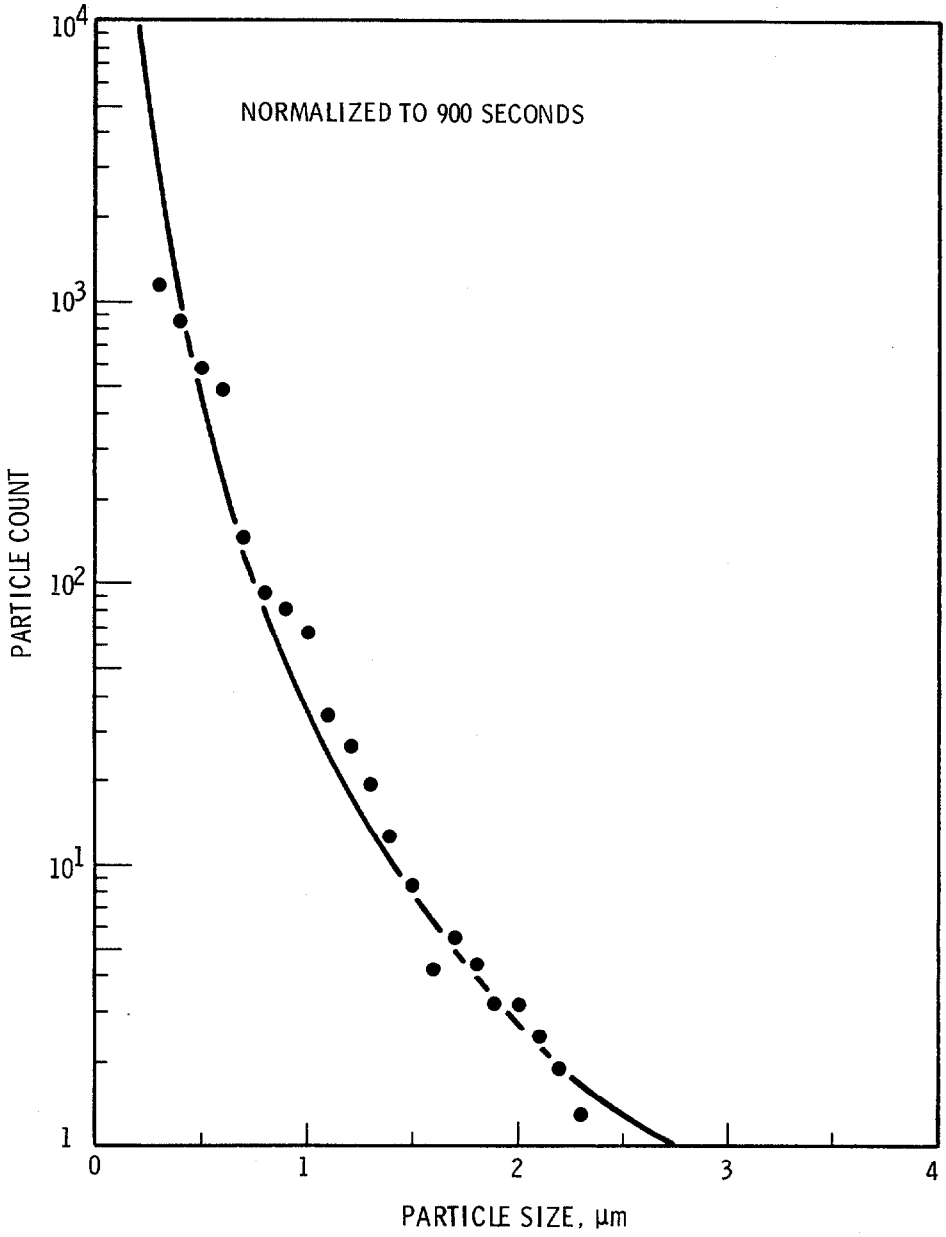

FIGURE 4
PARTICLE COUNT VERSUS PARTICLE SIZE IN AN
IDLING LIQUID-FED CERAMIC MELTER

and mass are less than 0.8 µm in dia. As was the case in idling, the liquid-feeding data shows that the particle count peaks at below the 0.32-µm size range. The maximum mass-loading for liquid-feeding occurs at 0.4 µm and particles up to 3.2 µm in dia were detected.

The particulate loadings in the off-gas line are based on the CSAS particle counts. The particles are assumed to be spherical and to have a particle density of 4.0 g/cm^3. Particle concentrations ranged between 12.8 and 14.1 µg/L gas. Using the average steady-state feed rate of 62 L/h and the average off-gas flow of 8590 L/min, the average steady-state particulate DF was calculated to be 1700. The aerosol spectrometer DF of 1700 is believed to be large because 1) a fraction

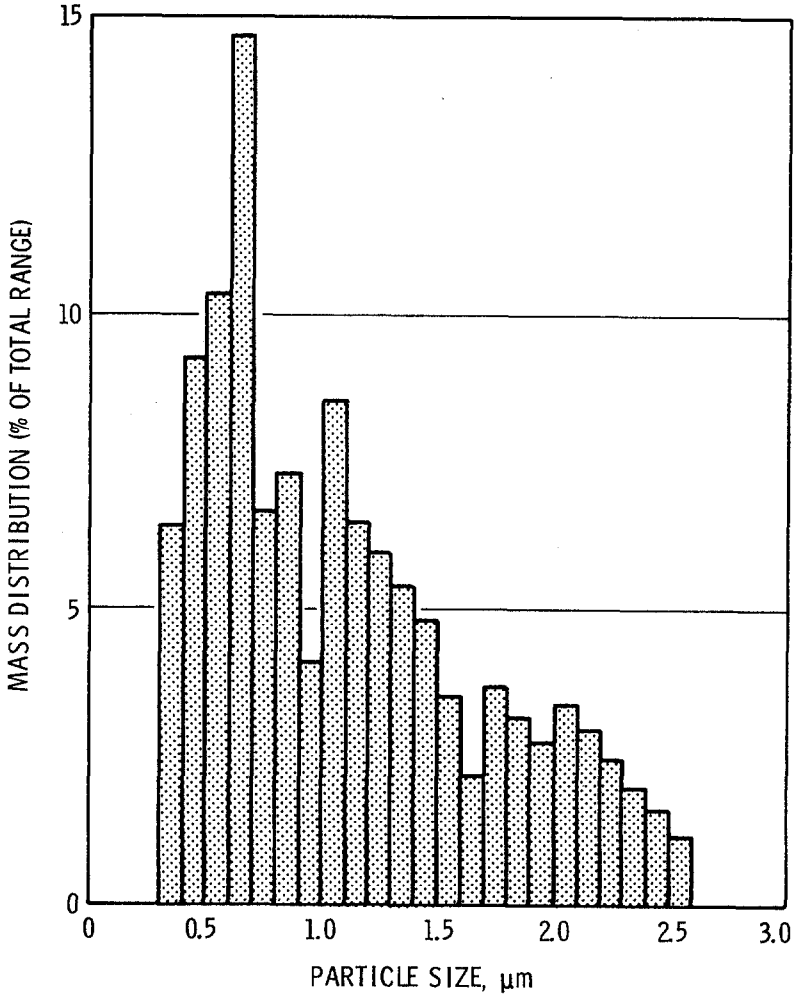

FIGURE 5
MASS VERSUS PARTICLE SIZE IN AN IDLING
LIQUID-FED CERAMIC MELTER

of the particles were smaller than the detection limit of the instrument, and 2) the sampling line to the spectrometer probe was not isothermal. It was insulated, but not heat-traced, and cooling may have caused water condensation in the sample tube. It was thought that water condensation caused deposition of the particles in the sample tube, thus reducing the particle loading seen by the spectrometer probe.

Table VII shows a steady-state liquid-feeding DF comparison from the scrubbing system, the aerosol spectrometer, and previous DFs from HEPA filter weight differences (data supplied by Jim Buelt, Research Scientist, PNL). Elements with oxide boiling points much higher than the glass temperature were chosen to calculate a nonvolatile DF from the data in Table IV. The DF based on those numbers should indicate the actual particle carry-over into the off gas. The average nonvolatile DF obtained from the sampling system was 4500, meaning that 0.02 wt% of the solids are leaving the melter by entrainment. The ratio of all of the elements into the melter and all of the elements collected in sampling system gives a much lower DF (520). This number compares well with the nominal DF of greater than 200 from previous data, but it is less than 1/3 of the DF based on the aerosol spectrometer data (1700). Elements with low DF's such as Li, B, Na, Ru, Sb, Te and Cs are

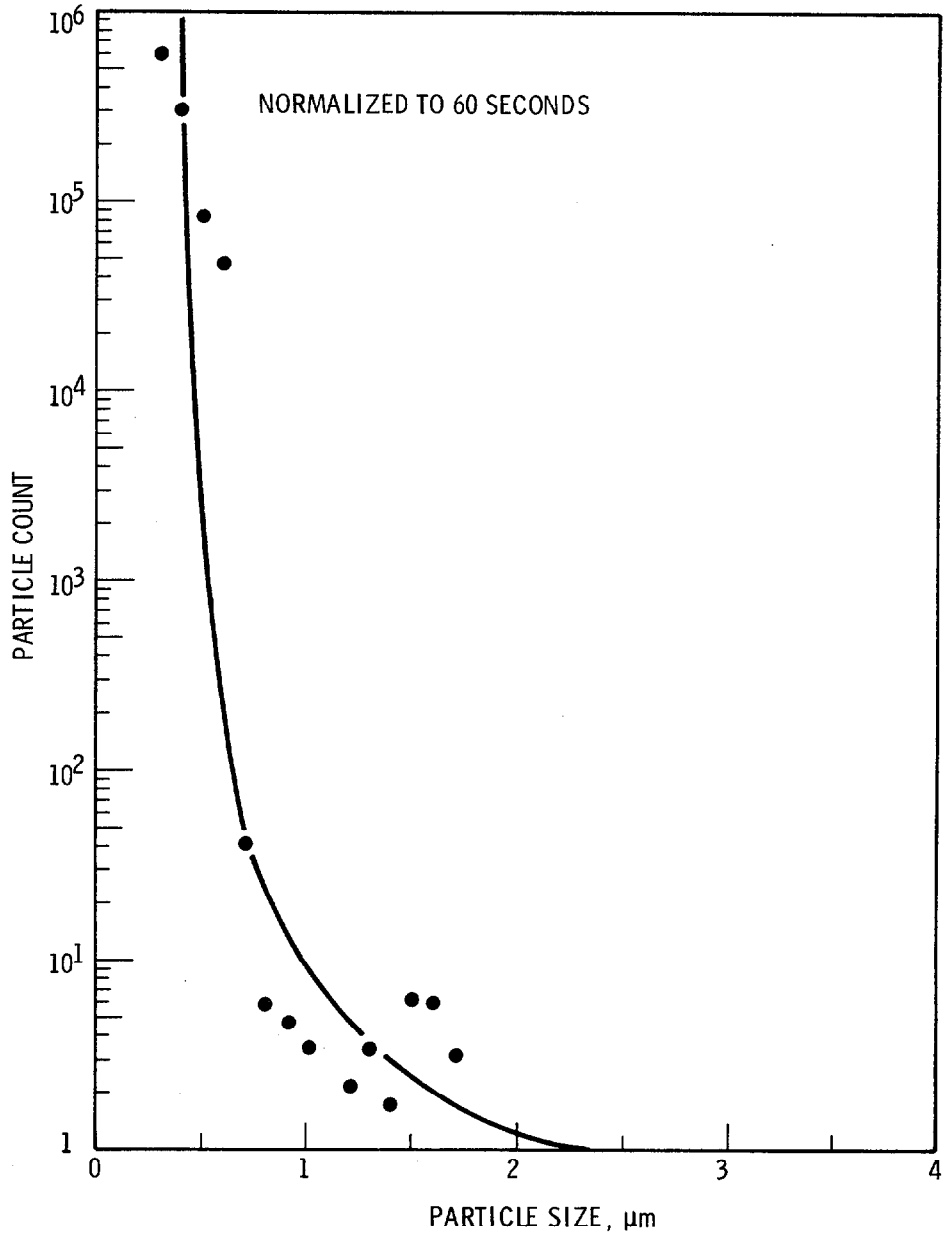

FIGURE 6
PARTICLE COUNT VERSUS PARTICLE SIZE DURING
FEEDING IN THE LIQUID-FED CERAMIC MELTER

leaving the melter by volatilization as well as by particulate entrainment. Previous LFCM loss numbers for power-reactor (acid) wastes have indicated Cs losses between 0.4 and 1.4 wt% (data supplied by Jim Buelt, Research Scientist, PNL), while this work shows higher losses of 0.91 to 24 wt% (and averaging 13 wt%).

Table VIII shows particulate loading in the off gas for idling, for steady-state liquid-feeding and for previous work from spray calcination.[5] The particle diameter ranges are similar for all three cases. The average particulate loadings for idling and spray calcination are roughly the same, while the particulate loading for liquid-feeding without any filtration is only 100 times that of spray calcination with sintered-metal filters. Operation of off-gas cleanup equipment

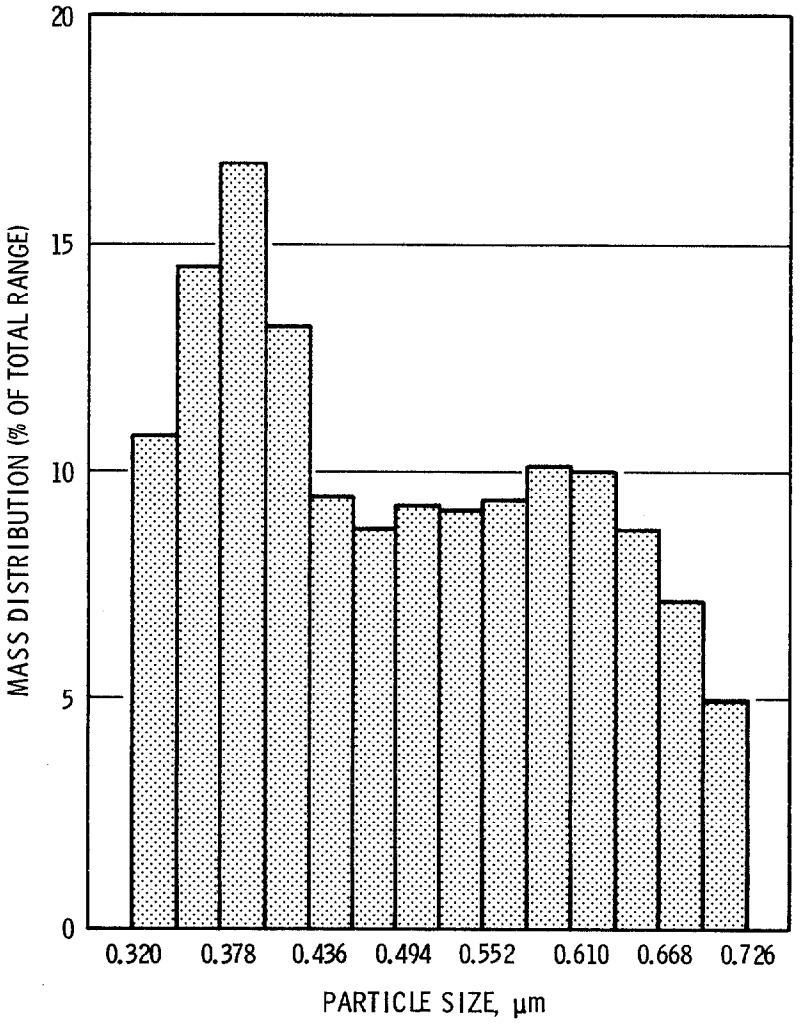

FIGURE 7
MASS VERSUS PARTICLE SIZE DURING FEEDING
IN THE LIQUID-FED CERAMIC MELTER

was the same for liquid-feeding as it was for spray calcination, with no adverse effects in spite of the higher particulate loadings.

The overall DF of 520 indicates that a total of 0.2 wt% of the solids are leaving the melter by volatilization and entrainment. As stated previously, the loss by entrainment alone is 0.02 wt% based on the nonvolatile average DF. The percentage of losses by volatilization based on these numbers is 90%. If one chooses a single nonvolatile element such as Fe or Sr instead of the six-element average (Table VII), the losses by entrainment are 0.05 wt% and the percentage of losses by volatilization is 70%. Thus, one can conclude that between 70% and 90% of the melter losses were by volatilization, with the remaining 10% to 30% being lost by entrainment.

Table VII. Decontamination Factor Comparison During Steady-State Liquid Feeding

Components	From Scrub Analysis*	From CSAS	From Previous Data**
Nonvolatiles†	4500	---	---
Cs	44	---	71 to 250
Overall	520	1700‡	200

* DFs were calculated for each scrub-sample period, then averaged.
** Data supplied by Jim Buelt, Research Scientist, PNL (acid waste-feeding of LFCM).
† Al, Si, Ca, Fe, Ni and Sr are considered nonvolatile.
‡ May be lower if volatiles are not condensed.

Table VIII. Particulate Loadings and Diameter Range in the Off Gas During Idling and Liquid-Feeding

	Idling*	Liquid-Feeding*	Spray Calcination**
Average Particulate Loading (μg/std L)	0.04	13.5	0.08
Maximum Particulate Loading (μg/std L)	0.143	---	---
Particulate Diameter Range (μm)	0.5 to 5.6	<0.3 to 3.2	0.5 to 5

* Based on aerosol spectrometer data.
** From Hanson.[5]

Conclusions

1. The average loss to the off-gas system of radionuclide substitutes during steady-state melter operation was: Ru = 0.16 wt%, Sb = 0.11 wt%, Te = 0.44 wt% and Cs = 13 wt%. It is not understood why Cs losses were high. Previous work with power-reactor wastes indicates Cs losses of between 0.4 and 1.4 wt%.

2. The average particle loadings in the melter off gas during melter idling are roughly the same as those from the sintered-metal filters of a spray calciner. Particulate loadings during liquid-feeding are approximately 100 times those from the sintered-metal filters of a spray calciner. Particle diameter ranges are roughly the same for idling, liquid-feeding and spray calcination.

3. During melter operation, less than 0.02 wt% of waste elements escaped the melter into the off-gas system.

4. Between 70 and 90 wt% of the elements leaving the melter in the off gas are volatilized. The remaining 10 to 30 wt% leave by physical entrainment.

5. Of the major glass elements, chloride and sodium are most prevalent in the off gas, followed by boron, cesium and lithium.

6. Losses of melter off-gas solids are typically highest during steady-state liquid-feeding and lower during startup or foaming states.

7. The melter plenum and off-gas system must be made of corrosion-resistant materials because of the potential chloride, sulfate and nitrate volatility for this process.

8. Oxygen is released from the melt during liquid-feeding and absorbed during idling.

References

1. Buelt, J. L., and C. C. Chapman. 1978. Liquid-Fed Ceramic Melter: A General Description Report. PNL-2735, Pacific Northwest Laboratory, Richland, Washington.

2. Brouns, R. A. et al. 1980. Immobilization of High-Level Defense Wastes in A Slurry-Fed Electric Glass Melter. PNL-3372, Pacific Northwest Laboratory, Richland, Washington.

3. Pye, L. D. 1979. Investigation of Controlling Mechanisms in Simulated Nuclear Waste Glass Melting and Gas Generation. Prepared for U.S. Department of Energy under Subcontract No. B-72814-A-F, New York State College of Ceramics, Alfred University, Alfred, New York.

4. Williams, John A. 1978. Thermal Analysis of Glass Batch and the Effect of Water. Paper presented at the 39th Annual Conference on Glass Problems at Ohio State University, Columbus, Ohio.

5. Hanson, M. S. 1980. Spray Calcination/In-Can Melting: Effluent Characterization and Treatment, PNL-3109, Pacific Northwest Laboratory, Richland, Washington.

DISCUSSION

CHRISTIAN: Did you find any evidence of enrichment of ruthenium or cesium in the particulate matter you collected?

OMA: Yes, there was an enrichment of about 50 times for cesium and 2.5 times for ruthenium compared to what we anticipated in the glass. I think that was shown in my paper.

CHRISTIAN: Were you able to keep the sampler line heated to 1100 degrees as you collected the semi-volatiles?

OMA: The sample line was heated to the same temperature as the plenum temperature. It was heated to about 200°C.

PENBERTHY: You noted that the cesium was more volatile than might have been hoped for. Did you do any studies or do you know of any studies which relate the boric oxide content of the glass matrix to the cesium volatility?

OMA: I am not aware of any. I am aware that boric oxide was the primary reason that we saw boron volatility.

PENBERTHY: There were some studies done by Dr. Lucy Oldfield at General Electric Company in England, in the early 50's. She determined that boric oxide, being an acid molecule, does not go out alone. It takes an alkali with it. That might be one of the reasons why the cesium went out.

OMA: That is very possible.

INCINERATION OF LWR-TYPE WASTE AT MOUND FACILITY

Barbara M. Alexander, Richard S. Grimm, and Jay W. Doty, Jr.
Monsanto Research Corporation
Mound Facility*
Miamisburg, Ohio 45342

Abstract

The Mound Cyclone Incinerator, demonstrated over several years for the combustion of radwaste containing plutonium, is now being developed for volume reduction of radwaste containing mixed beta- and gamma-emitters, from LWR facilities. To this end, a laboratory-scale feasibility study was developed and executed.

Development of the feasibility study was based on known characteristics of LWR waste and on operating data compiled for the Mound Cyclone Incinerator since 1975. Feed spiked with several isotopes found in LWR waste was burned in the laboratory-scale cyclone incinerator, and samples were collected and analyzed. From these data, the applicability of cyclone incineration was demonstrated, and an efficient scrub liquor composition was chosen for the offgas treatment system. A Health Physics survey of the incinerator system after incineration of 220 μCi of beta/gamma activity showed no exposure readings above background level.

Future work planned includes incineration of simulated LWR waste in the full-scale Mound Cyclone Incinerator to begin later this year.

Introduction

Operation of the cyclone incinerator began at Mound Facility in 1975. The incinerator was originally developed to burn low-level plutonium-238-contaminated waste generated at the facility. The cyclone incinerator proved superior to former designs in several ways. It reduced handling of the waste, since waste can be incinerated in-situ in the drum in which it was collected. Also, the cyclone effect within the drum produced more efficient combustion of the waste, due to high turbulence, high temperature, and high excess oxygen.

Burning of plutonium-contaminated waste in the Mound Cyclone Incinerator began in December 1976. Since that time, over nine tons of 2:1-compacted waste have been successfully incinerated. The average volume reduction for this waste was 97.7%, while the average weight reduction was 90.8% (including production of secondary wastes). Waste containing paper, wood, rubber, polyethylene, polypropylene, polystyrene and polyvinyl chloride has been routinely incinerated. The composition of the typical Mound waste fed to the incinerator is given in Table I. Maintenance required by the cyclone incinerator system has been minimal.

The offgas treatment system of the Mound Cyclone Incinerator consists of a deluge tank in which offgas is sprayed with a scrub liquor composed of aqueous NaOH (caustic) solution, followed by a venturi scrubber for removal of fine particles, and HEPA filters for complete particulate removal. This system efficiently neutralizes acid gases produced

*Mound Facility is operated by Monsanto Research Corporation for the U.S. Department of Energy under Contract No. DE-AC04-76-DP00053.

Table I. Composition of typical feed for Mound Cyclone Incinerator.

	wt %
Paper	34
Plastics	
Polyvinylchloride	9
Polyethylene	31
Polypropylene	9
Rubber	14
Cloth	3
	100

during combustion and removes all plutonium activity from the offgas. Because the offgas treatment removes essentially 100% of particles from incinerator offgas, waste containing any radioisotope (such as plutonium-238) which does not volatilize in the combustion environment should be amenable to cyclone incineration, using the present offgas treatment system.

The cyclone incinerator system is now being developed for incineration of dry, combustible waste from nuclear power plants, both BWR's and PWR's. For this purpose, a bed of silver zeolite has been installed in the incinerator offgas system to enchance the iodine removal efficiency of the system.

This paper details the execution and results of the feasibility study just completed on the laboratory-scale Mound Cyclone Incinerator. Data gathered during the feasibility study will form a partial basis for a safety analysis report for the use of the cyclone incinerator in a nuclear reactor facility.

Design Basis

The Mound Cyclone Incinerator feasibility program has been geared primarily toward incineration of dry, combustible waste produced by LWR facilities. In designing the experimental portion of the program, characteristics and generation rates for this type of waste were carefully studied.

Data on solid waste generation by LWR's were gathered from three sources: WASH-1258[1], ERDA-76-43[2], and ORP-TAD-77-2[3]. The category of dry solid waste includes HEPA filters, charcoal, clothing, plastic, paper, wood, metal, rubber and glass in various proportions. Approximately 80% of this dry solid waste is combustible[2]. Although 45% of all solid waste produced by BWR's and PWR's is dry, this waste contains less than 5% of the total activity found in LWR solid waste[3]. The volume of this dry solid waste could therefore be greatly reduced in volume by incineration without producing highly radioactive residues.

The report, ORP-TAD-77-2, which is the most current report referenced, is the only source which lists the radionuclide content of dry and wet solid wastes separately. Data from actual operating reports or radioactive effluent reports of BWR's and PWR's were used in producing the average annual values for the radionuclide content of dry solid waste from LWR's, as listed in Table II and Table III.

Table II. Radioisotopes in dry solid waste from pressurized water reactors.*

Isotope	1975 Curies**	1975 Percent	1976 Curies†	1976 Percent
Co-57	0.6	0.9	-	-
Co-58	24.3	35.2	17.1	16.5
Co-60	21.5	31.2	18.2	17.6
Cs-134	6.1	8.8	15.1	14.6
Cs-137	11.7	17.0	28.9	27.9
Mn-54	3.6	5.2	1.1	1.1
Nb-95	0.1	0.1	0.6	0.6
Nb-97	-	-	0.5	0.5
Sb-125	0.3	0.4	-	-
Other	0.8	1.2	22.0	21.2
Total	69.0	100	103.5	100

*From reference (3).
**Based on study of 812.7 m^3 of waste.
†Based on study of 877.4 m^3 of waste.

The radionuclides found in LWR solid waste are beta- and gamma-emitters. Most of these contaminants are non-volatile, and it was anticipated that these could be removed from incinerator offgas by removing all particulate matter. Iodine is an exception, however, as it may form compounds which are highly volatile, even at room temperature. Because it is difficult to contain, iodine was one of the contaminants chosen for study. To promote chemical absorption of iodine in the deluge tank, several chemical additives to the scrub liquor were tested. A bed of silver zeolite, which is highly efficient in adsorbing volatile iodine compounds, was also added to the incinerator offgas system.

Cobalt and cesium were also studied in the incinerator system, since isotopes of cobalt and cesium are responsible for a great percentage of the total dry solid waste activity from both BWR's and PWR's. (See Tables II and III.)

Table III. Radioisotopes in dry solid waste from boiling water reactors.*

Isotope	1975 Curies**	1975 Percent	1976 Curies†	1976 Percent
Co-58	0.5	1.1	0.36	1.1
Co-60	13.3	28.9	19.6	60.1
Cr-51	1.5	3.3	1.6	4.9
Cs-134	4.0	8.7	0.3	0.9
Cs-137	6.6	14.3	3.0	9.2
Fe-59	-	-	0.01	0.03
I-131	-	-	0.1	0.3
Mn-154	12.1	26.3	4.2	12.9
Nb-95	0.02	0.04	-	-
Zn-65	1.0	2.2	1.09	3.3
Zr-95	0.27	0.6	-	-
Other	6.73	14.6	2.33	7.2
Total	46.0	100	32.6	99.93

*From reference (3).
**Based on study of 507 m^3 of waste.
†Based on study of 1015 m^3 of waste.

Section 50 of the Code of Federal Regulations, Title 10, Chapter 1, gives guidelines for the release of airborne radioactivity from LWR plants. A major thrust of the cyclone incinerator feasibility study has been to ensure that incineration of LWR solid waste does not significantly increase airborne emissions from the LWR plant. Efforts have been made to maximize removal of activity from incinerator offgas, and offgas emissions have been sampled during each run.

Experimental Plan

The experimental plan for the cyclone incinerator feasibility study was designed sequentially to obtain the greatest amount of data from the smallest number of experiments. The schedule of experiments performed is shown in Table IV.

Feed to the laboratory-scale cyclone incinerator system was prepared according to the composition given in Table I. This composition, which is the same as that typically burned in the Mound Cyclone Incinerator, was chosen in the absence of quantitative data on the composition of LWR waste. The chosen composition is believed to be representative of waste originating from LWR facilities, as it contains many of the same materials

Table IV. Laboratory-scale experiments performed in feasilbity study.

Run No.	Date	Spike	Scrub Liquor	Length of Burn (min)
			Screening Experiments	
1	09/07/79	Cs-137	Caustic + 200 g Hypophosphite	64
2	09/11/79	0.1 g KI	Same	39
3	09/14/79	Co-60	Same	40
4	09/20/79	1.0 g KI	Caustic Only	41
5	09/24/79	Cs-137	Same	50
6	09/27/79	Co-60	Same	46
7	09/28/79	Co-60	Caustic + 200 g Hypophosphite + 200 g KI	52
8	10/03/79	1.0 g KI	Same	48
9	10/04/79	Cs-137	Same	49
10	10/05/79	Co-60	Caustic + 200 g KI	57
11	10/08/79	Cs-137	Same	54
12	10/15/79	1.0 g KI	Same	58
13	10/18/79	1.0 g KI	Caustic + 200 g Hypophosphite	59
			Concentration Experiments	
17	11/16/79	1.0 g KI	200 g KI, pH 10.0	54
18	11/26/79	Same	100 g KI, pH 12.0	63
19	11/28/79	Same	300 g KI, pH 12.0	75
20	11/30/79	Same	100 g KI, pH 8.0	58
21	12/03/79	Same	300 g KI, pH 8.0	50
22	12/04/79	Same	200 g KI, pH 10.0	35
23	12/06/79	Same	300 g KI, pH 12.0	55
24	12/07/79	Same	300 g KI, pH 8.0	48
25	12/10/79	Same	100 g KI, pH 12.0	49
26	12/11/79	Same	100 g KI, pH 8.0	52
27	12/12/79	Same	200 g KI, pH 10.0	54
29	01/14/80	Same	300 g KI, pH 8.0	48
			Full Set of Experiments	
30	02/27/80	I-131	300 g KI, pH 10.0	56
31	03/04/80	Cs-137	Same	51
32	03/06/80	Co-60	Same	57
33	03/11/80	Blank	Same	59
34	03/11/80	Cs-137	Same	50
35	03/13/80	Co-60	Same	52
36	03/14/80	I-131	Same	42
37	03/17/80	Blank	Same	36
38	03/18/80	Co-60	Same	48
39	03/20/80	I-131	Same	40
40	03/20/80	Cs-137	Same	45
41	03/21/80	Blank	Same	57
			Verification Experiments	
42	06/12/80	Mixture	300 g KI, pH 10.0	53
43	06/13/80	Same	Same	50
44	06/23/80	Same	Same	55
45	06/24/80	Same	Same	55
46	06/25/80	Same	Same	45

reported in LWR waste. In each experiment, 1500 g of feed was spiked with the isotope(s) of interest and then burned. A typical bag of feed is shown in Figure 1. A jar of ash remaining after incineration is shown in Figure 2.

Four different scrub liquor compositions were tested to identify the best candidate for further study. The four compositions tested were caustic solution containing potassium iodide, sodium hypophosphite, both, or neither. During these experiments, feed was spiked with approximately 10 μCi of cobalt-60, 10 μCi of cesium-137, or 1 g of stable potassium iodide.

After a scrub liquor composition had been chosen, experiments were performed on feed spiked either individually or simultaneously with cesium-137, cobalt-60, and iodine-131. A total of approximately 10 μCi of activity was used in each spike. Results of these experiments further characterized the incinerator system performance during short-term reuse of scrub liquor as well as in the presence of multiple contaminants.

Experimental System

Feasibility study experiments were performed on the laboratory-scale cyclone incinerator system. This system is approximately one-ninth the size of the full-scale cyclone incinerator, and employs a similar offgas system. Figure 3 is an artist's representation of the laboratory system. Note that the silica gel bed pictured was bypassed during the feasibility study.

Hardware

In the laboratory-scale unit, combustion takes place in a modified 6-gal steel drum. Combustion air is introduced through four inlets at the top, near the outer wall of the drum. This helps to cool the drum and imparts a swirling motion to the burning waste. Burning is more efficient due to this turbulence. Combustion air is induced by means of two blowers at the discharge end of the incinerator offgas system, so that the pressure within the incinerator system is maintained below atmospheric pressure throughout, ensuring that activity is always contained.

From the combustion chamber, the offgas goes to a fluidized bed spray scrubber, where it passes through two stages of glass bead packing, washed by a countercurrent spray of caustic. Here the offgas is cooled, acid gases are neutralized, and many of the entrained particles are removed. A stainless steel wire mesh pad in the top of the spray scrubber removes droplets of caustic from the offgas before it enters a glass-fiber prefilter, rated as 90-95% efficient for removal of a 0.3 μm particle. The offgas then passes through an iodine adsorber containing silver zeolite, before leaving the incinerator offgas system through HEPA filters. Scrub liquor is recycled to the spray tower after being filtered and cooled.

During each experiment, the offgas was sampled at four locations, as indicated on the diagram in Figure 4. The four locations were: following the spray scrubber, before and after the silver zeolite bed, and after the final HEPA filter. Samples were obtained by pulling 9 ft^3/hr of offgas through a Millipore filter, bubbling it through a caustic solution, and finally passing it through a small silver zeolite bed. All particulate matter should remain on the filter paper, with only gaseous species appearing in bubbler solutions.

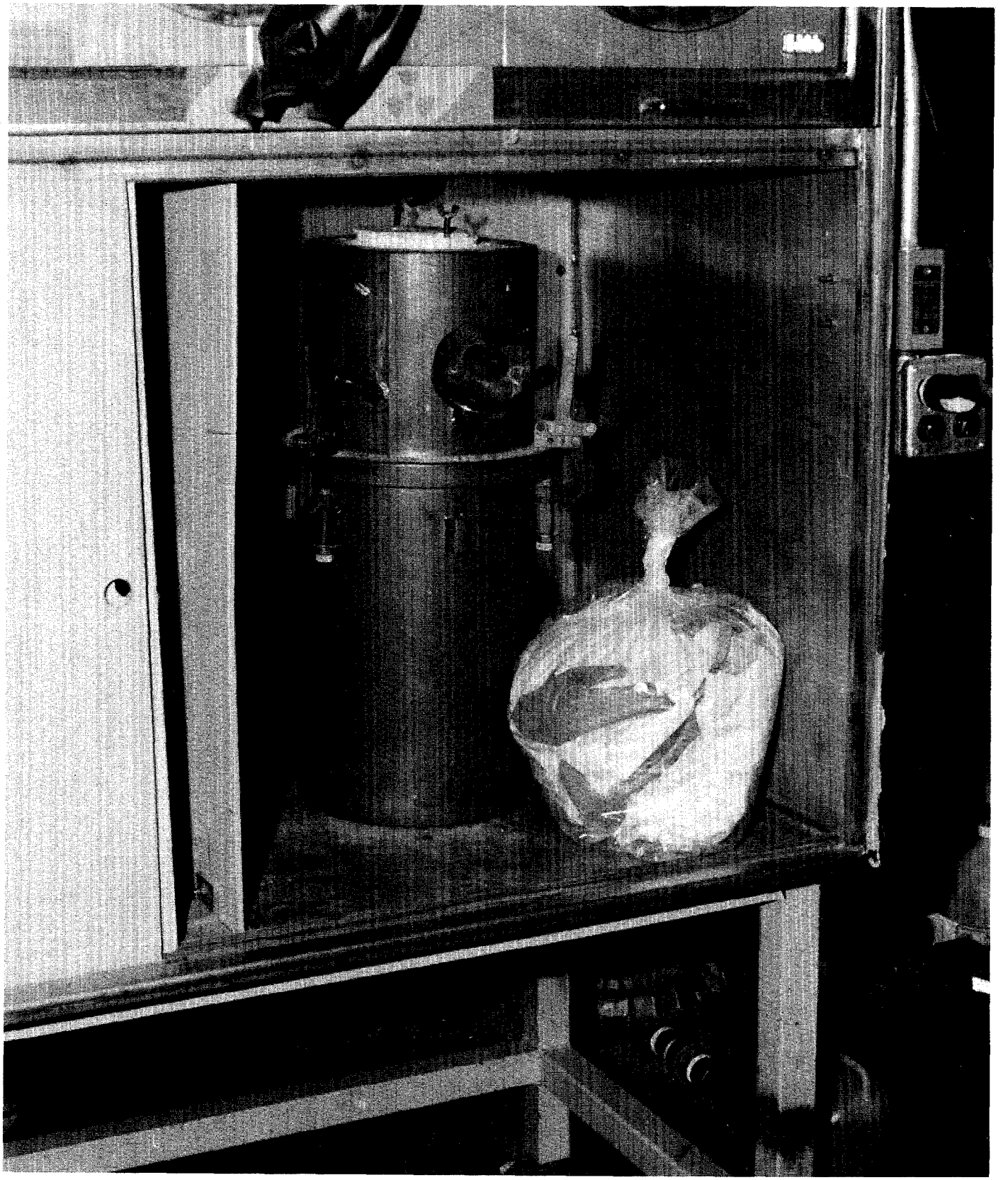

Figure 1 Typical feed charge and laboratory-scale combustion chamber.

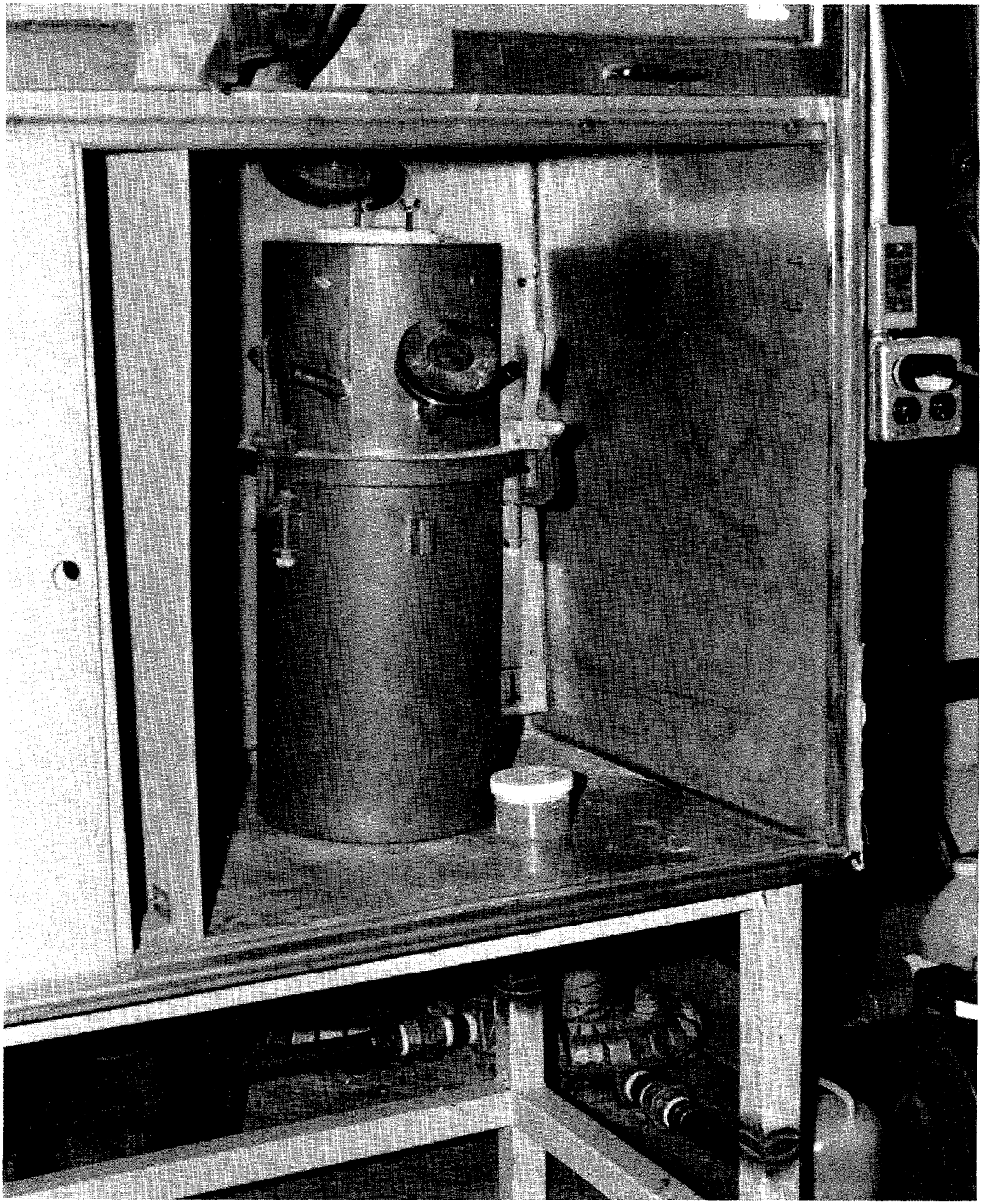

Figure 2 Jar of residual ash and laboratory-scale combustion chamber.

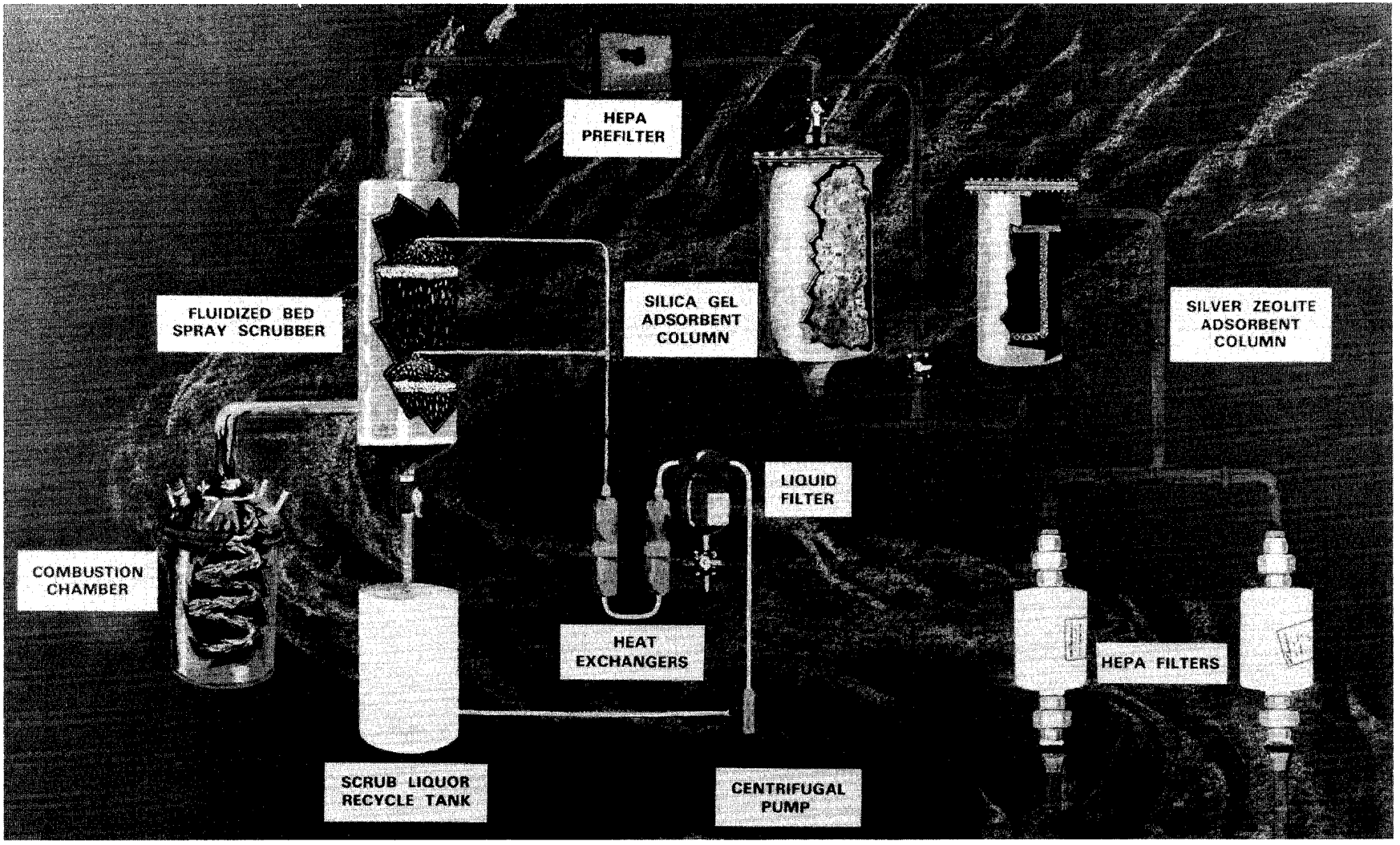

Figure 3 Laboratory-scale cyclone incinerator system for incineration of beta- and gamma-contaminated waste.

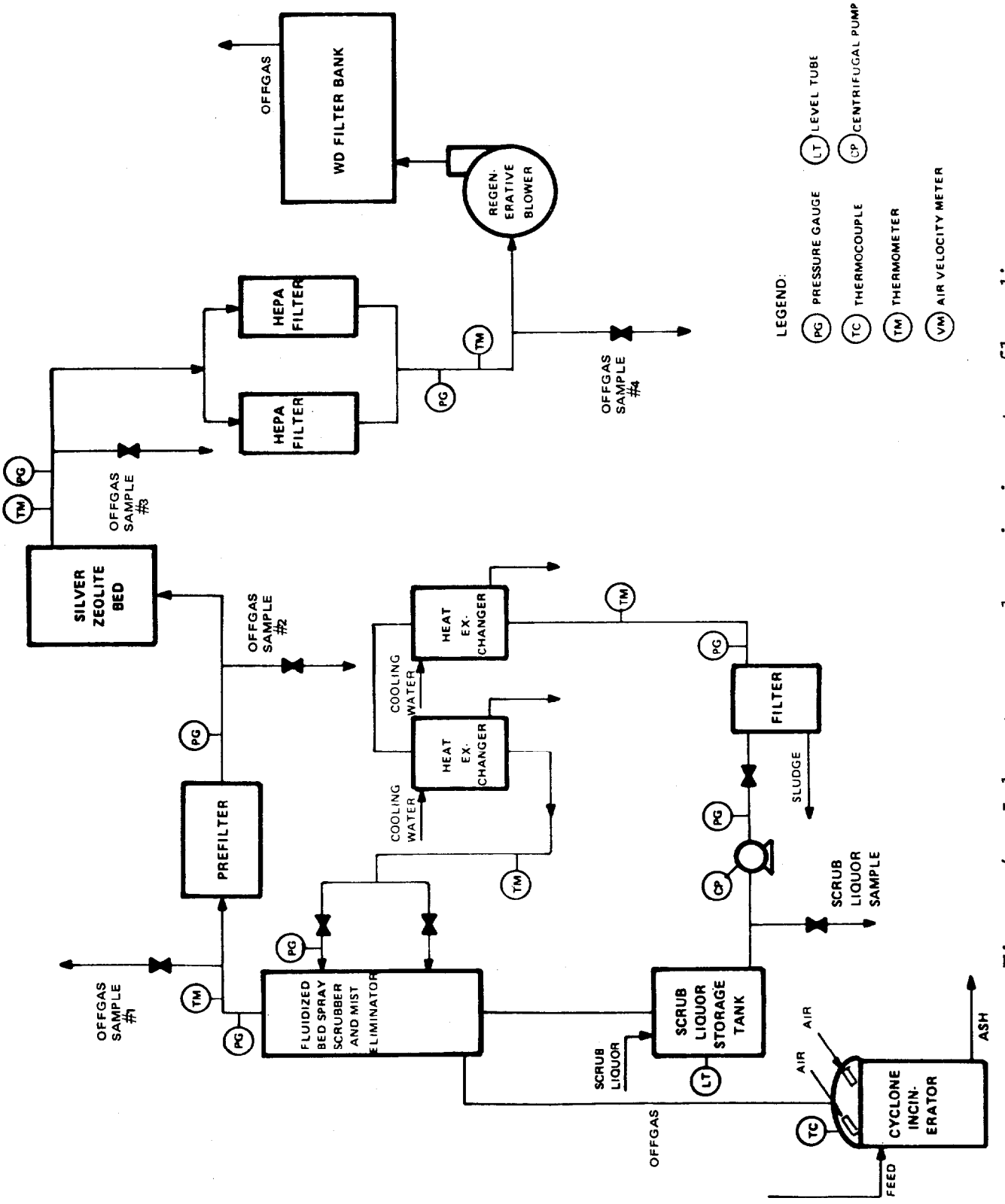

Figure 4 Laboratory cyclone incinerator flow diagram.

Liquid samples were screened for the presence of nonradioactive iodine and chloride by the use of HNU ion specific electrodes, connected to an Orion Model 801A pH meter. Radioactive species were detected by gamma-counting, using the Canberra Scorpio System. The detection system consists of a Ge(Li) detector connected to a multichannel analyzer, which separates gamma-peaks according to their energies. The attached PDP-11 computer uses Scorpio software systems to compare unknown spectra to spectra of known activity. Therefore, peak areas can be converted to activity levels.

Operating Characteristics

Operating characteristics of the laboratory-scale incinerator are shown in Table V. These parameters were obtained from a series of "cold runs" performed prior to the start of the feasibility study.

Table V. Operating parameters for Laboratory Cyclone Incinerator.

Feed (g)	1500.00
Ash (g)	35.5
Sludge (g)	2.0
Particles filtered from offgas (g)	3.9*
Weight reduction	97.2%**
Length of burn (min)	35.0
Offgas flow rate (actual ft^3/min)	35.5
Scrub liquor volume (liters)	20.0
Temperature:	
In Combustion Chamber	950°C
Following spray scrubber	47°C
Following final HEPA filter	29°C

*Figure may be high, due to adsorbed water.
**Based on ash, sludge, and particles.

The iodide-specific electrode used in the study is sensitive to iodide in a concentration range from $5x10^{-8}$ to 1 mole/liter. The chloride-specific electrode operates from $5x10^{-6}$ to 1 mole/liter of chloride. Electrodes were calibrated by graphing readings obtained from standard solutions of known concentration. Unknown concentrations were then determined by comparison with the graph. Accuracy is probably within ±10%.

For use of the Canberra Scorpio System, standard samples of known activity were prepared in four different geometries, corresponding to ash samples, filter paper samples, sludge samples, and liquid samples (which include both bubbler solutions and scrub liquor samples). Quantities of radioisotopes as small as several picocuries (10^{-6} microcuries) could be

detected by this system by counting for 10,000 sec. Samples of higher activity required shorter counting times. Accuracy varied depending on activity level, with high activity samples showing the best accuracy.

Experimental Results

Results of the screening experiments and the concentration experiments were used to select an optimum scrub liquor composition for use in burning beta-gamma waste. Chloride and iodide concentrations in the offgas directly downstream of the spray towers (Bubbler #1) were measured, and are listed in Table VI. Scrub liquor composition in each experiment may be found in Table IV.

Table VI. Chloride and Iodide Content - Bubbler #1.

Run No.	Chloride Content (mole/liter x 10^5)	Iodide Content (mole/liter x 10^6)
1	3.08	0.03
2	3.82	0.57
3	3.02	0.81
4	3.21	2.98
5	3.88	2.02
6	3.76	3.52
7	3.89	1.32
8	4.34	1.06
9	3.49	1.06
10	6.38	0.75
11	4.20	1.11
12	3.59	0.26
13	3.81	1.71
17	3.71	0.25
18	6.55	9.00
19	4.50	1.18
20	10.5	17.5
22	6.60	1.08
23	9.70	0.69
24	3.70	1.70
25	5.90	0.23
26	8.20	5.00
27	3.05	0.08
29	3.40	0.14

Chloride in the offgas is formed by combustion of polyvinyl chloride in the feed material. This chloride is troublesome, both because of its corrosiveness and because it competes with iodine for adsorption onto the silver zeolite downstream of the spray scrubber. Therefore, removal of chloride from the offgas also aids in the removal of iodide.

For optimum removal of both chloride and iodide from incinerator offgas, a scrub liquor containing 300 g of potassium iodide at a pH of 10 was chosen for use in incineration of beta-gamma waste.

With the chosen scrub liquor, the full set of experiments was then performed to determine the effect of repeated reuse on scrub liquor performance. In these twelve experiments, feed was spiked with either cesium-137, cobalt-60, iodine-131 or no radioisotope. Results of gamma-

counting of samples from these experiments are shown, along with all other experiments involving radioactive spikes, in Tables VII, VIII, IX, and X. The data lead to the conclusion that short-term reuse has no adverse effect on scrub liquor performance.

The verification experiments were performed to evaluate the effect of incinerating combinations of contaminants. In each experiment, feed was spiked with a mixture of cesium-137, cobalt-60, and iodine-131. Results in Tables VII, VIII, IX, and X seem to indicate no difference in incinerator system performance when feed is spiked with several isotopes instead of just one.

Table VII. Spikes - feasibility study.

	μCi		
Run No.	Cs-137	Co-60	I-131
1	9.896		
2			0.1 g KI
3		9.44717	
4			1.0 g KI
5	7.760		
6		9.40690	
7		9.40381	
8			1.0 g KI
9	9.2948		
10		9.38221	
11	9.26268		
12			1.0 g KI
13			1.0 g KI
30			5.26408
31	8.61337		
32		15.44713	
33	----------	Blank ----------	
34	9.52398		
35		15.40822	
36			12.24264
37	----------	Blank ----------	
38		13.03537	
39			10.85397
40	8.911282		
41	----------	Blank ----------	
42	2.085176	3.79130	3.70434
43	2.08504	3.46736	3.04560
44	2.08373	3.72724	3.66724
45	2.08359	3.72590	3.65687
46	2.083461	3.72456	3.75739

Table VIII. Ash - feasibility study

Run No.	μCi Cs-137	Co-60	I-131
1	6.37681		
2	0.454900		
3	5.27239E-02	6.78609	
4	0.113301	1.02125	
5	7.06594	0.364837	
6	1.44813E-01	6.65403	
7	5.31231E-02	6.52869	
8	4.95223E-02	1.78614	
9	4.48263	0.820946	
10	0.559472	6.36772	
11	7.74630	1.13737	
12	0.29221	0.497628	
13	0.232682	0.319285	
30			0.0929252
31	6.691912	0.0190804	
32	0.889981	13.177797	<2.45321E-03
33	0.1047759	0.357165	<4.18813E-04
34	8.096747	0.092075	<1.84307E-03
35	0.400555	13.35044	<2.36715E-03
36	0.137836	0.608877	2.20584E-02
37	0.957181	0.234038	1.87512E-03
38	0.081875	10.45480	<1.98821E-03
39	0.0418846	0.710272	1.62536E-02
40	8.05359	0.300060	<1.81655E-03
41	0.0972415	0.0654399	<8.22506E-04
42	2.02574	3.00858	6.13687E-02
43	1.48920	2.80312	5.15181E-02
44	2.18908	3.79032	5.161106E-02
45	1.15894	1.79954	4.30281E-02
46	1.70983	2.73720	6.11650E-02

Table IX. Sludge - feasibility study

Run No.	μCi Cs-137	Co-60	I-131
1	5.65409E-02		
2	5.78861E-02		
3	3.86190E-02	5.75506E-02	
4	2.79219E-02	6.47111E-02	
5	6.88362E-02	4.52751E-02	
6	0.10895	0.20066	
7	0.061917	0.185972	
8	0.060928	0.212715	
9	0.0323128	0.0637224	
10	0.035669	0.139654	
11	0.0247486	0.0257595	
12	0.0385211	0.0621231	
13	0.0280972	0.0262598	
30	1.96708E-03	3.30711E-03	1.0267E-02
31	0.0634983	0.0046962	0.00856900
32	0.0435181	0.0778596	0.00882313
33	0.0135341	0.0422548	0.0034104
34	0.055925	0.0830407	<6.27898E-04
35	0.030172	0.0909192	0.00258345
36	0.0323216	0.1402521	0.01844037
37	0.0427344	0.1846109	0.0270113
38	0.0152172	0.2204837	0.0141582
39	0.0099533	0.1595393	0.0158724
40	0.0493249	0.2138530	0.0333270
41	0.0479168	0.2270011	0.0224973
42	3.23593E-02	9.76182E-02	<6.38771E-04
43	0.125364	0.2900130	0.0119700
44	3.75633E-02	8.34224E-02	2.41446E-03
45	3.08676E-02	7.61605E-02	5.10130E-03
46	3.14112E-02	7.72938E-02	8.685465E-03

Table X. Scrub liquor - feasibility study

Run No.	μCi Cs-137	Co-60	I-131
1	4.969335E-04		
2	4.33334E-04		
3	6.79062E-04	3.53103E-04	
4	3.40829E-04	1.60982E-03	
5	4.29642E-04	3.66082E-04	
6	8.55114E-04	2.01953E-03	
7	<5.10753E-05	6.21439E-04	
8	5.59623E-04	2.7038E-03	
9	3.67464E-04	1.27858E-03	
10	<9.55338E-05	2.47138E-03	
11	2.46575E-04	1.02982E-03	
12	5.50436E-04	3.71139E-03	
13	7.23079E-04	1.21064E-03	
30	<7.54836E-06	<1.35946E-05	1.91577E-02
31	<5.91547E-05	<5.71850E-05	0.0127342
32	3.30042E-04	<6.73931E-05	0.0111390
33	<3.1336E-04	<1.16106E-03	6.82610E-03
34	7.496096E-04	5.32495E-04	5.87461E-03
35	1.056607E-03	5.17962E-04	5.902009E-03
36	<4.66073E-04	<1.29426E-03	0.0208482
37	<4.49822E-04	<1.42916E-03	1.53520E-02
38	1.74011E-03	3.062655E-03	0.0154041
39	<4.84847E-04	3.92074E-03	0.0306998
40	1.597652E-03	2.13453E-03	0.03933885
41	1.63734E-03	<1.24591E-03	2.46098E-02
42	6.60050E-04	1.07885E-03	3.62065E-03
43	8.29388E-04	1.32901E-03	9.09582E-03
44	8.45435E-04	<1.88237E-05	4.62326E-03
45	1.41041E-03	9.55583E-05	1.15494E-02
46	1.081108E-03	<9.0E-05	1.66138E-02

Discussion

The non-volatile nature of cobalt in incinerator feed is evident from its distribution in the incinerator system. The great majority of its activity remained in incinerator ash, as expected. An average of 85.8% of the original cobalt-60 activity was found in the ash, 3.2% in the sludge, and 8.5% in the scrub liquor, leaving only 2.5% in other areas of the incinerator system, e.g., on the offgas filters.

Cesium-137, like cobalt, remained largely with the incinerator ash following combustion. It is also non-volatile under the conditions of cyclone incineration. An average of 82.6% of the initial activity was found in the ash, 1.8% in the sludge, and 4.0% in the scrub liquor; 11.6% was therefore distributed through the rest of the incinerator system. This may indicate that cesium is slightly more volatile than cobalt, or that it forms smaller particles, which are not removed as efficiently in the spray scrubber. Cesium activity was detected in offgas bubbler solutions only three times. If these readings are correct, they would indicate a volatile form of cesium-137. Since there are so few occurrences, however, the readings are believed to be due to counting error, or perhaps the presence of a hole in a filter paper.

Frequently, cesium-137 activity was found on filter paper samples. The maximum amount of cesium activity detected in the final incinerator offgas was 4.82681×10^{-5} μCi of cesium-137. Because of the sampling rate, this would correspond to a total offgas release of 1.1423×10^{-2} μCi, or 7.61563×10^{-3} μCi per kilogram burned. For a reference LWR facility, burning 275,000 ft^3 of combustible waste per year, at an average density of 15 lb/ft^3, the total cesium-137 released would amount to 0.001295 Ci/yr. The maximum amount of cobalt-60 released would probably be comparable.

Iodine-131 was detected on filter paper #1 in three experiments and on filter paper #2 once. On filter papers #3 and #4, the iodine activity was, in all cases, less than the lower detection limit for the detector. Iodine-131 was found in a bubbler solution only once, in bubbler #4. This value is most likely in error.

In the spiked feed, iodine-131 was present in the form of sodium iodide. Its relative disappearance from ash samples, especially as compared with cesium and cobalt in the last five runs, would indicate that the iodine volatilizes almost completely during combustion. The boiling point of sodium iodide is 1304°C, higher than the maximum temperature reached in incinerator offgas (see Table V). Therefore, the iodine probably reacts in the combustion chamber to produce a lower boiling compound, such as I_2(B.P. 184.4°C), HI (B.P. 127°C), or CH_3I (B.P. 42.4°C). CH_3I is not likely to be the species formed, as the species seems to be almost totally condensed following the spray scrubber, where the offgas temperature is approximately 47°C. Because HI is slightly more stable than I_2, and because of the high solubility of iodine-131 in the scrub liquor, HI is the most likely form for iodine-131 in incinerator offgas.

The distribution of iodine-131 in the incinerator samples is 0.9% in the ash, 0.4% in the sludge, and 85.7% in the scrub liquor. The remainder of of the iodine-131 (13%) probably was deposited on filters in the offgas system or decayed away before sample analysis. The iodine adsorption

efficiency of the silver zeolite bed could not be determined for the experiments performed due to the low level of iodine present in incinerator offgas.

It is obvious from the reported data that radionuclides in the incinerator system do carry over from one run to the next. To determine if any "hot spots" existed in the incinerator system, the system was surveyed with a gamma-survey instrument. Particular attention was paid to obvious locations such as the burn chamber, recycle tank, and scrub liquor filter. None of the readings obtained exceeded background levels for the building (0.1-0.2 mrem/hr), even after 100 μCi of cobalt-60, 74 μCi of cesium-137, and 46 μCi of iodine-131 had been incinerated.

Conclusions

Results of the screening experiments and concentration experiments led to the choice of a scrub liquor of pH 10.0 and a KI concentration of 15 g/liter.

Offgas samples taken during the feasibility study show that cesium, cobalt, and iodine are all effectively contained by the cyclone incinerator offgas system. It is anticipated that all other contaminants found in LWR waste would also be contained in a similar fashion.

Exposure to the incinerator operator was not increased above background levels by incineration of 220 μCi of beta/gamma activity. The latter findings confirm the safety and efficiency of cyclone incineration as a volume reduction method for LWR waste. Further studies will be performed to verify these conclusions.

Future Work

For the future, a small number of experiments will be performed, using iodine-131 in the form of I_2 in the spike, to see if the chemical form affects the behavior of iodine in the offgas. Experiments will also be performed in which KI is absent from the scrub liquor, so that the actual effect of the addition of KI can be determined.

In November, burning of spiked waste in the full-scale Mound Cyclone Incinerator will begin. Waste spiked with cobalt-60, cesium-137, and iodine-131 will be burned simultaneously to verify that data obtained from laboratory-scale experiments is valid in full-scale operation.

References

1. Final Environmental Statement Concerning Proposed Rule Making Action: Numerical Guides for Design Objectives and Limiting Conditions for Operation to Meet the Criterion "As Low As Practicable" for Radioactive Material in Light-Water-Cooled Nuclear Power Reactor Effluents, U.S. Atomic Energy Commission, Directorate of Regulatory Standards, 7-73, WASH-1258.
2. Alternatives for Managing Wastes from Reactors and Post-Fission Operations in the LWR Fuel Cycle, U.S. Energy Research and Development Administration, 5-76, ERDA-76-43.
3. An Analysis of Low-Level Solid Radioactive Waste from LWR's through 1975, U.S. Environmental Protection Agency, Office of Radiation Programs, 11-77, ORP-TAD-77-2.
4. Barbara M. Alexander, Feasibility Report: Incineration of LWR-Type Waste in the Mound Cyclone Incinerator, Monsanto Research Corp., (to be published).

DISCUSSION

LOYSEN: Can you give me some idea of the volume of liquid used per unit volume, or weight, of waste incinerated and whether any attempt was made, or will be made, to further reduce the volumes of liquid that will be produced? Lastly, do you have any plans for a pilot plant or larger scale construction of the facility?

ALEXANDER: I assume you are speaking of the scrub liquid when you refer to liquid waste volume. The volume of scrub liquid produced is totally dependent on the percentage of polyvinyl chloride in the feed. As I mentioned before, combustion of polyvinyl chloride produces chloride in the offgas which reacts in the scrub liquid to form salt. The scrub liquid can then be reused until the salt builds up to an unacceptable level, which is about 10%. At that point, it has to be removed and replaced. The typical feed composition we have been using which is 9% polyvinyl chloride, produces so much chloride that the scrub liquid has to be changed after approximately 75 cycles. The batch of scrub liquid is about 100 gallons. So, the volume of waste liquid produced is totally dependent on the amount of polyvinyl chloride in the feed. With respect to your second question concerning the size of the pilot plant, a 55-gallon container is the largest combustion chamber we are planning to evaluate. Although many people have expressed the opinion that it is too small, we found that, with the amounts of waste that are produced, a single cyclone incinerator chamber operated in two shifts could accommodate all the waste from approximately 90% of the LWR facilities in this country. Seventy percent of the LWR facilities could get along with a single cyclone incinerator and operate it on only one shift to handle all of their combustible waste in one year. That includes all the solid waste consisting of rags, plastic, paper and so forth, but does not include resin.

EVONIUK: What is the gas flow rate that you have coming through your scrubber? What are the concentrations of SO_x, NO_x and chloride that would be entering your silver zeolite backup for iodine capture?

ALEXANDER: In the full-scale unit, we operated at about 300 cfm for the offgas rate. The SO_x is dependent on the amount of rubber in the feed. It has always been extremely low. I think 25 ppm was the highest detected and that was reduced to a non-detectible level leaving the scrub tank. In other words, the SO_2 has all been controlled in the scrub liquid. On the other hand, we have measured in the range of 100 ppm for NO_x. The readings are variable around that amount.

EVONIUK: What about the chloride? Is it completely taken out in the scrubber?

ALEXANDER: The chloride level has been measured at 300-600 ppm coming out of the burning chamber. That concentration is reduced to approximately 50 ppm in the effluent from the scrubber.

EVONIUK: Have you seen any chloride being picked up in your silver zeolite?

ALEXANDER: No.

EVONIUK: Have you measured for chloride downstream of the zeolite?

ALEXANDER: In the early experiments, when we were using non-radioactive iodine, we did measure downstream of the zeolite. This was with the laboratory scale unit. By the time it reached that point, the levels were very low to begin with and they were reduced to a very small amount further by passing through the silver zeolite bed.

EVONIUK: The reason I asked is that the chloride at that temperature is probably taken out in the silver zeolite bed and may poison it and make it inactive.

ALEXANDER: That is the reason that we evaluated the chloride removal in our scrub liquid, because we wanted to minimize the amount of chloride that would reach the silver zeolite.

DENNISON: Returning to your comment regarding scintillation vials, I have one question. Did you evaluate them with liquids that were toluene-based versus kerosene-based, which you indicated in your slide? And, were the vials crushed? Also, did they contain the usual isotope of hydrogen?

ALEXANDER: These were non-contaminated scintillation vials that we burned. They were filled with a toluene base scintillation cocktail. They were not crushed. They were fed whole.

CHRISTIAN: Was the gas temperature going into your fluidized bed scrubber 1000°C?

ALEXANDER: No. There was some heat loss by radiation and convection in the offgas line. It was reduced to approximately 700°C before entering the fluidized bed spray scrubber. The place where it entered was below the level of the glass packing, so I am sure that the temperature was reduced even further by contact with the liquid before it reached the glass packing.

CHRISTIAN: How much particulate loading did you have in your gas stream? Was it quite small?

ALEXANDER: I really cannot say. We are intending to do some EPA method sampling of the offgas stream. That is the kind of data we are looking for, e.g., particulate levels, SO_2, NO_x, to get a better fix on what is produced.

CHRISTIAN: This device is new in concept to me. Maybe it is an established concept. My interest in it is whether it might be applicable to an offgas stream similar to what might be exiting from a slagging pyrolysis incinerator, which leaves the secondary combustion chamber around 1400°C, perhaps 1200-1400°C, and has about 7 g/m^3 of particles.

ALEXANDER: I would be pleased to discuss this with you at another time, as time is getting short.

DEITZ: We have studied the ignition of many carbons in a flow of excess air, including non-activated carbons such as cokes, and have found that the addition of small amounts of inorganic salts will lower the temperature of ignition significantly. It would seem to me that your materials could be doped and the ignition started at a significantly lower temperature.

ALEXANDER: I am not sure what the point is. Are you saying that we don't need to operate at this high a temperature to burn the waste?

DEITZ: The ignition to form CO_2 and CO starts at lower temperatures. Once ignited, the heat of combustion will determine the peak temperature.

BROWN: How much can you burn per hour?

ALEXANDER: We burn about 60 pounds per hour and the density is, I think, about 17 lbs. per cubic foot of dry solid waste.

BROWN: If you had a couple of million pounds of waste, this might not be the best way to do it.

ALEXANDER: This is an ideal incinerator for an individual installation.

FREEMAN: A few comments about some of the initial work we did. We chose the incinerator design to incinerate in the drum itself for two reasons: (1) The feed does not have to be treated in any way. With many of the other incinerators you have to chop it and otherwise prepare it, sort it, etc. In fact, it was thought at one time that you might be able to take some of the drums that are underground in Idaho, disinter them, straighten out the drums, put them into an oversize drum, and burn them in situ. (2) At the end of the burn, the ashes can be processed further. The drum can be compacted, and you end up with a safe configuration and a lot of reduced volume. Another question was asked about how big a unit you should have. Instead of working with a bigger burn chamber, we thought of using multiple small burn chambers with a large offgas handling system. You could have two or three 55-gallon drums feeding one offgas handling system.

INCINERATION OF CONTAMINATED ORGANIC SOLVENTS IN A FLUIDIZED-BED CALCINER

R. E. Schindler
Exxon Nuclear Idaho Co., Inc.
Idaho Falls, Idaho

Abstract

The reprocessing of expended reactor fuels at the Idaho Chemical Processing Plant (ICPP) generates contaminated organic solvents. An evaluation of potential management alternatives shows that several are suitable for management of contaminated solvents containing tri-butyl phosphate (TBP):

1) The solvent could be burned in a commercially-available burner which absorbs the phosphorus on a fluidized-bed of limestone leaving a solid product for burial.

2) The solvent could be burned in a small fluidized-bed calciner which solidifies non-radioactive feed by in-bed combustion of the contaminated solvent. The fluidized-bed absorbs the phosphate forming a solid product for burial.

3) The solvents could be solidified with a gel or sorbant for burial if the reprocessing system were modified to reduce the solvent volume.

4) The contaminated solvent could be burned in an existing fluidized-bed calciner designed for solidifying high-level aqueous wastes.

Burning the solvent in the existing calciner was selected for process verification because it provides an existing burner, off-gas system, and solids transfer and storage system. No additional wastes are generated.

A set of four pilot-plant tests verified the absence of adverse effects from the phosphorus in the fuel when calcining simulated ICPP aqueous wastes. Essentially all of the phosphorus remained in the calcined solids with only a neglegible quantity remaining in the scrubbed off-gas. Combustion efficiency was high (93-96%). There were no observable adverse effects on solids in the scrubbing system, corrosion rates, or solids flowability (for retrieval).

Conclusions of general applicability are: 1) alternative technologies are available for disposal of contaminated solvents, and 2) the use of an existing fuel-using facility, e. g., calciner or incinerator--designed for contaminated wastes will usually be cost effective.

I. Introduction

The aqueous reprocessing of expended fuel elements at the Idaho Chemical Processing Plant (ICPP) leaves contaminated organic solvents requiring disposal or management. The solvents from a fuel reprocessing campaign are: 1) about 2 m^3 of extraction solvent consisting of 6% tri-butyl phosphate (TBP) in dodecane (30% TBP may be used in the future) contaminated with transuranics, fission products, and degradation products, and 2) 10 to 30 m^3 of washing solvent consisting of AMSCO (kerosene) contaminated with about 1% TBP and small concentrations of transuranics and fission products. Potential alternatives for disposal or management of the contaminated solvents were evaluated.

The difficulty with burning--the "obvious" first choice for a disposal method--is the formation of a fume when TBP is burned. The phosphorus forms an oxide, P_4O_{10}, which can exist in 3 forms[1] all of which can condense at elevated temperatures (up to about 500°C) forming a solid fume or (wall) deposit. The P_4O_{10} will react with water vapor generated during combustion to form[1] meta phosphoric acid, $(HPO_3)_n$ which condenses at elevated temperatures[1] (depending on n) forming a glassy solid deposit or a fine fume that will plug filters. Hence, a solvent burning system requiring HEPA filters for radionuclide retention must remove the phosphoric acid and/or phosphorus oxide fume from the effluent before it reaches the filters.

II. Alternatives for Management of Contaminated Solvents

An evaluation of potential alternatives for disposal of TBP-containing, contaminated solvents shows several alternatives of tested or potential suitability for ICPP solvents:

A. Fluidized-Bed Burner

A fluidized-bed solvent burner has been developed by Gale[2] and is being patented by Energy Incorporated (EI). The solvent is burned at 800°C in a fluidized bed of limestone with which the phosphorus oxides react. A jet grinder removes reacted calcium and renews the surface of the bed particles. The calcium phosphate and limestone attrited from the bed are collected by a cyclone to form a solid by-product waste. The proposed[2] off-gas system contains a cyclone, a cooler, a sintered-metal filter, and a HEPA filter. A 146-mm diameter prototype with a simplified off-gas system was tested for 130 hr. The fluidized-bed burner basically converts the contaminated solvent to solid waste.

B. Fluidized-Bed Calciner

Aqueous radioactive wastes are solidified routinely[3,4] at the ICPP in a fluidized-bed calciner heated by in-bed combustion (at 500°C) of kerosene. Effluent clean-up technology is well established[5]. The concept could be reversed, with contaminated solvents burned while calcining a non-radioactive feed. Pilot-plant tests described later verified the retention of the phosphorus (from the TBP) in the solids. A calciner for burning contaminated solvent would be similar to a fluidized-bed burner in use of a fluidized bed, having roughly the same space requirement and likewise converting the liquid waste to a solid waste. Differences are formation of fresh bed surface by calcining feed rather than jet grinding and addition of fresh limestone, and different operating temperatures.

C. Oil Burner with Off-Gas System

The addition of a filtration system on the off-gas duct from an ordinary oil burner is an apparent choice for solvent burning. However, development is needed on the off-gas system because of high concentrations of solids in the burner effluent. Effluent samples (cascade impactor) taken from an existing oil burner burning 20 L/hr of solvent containing 1 to 3% TBP contained about 1 g/m^3 of total solids of which 30 mg/m^3 were submicron. The 1- to 30+-micron-diameter particles were essentially all (carbonaceous) soot, but the submicron particles were mostly a phosphorus compound. A more efficient burner would undoubtably reduce the soot concentration but not the concentration of phosphoric acid (or oxide) fume. Hence, a filtration system with a HEPA filter for radionuclide retention would need a pre-filtration system with a collection efficiency of at least 90% for submicron particles (99+% if 30% TBP is burned) to prevent excessive clogging of the HEPA filters. In addition, deposition on surfaces would be

troublesome.

D. Solidification

A moderate volume of contaminated solvent could be solidified with a gel or sorbant and stored as a solid waste. A (feasible) process modification to eliminate the washing column would reduce the ICPP waste solvent volume to the 2 m^3/yr of extraction solvent which would solidify to 20 to 30 drums of solidified solvent. The solidified solvent could then be stored at an on-site solid-waste storage facility. Required would be: 1) the process modification to reduce the solvent volume, 2) some development on the solidification procedure, and 3) facilities in which to solidify the solvent. General application of this option would depend on access to a solid waste storage facility at which the solidified solvent could be accepted.

E. Existing Calciner

The multiple use of an existing facility will often be cost effective. The ICPP has two existing fluidized-bed calciners designed to solidify aqueous HLW--the (soon to be shut down) Waste Calcining Facility (WCF) and the almost-complete New Waste Calcining Facility (NWCF). Figure 1 shows the flowsheet for the NWCF. In bed combustion of kerosene provides the process heat for fluidized-bed calcination of the aqueous wastes; the resulting solids are transported pneumatically to storage bins. If the contaminated solvent could be burned as part of the fuel in the NWCF, the NWCF would supply the burner (calciner), off-gas system, and solids storage systems. The required facility modification would be an upgrade of the fuel supply system to one (of four) fuel nozzle to allow the use of contaminated fuel.

The burning of the contaminated solvents in the NWCF is the alternative selected for process verification because:

1) No by-product waste streams are generated. Instead, two waste streams are combined for processing in one facility with the resulting solids stored in one existing storage facility.

2) Cost effective use is made of existing facilities designed for solidifying radioactive wastes.

III. Test Program

Four pilot-plant tests were conducted to verify that the phosphate in the fuel had no adverse effect on calciner operation. the composition of the simulated plant wastes used in 3 of the tests are tabulated in Table I. Solid calcium nitrate is added to the feed before calcining to react with the fluoride during solidification. The Ca:F mole ratio is 0.55 for straight HLW and 0.7 for a blend of HLW and ILW.

The pilot-plant tests were conducted in two different pilot-plant calciners. The 30-cm calciner has a 30-cm square fluidized bed with one fuel nozzle and one feed nozzle. It normally burns about 6 L/hr of fuel. The off-gas system, shown in Figure 2, contains a cyclone for fines collection and a recirculating scrubbing system with a quench (cooling) tower and a venturi scrubber. The 15-cm calciner has a 15-cm fluidized-bed in which about 2 L/hr of fuel is burned solidifying about 7 L/hr of feed. The off-gas system contains a cyclone and an abbreviated scrubbing system that cools and scrubs with a venturi scrubber.

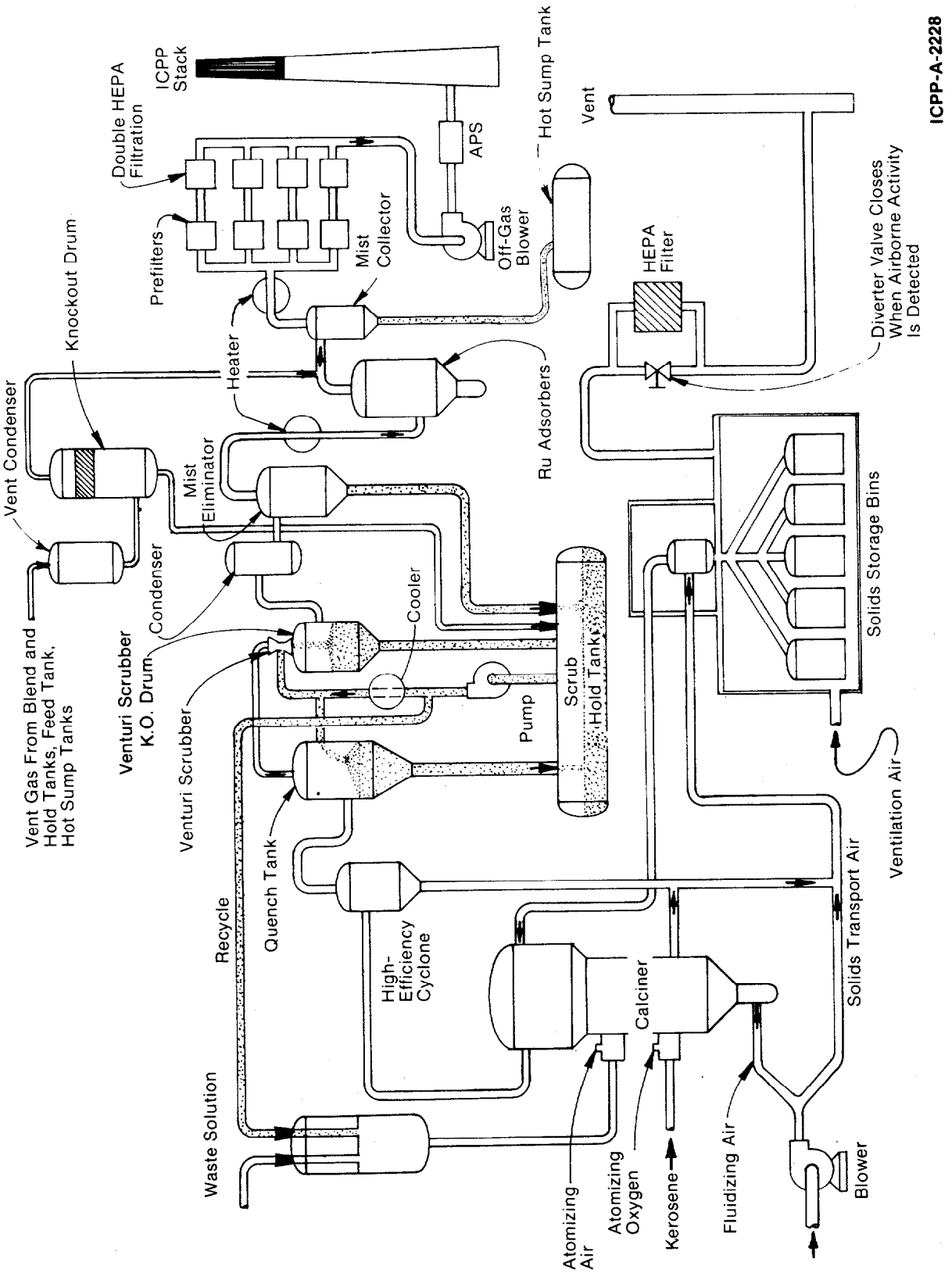

Figure 1: NWCF Flowsheet

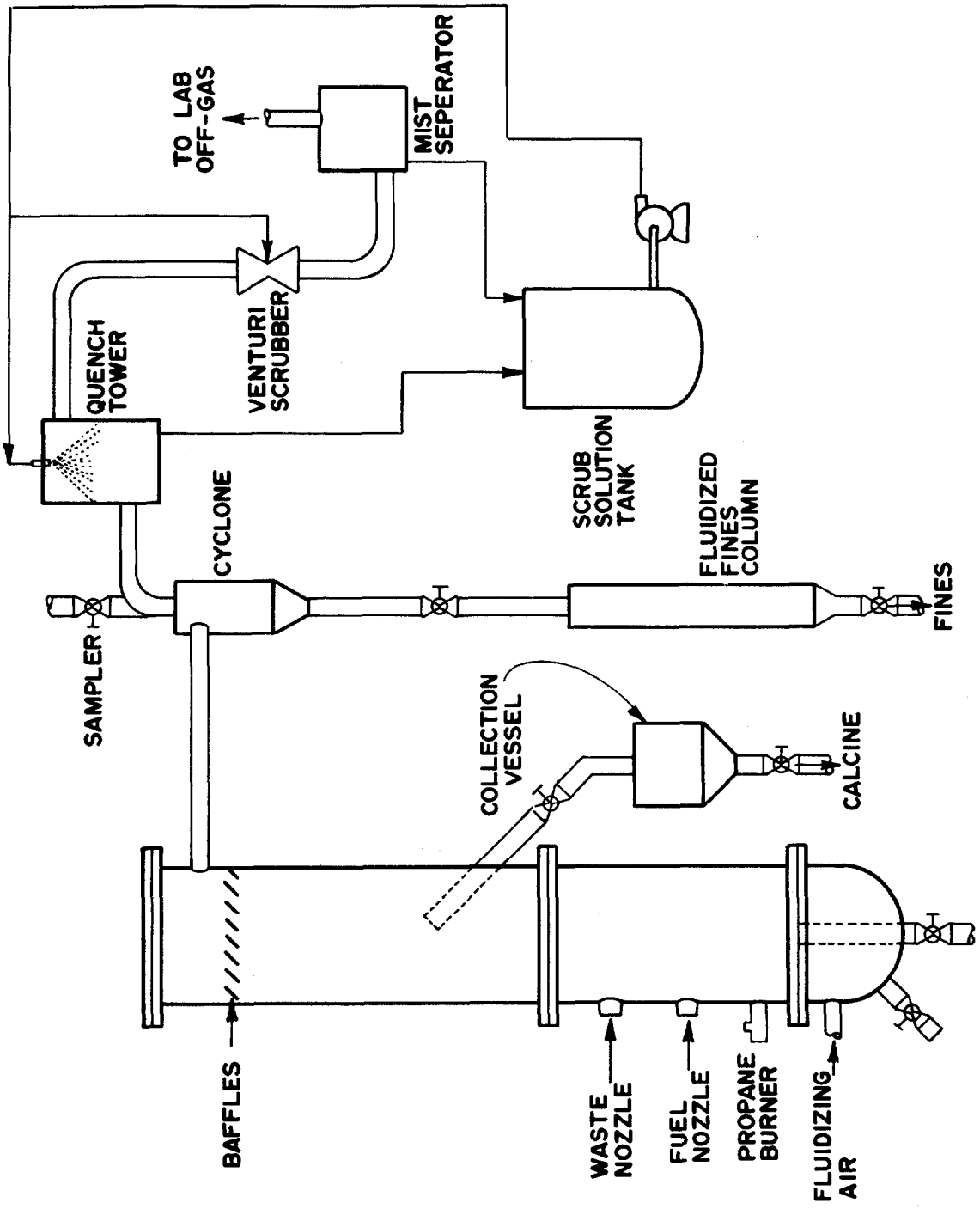

Figure 2: Pilot-Plant 30-cm Calciner

The four pilot-plant tests are described below:

Table I

Composition of Simulated Wastes

Component	Composition (M)		
	Normal HLW	Dilute HLW	ILW
Al	0.66	0.45	0.52
B	0.2	0.12	0.011
Cr	-	0.012	--
Cl	-	0.01	0.057
F	3.25	1.64	0.027
Fe	-	0.01	0.057
H^+	1.28	1.6	1.64
Hg	0.002	-	0.01
K	-	0.006	0.21
Mg	-	0.008	-
Mn	-	0.0008	0.016
Na	-	0.08	1.30
Ni	-	0.002	0.004
NO_3	2.2	1.29	5.15
Pb	-	-	0.003
PO_4	-	-	0.02
SO_4	-	0.05	0.06
Zr	0.37	0.23	0.05

1. Blended Waste in the 30-cm Calciner

The 30-cm calciner calcined a 7:1 blend of dilute HLW and ILW for 100 hr. The test demonstrated: 1) efficient combustion with 5% TBP in AMSCO, 1% TBP in AMSCO, and 5% TBP in tetradecane, 2) absorption of the phosphate in the fluidized bed, and 3) the absence of phosphoric acid fume in the scrubbed off-gas. There was a tendency of the solids to cake that was determined later to be a result of the feed properties rather than the phosphate.

2. Normal HLW in the 30-cm Calciner

The 30-cm calciner calcined normal HLW (with simulated fission products added) at a higher-than-normal feed rate to produce solids for other development programs. The fuel was 5% TBP in kerosene. Samples of the solids were used to verify the absence of adverse effects of the phosphate on the flowability of the calcine.

3. Blended Waste in the 15-cm Calciner

The 15-cm calciner was operated for 96 hr with a 7:1 blend of "normal" HLW and ILW to generate solids for solids flowability evaluation. The calciner operated for 40 hr burning normal kerosene to generate baseline (phosphate-free) calcine samples, then for 56 hr burning 5% TBP in kerosene to generate a phosphate-containing calcine from the same feed. The absence of an adverse effect of the phosphate on the retrievability of blended-waste calcine (7:1) was verified by comparison of the solids flowability of the calcine samples.

4. J. A. Weilang and W. A. Freeby, The Fifth Processing Campaign in the Waste Calcining Facility, FY-1972, ICP-1021, 1973.

5. R. E. Schindler, Removal of Particulate Solids from the Off-Gas of the WCF and NWCF, ICP-1157, 1978.

OFFGAS TREATMENT FOR RADIOACTIVE WASTE INCINERATORS*

L. A. Stretz and R. A. Koenig
Los Alamos Scientific Laboratory
Los Alamos, New Mexico 87545

Abstract

Incineration of radioactive materials for resource recovery or waste volume reduction is recognized as an effective waste treatment method that will increase in usage and importance throughout the nuclear industry. The offgas cleanup subsystem of an incineration process is essential to ensure radionuclide containment and protection of the environment. Several incineration processes and associated offgas cleanup systems are discussed along with potential application of commercial pollution control components to radioactive service. Problems common to radioactive waste incinerator offgas service are identified and areas of needed research and development effort are noted.

Introduction

During the past several years a great deal of time, money, and effort have been expended to develop and demonstrate processes for the volume reduction of radioactive waste. Incineration of the combustible fraction of the transuranic (TRU) and low level (LLW) waste streams is recognized as an effective method for the reduction of waste volume and in some cases, resource recovery. The offgas cleanup subsystem of an incineration process is essential to ensure radionuclide containment, protection of the environment, and public health and safety.

As each of several incineration systems have been developed, different offgas cleaning subsystems have been utilized. The demands placed on the offgas cleaning equipment are a function of incinerator type, waste material, and radioactive content of the waste. These demands can be site specific but frequently are common to all incinerators in radioactive service. The purpose of this paper is to summarize the results of a study of radioactive waste incinerator offgas systems which was designed to identify generic requirements and problems, evaluate system operating experience, consider commercial offgas cleaning technology with potential applications in radioactive service, identify needed research and development efforts, and recommend R&D paths to be followed.

*The Los Alamos Scientific Laboratory requests that this work be identified as performed under the auspices of the US Department of Energy, Contract W-7405 ENG-36.

Incineration Systems

Early attempts to incinerate radioactive wastes met with operational and equipment problems such as feed preparation, corrosion, inadequate offgas cleanup, incomplete combustion, and inadequate isotope containment.[1,2] The US Department of Energy (DOE) continues to sponsor research, development, and demonstration of radioactive waste incineration. In addition, several industries are developing proprietary incineration system designs to meet specific radwaste processing requirements.

Incineration processes can generally be divided into categories by combustion process which include pyrolysis (starved air), excess air, slagging (high temperature excess air), fluidized bed, and combination systems. All of these processes have received attention in the past few years of radioactive waste treatment development efforts.

Major development efforts in the United States are listed in Table 1. Detailed reviews of radioactive waste incinerator technology are available.[3,4]

Waste Materials

The majority of radioactive waste incinerator development efforts have been directed toward treatment of TRU waste from defense related operations. Current work is being done to demonstrate applicability of this technology to waste from commercial nuclear power operations including power plant trash, contaminated liquids, and spent ion-exchange resins. At least two systems utilizing fluidized bed combustion are being offered on the commercial market to incinerate nuclear power plant wastes. A joint program involving Helix, Inc., the US Department of Energy, and Los Alamos Scientific Laboratory is underway to modify the Los Alamos Controlled Air Incinerator (CAI), which was developed and demonstrated for TRU wastes, for use with power plant wastes and spent ion-exchange resins.

Waste types for which various incineration processes have been developed and tested are also indicated in Table I. The composition of waste streams vary from site to site but are generally made up of a mixture of materials. Typical materials include cellulosics such as paper, cardboard boxes, chemical wipes, tissue paper, rags, used protective clothing, and wood chips; plastics such as polyethylene bags, PVC shoe covers, and miscellaneous plastic film; rubber materials such as latex gloves, neoprene pads and gaskets, hypalon gloves, and other rubber protective apparel; and miscellaneous trash such as floor sweepings. Spent ion-exchange resins are another high volume waste for potential incineration in some facilities along with small quantities of cleaning solvents and miscellaneous liquids.

Generic Offgas Requirements

There are several requirements placed on incinerator offgas systems which are common to most installations. The cleanup

requirements include containment of radioactive material, removal of particulates, removal of acid gases, and removal of volatilized heavy metals and inorganic salts. Health and safety considerations result in a preference for components of high reliability and maintainability with designs which do not allow buildup of contaminants resulting in high radiation fields.

Offgas Systems Tested

Several offgas systems have been utilized throughout the development phase of radioactive waste incineration technology. These systems can be divided into two general categories, aqueous sytems and dry systems, although certain types of components are common in both systems. For purposes of this discussion, any system which saturates the offgas stream with water vapor is considered to be an aqueous system.

Aqueous Systems

As indicated in Table I, most of the radioactive waste incinerator systems developed in the United States have utilized aqueous offgas cleaning systems. Many of these systems are similar in design and are discussed as a group rather than individual systems.

The general aqueous system design consists of quench, particle scrubber, absorber, offgas conditioning, and final filtration components. Some systems combine two or more of the steps in single units, these typically being the quench and scrubber or the scrubber and absorber steps. The Los Alamos CAI offgas system shown in Figure 1 represents one system in which the above steps are accomplished in separate units. High energy aqueous systems have performed well, with some individual systems experiencing erosion or corrosion problems related to design. Low energy systems have been less effective in particulate removal. The main disadvantage of aqueous systems is the generation of a secondary waste stream consisting of spent scrub solution.

There has not been a great deal of experience with incinerator offgas cleaning with LLW feed and resulting fission product loading. Tests done at the Mound facility with iodine indicated that about 90% of the material was removed from the offgas in the scrub system with the remainder trapped in a silver zeolite bed which was added to the system for the testing.

A major benefit of the aqueous cleanup system is the high particulate removal efficiency for a wide range of particle sizes resulting in long potential life of the final high efficiency particulate air (HEPA) filters. Also, with proper design of equipment, volatilized materials can be condensed into the liquid scrub solution rather than plating out on component surfaces. Aqueous systems can be designed with flexibility to handle a wide range of offgas flows, compositions, and particulate loadings.

Table I. Incinerators and Wastes

Facility/Company	Type of Process	Design Waste	Waste Tested	Offgas System
LASL/DOE	Controlled Air	TRU	TRU/LLW	Aqueous
SRL/DOE	Controlled Air	TRU	Simulated	Aqueous
SRL/DOE	Controlled Air	LLW	Simulated	Dry
Mound/DOE	Cyclone	TRU	TRU/ Simulated LLW	Aqueous
Rocky Flats/DOE	Fluidized Bed	TRU	Suspect TRU	Dry
Rocky Flats/DOE*	Single Hearth	Suspect TRU	--	Aqueous
Rocky Flats/DOE*	Rotary Kiln	TRU	--	Aqueous
Penberthy Electromelt**	Glass Melter	LLW	--	--
Westinghouse*	Controlled Air	Uranium	Uranium	Aqueous
Aerojet Energy Conversion**	Fluidized Bed	LLW	Simulated/ tracer	Aqueous
Newport News Industrial Corp.** (Energy Inc.)	Fluidized Bed	LLW	Simulated	Aqueous
Ontario Hydro*	Batch Pyrolysis	LLW	LLW	Dry

*Production units
**Offered Commercially

Dry Systems

Dry offgas systems have been used or proposed on several radioactive waste incinerators, some of which are identified in Table I. Typical dry offgas systems, such as the one shown in Figure 2, consist of particulate removal, acid gas neutralization, gas cooling, and final filtration.

Particulate removal is accomplished by one or more components such as dry cyclones, sintered metal or ceramic filters, or baghouse (fabric) filters. Design of the components depend upon the type of incinerator in use and the specific waste stream.

Acid gas neutralization is accomplished by one of several methods. Some incineration designs, such as fluidized bed, utilize in situ neutralization by reaction with sodium carbonate or similar

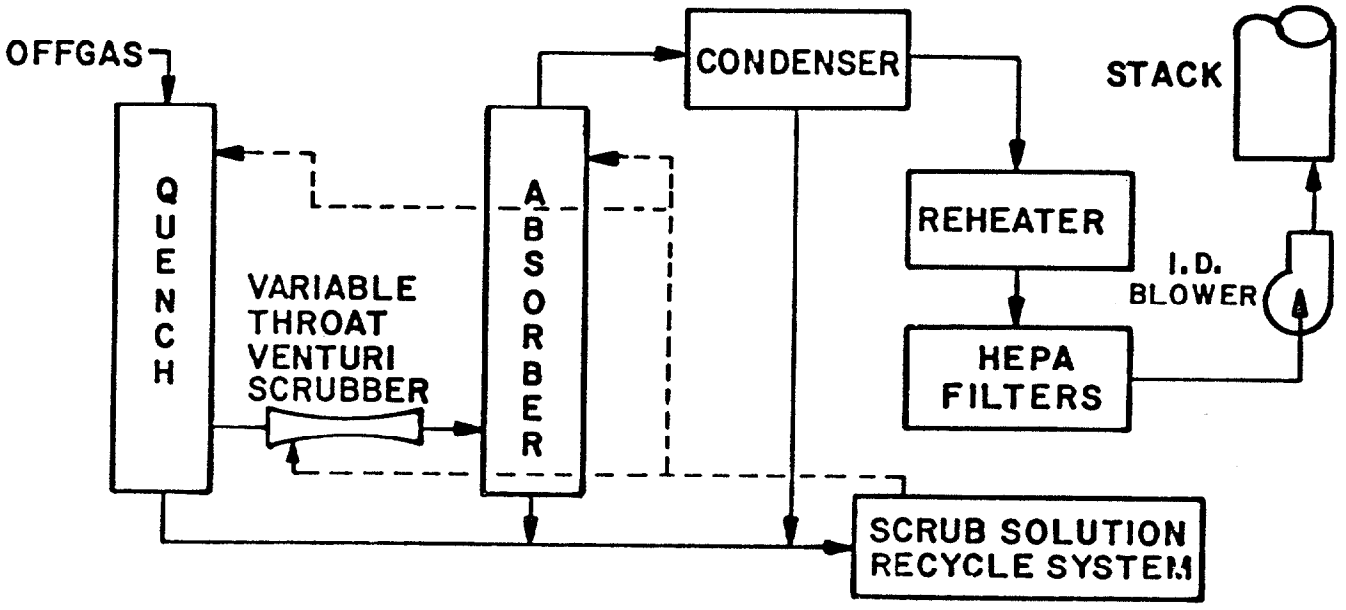

Figure 1. Typical Aqueous Offgas System.

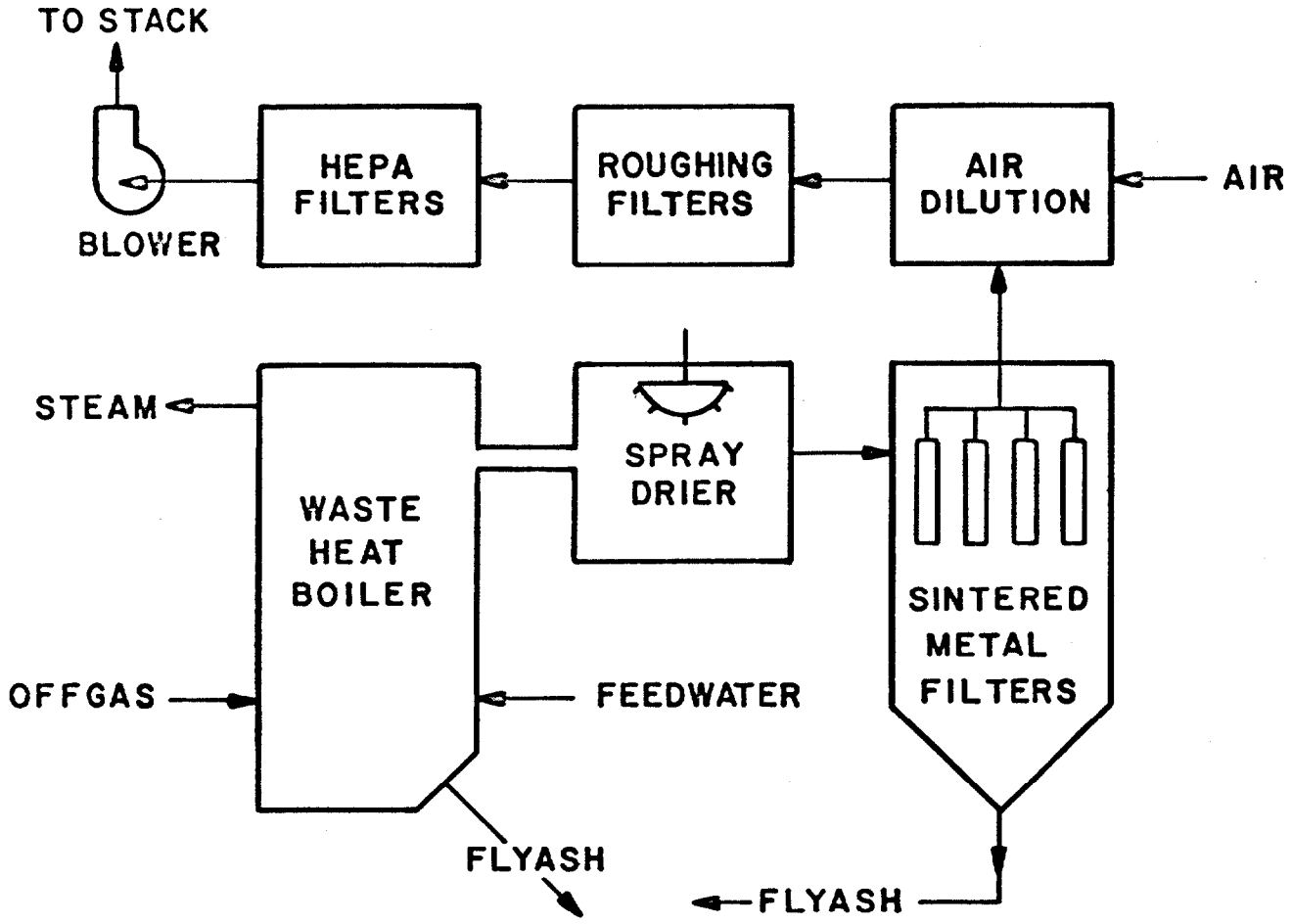

Figure 2. Typical Dry Offgas System.

bed material. Other typical methods involve spray drying to both cool and neutralize by using an alkaline spray solution or by precoating filter elements with sodium carbonate or similar material to neutralize the gases.

Gas cooling is accomplished by spray drying, cool air dilution, or heat recovery techniques. The gas cooling step is critical to overall system performance and must be designed with careful consideration of potential problems.

Dry systems offer the advantage of eliminating the secondary aqueous waste stream but generally produce a secondary solid waste consisting of salts from acid gas removal and unreacted neutralizing agents. This secondary waste can frequently be combined with the incinerator ash for disposal.

Some problems have been reported with dry offgas systems in radioactive waste incineration systems. Problems encountered include condensation of volatile metal compounds and inorganic salts on heat exchange and other surfaces resulting in tube plugging, lost heat exchange capacity, and high corrosion rates; plugging of high temperature filters due to high face velocities and/or condensation of volatile components in the filter elements; fires in high temperature filter housings resulting from carryover of uncombusted material from the incinerator; and rapid blinding of the HEPA filters resulting from the condensation of volatile species downstream of the primary filters. The majority of the problems identified with dry systems are related to the system design rather than any fault in the dry system concept.

Commercial Equipment

The majority of the offgas systems installed utilize commercial components with modifications as required for radioactive service. Commercial scrubbers and filters are available from numerous sources. The main thrust of the commercial scrubber and filter industry is to allow customers to meet legal emission limits as economically as possible. In the specialized area of radioactive waste incinerator offgas cleaning, requirements may be more severe due to the potential release of radioactive material in the particulate. For this reason most systems employ HEPA filters as a final cleanup step.

Long HEPA life is desirable to lessen secondary waste (spent filters), operating complexity (changing contaminated filters), and personnel exposure. This can best be ensured by employing components with high efficiency for a wide range of particle sizes. Generally, the most efficient particulate removal in aqueous systems is achieved with fibrous bed scrubbers, high-energy spray towers, and high energy venturi scrubbers. In dry systems, particulate removal capabilities at the level required for radioactive service is attainable with sintered metal or ceramic filters and fabric filter systems.

Most commercial equipment will require extensive modification prior to use in radioactive service. The type and extent of

required changes are related to the type of waste material being burned. Provisions must be made to assure removal of material from sumps and housings to prevent formation of high radiation fields. In components where routine maintenance is required, such as bag replacement in fabric filters, modifications to allow the procedure to be done remotely or to protect personnel from exposure are essential. Consideration must be made for nonroutine procedures as well. Such operations as replacing sintered metal filter elements, replacing absorber tower packing, and valve and pump repair, among many others are procedures which require special consideration in radioactive service.

Needed R&D Efforts

Additional research, development, and demonstration efforts appear to be needed in several areas. These include recycle and disposal of aqueous scrubber blowdown solutions, improved reliability and maintainability in fabric filter systems, and investigation of fission product behavior in incineration offgas systems. Methods for sampling, monitoring, and evaluating decontamination factors for incinerator offgas systems also need to be improved.

Summary

This paper presents a brief summary of the areas and concerns addressed in the Radioactive Waste Incinerator Offgas Systems Study. The areas of generic offgas requirements, operating problems, commercial equipment application, and R&D needs have been addressed in detail in the final report of the study.[5] Both aqueous and dry offgas systems have been developed and utilized in radioactive waste incinerator offgas cleaning, each with its own advantages and disadvantages. Additional development and testing is in order with both aqueous and dry systems, particularly in application to LLW incineration. Major problems experienced in current systems can be solved by design changes and materials selection.

References

1. General Manager's Task Force, "Incineration of Radioactive Solid Wastes." USAEC Report WASH-1168 (August 1970).

2. B. L. Perkins, "Incineration Facilities for Treatment of Radioactive Wastes: A Review." Los Alamos Scientific Laboratory report, LA-6252 (July 1976).

3. L. C. Borduin and A. L. Taboas, "US DOE Radioactive Waste Incineration Technology: Status Review." Waste Management '80, Vol 2, pp 623-660 (March 1980).

4. L. A. Stretz, C. R. Allen, and M. D. Crippen, "Combustible Radioactive Waste Treatment by Incineration and Chemical Digestion." Presented to American Institute of Chemical Engineers, August 1980, Portland, OR (also Hanford Engineering Development Laboratory report HEDL SA-2064).

5. L. A. Stretz, "Radioactive Incinerator Offgas System Study: Final Report," Los Alamos Scientific Laboratory, to be issued.

DISCUSSION

CHRISTIAN: Since the technology has been basically developed for the different needs of offgas treatment, what do you feel is the best method of cooling high temperature gases that are laden with volatile materials such as metals and salts?

STRETZ: My personal feeling is that the best method is through an aqueous quench system with a wetted wall type column to assure that these volatile products do go into the scrub solution and not onto the equipment. I have some personal prejudices along those lines because I was involved in developing such a system. From the standpoint of volatile components, I find that this is probably the most attractive.

LILLYMAN: Have you any information on the carryover of radioactivity from the combustion chamber into the cleanup system? How extensive is it?

STRETZ: The carryover into the cleanup system is greatly dependent upon the incinerator type that is being used. An incinerator that uses an extremely turbulent combustion area will typically have very high particulate carryover. This will be where the majority of the activity will enter the offgas system. Other designs that provide for a quiescent type of burning minimize this problem. But, it can best be said that it really depends on the incinerator design. I know that this does not give you a specific answer to the question.

LILLYMAN: Have you measured any figures on this at all?

STRETZ: We have not taken a look at fission product carryover in our system. Our work has been with transuranics. To date,

we have seen very little activity in the scrub solution. The majority of the activity remains in the ash in the incinerator. Once again, I think that is a feature of the controlled air incinerator.

LILLYMAN: Then what are we talking about, something under 1%?

STRETZ: I would say, probably less than 5%. That is just a guess. We do need to do more work on quantifying it and that is one of the things we have in our plans at this time. That is to say, to look at this kind of problem.

RIMSHAW: I would like to bring up one problem on combustion that I do not think has been explicitly stated here. That is, you get about a 0.5%, or maybe 1%, of high boiling organic compounds that plate out in soot. One solution for this that you may be familiar with is high temperature filtration with silicon carbide filters. They oxidize this material right in place at a high temperature. How would you take care of this if you did not use silicon carbide? I think what Jerry Christian was probably asking you was, how do you take care of the particulate carbon and high boiling organics that will plate out, plug your system, and cause you trouble in a lot of ways?

STRETZ: I don't look at it as a problem to handle in the offgas system, but rather as one to handle by the efficiency of the combustion process. I am aware that a type of system has been used, where you actually burn the soot in place on filter elements. For the type of waste that we are looking at and burning, I believe the incinerator combustion efficiency can be high enough to prevent these materials from becoming a serious problem. Maybe I don't understand the problem you have presented.

RIMSHAW: Maybe you don't, because usually one problem in all these systems is fires in the filter bags. You mentioned that you had a fire in the filter bag. These deposits are flammable and this is one of the problems.

STRETZ: I stated that I had heard a report of a fire in filter bags and this is one of the reasons why I stated that I favored using an aqueous quench system to assure that these products go into the scrub solution rather than being on the equipment surfaces.

RIMSHAW: This is true, but then you have a mess in your scrub solution; you have these oily organics. I was just wondering how you would cope with it. That just seems to be a real problem in all these combustion systems, i.e., there is always a certain amount of high boiling volatiles that escape and condense out.

DEVELOPMENT OF THE PROCESSING SYSTEM FOR PLUTONIUM CONTAMINATED HEPA FILTERS

Katsuyuki Ohtsuka
Power Reactor and Nuclear Fuel Development Corporation
M. Buseki, Tokyo Nuclear Services Company, Ltd.
T. Inoue and Y. Itoh, Nitta Belting Company, Ltd.

ABSTRACT

Volume reduction and stabilization for the nipple-connecting type of HEPA filter installed in the exhaust systems of the production facility for plutonium fuel have been studied and evaluated by Power Reactor and Nuclear Fuel Development Corporation (PNC), Japan. This was necessitated because of the larger size of these filter units compared to the conventional sizes 5 and 3 filters installed in other facilities of PNC.

The nipple-connecting type of HEPA filter can be considered to consist of three elements, a couple of nipples, wood frame, and filter medium together with asbestos separators. Separation into these three elements was needed in order to proceed to succeeding stages of the disposal chain. By the end of 1978, shredding, sawing, and cutting methods had been tried in using the prototype machine which had been built to prove the various functions for design of complete processing by an automatic control system. As a result, development of the automatic processing machine was designed upon the drill-cutting method.

I. Introduction

At present, a quarter of the total plutonium-contaminated waste from the production facilities for plutonium fuel consists of the HEPA filters used in the exhaust systems of PNC. It has become necessary to reduce and stabilize this waste in order to establish effective storage and control.

The nipple-connecting type of HEPA filter can be considered to be composed of the three elements shown in Figure 1. A first stage of the processing system therefore requires separation of the filter into these elements: wood frame, metal nipples, and glass fiber medium along with asbestos separators. This first stage will provide products which can be processed easily in succeeding stages of the system, such as incineration or melting. The prototype equipment was constructed as an experimental model on which design and development could be undertaken for the filter processing system.

II. Design Policy of the Processing System

1. Design Policy

(1) The system should be installed in a sealed containment in order to prevent plutonium dispersion and there should be no possibility of deterioration in case of an earthquake, fire, or other incident.

(2) The system should be operated remotely by means of an automatic control system developed for positive safety.

(3) A suitable cutting method should be developed to separate each element of the filter in the form required.

(4) The system should be compact and the processing time should be reduced to a minimum.

2. Design Specification

(1) Filter to be processed:

Nipple-connecting type of HEPA filter

No. 1 Size 5 24" x 24" x 20" (excluding nipples)

No. 2 Size 3 12" x 12" x 18" (excluding nipples)

(2) Desirable system performance

Render two Size 5 filters per hour.

(3) Dimensions of containment

The system should be installed in a glove box to be 3 meters high x 3 meters long x 1 meter wide.

(4) Design scope

The work covers the sequence of receiving the filter in the containment, separating into elements, packing the separated elements and providing them to the next stage of the processing system.

III. Study of the Processing System

1. Selection of Cutting Tools

Much of the study and research was conducted in the cutting characteristics of a face cutter and twist drill to experiment in cutting the plywood board that comprises the filter frame. As a result, the following were observed in the performance of the face cutter.

(1) It is difficult to obtain uniform and steady cutting because of the alternating direction of the grain of the plies of wood in the plywood.

(2) Useful life of the cutter is short, requiring cutter replacement too frequently.

(3) It caused an abnormally heavy dispersion of cutting dust.

(4) The filter is difficult to hold in place because of excessive torque imposed on the filter by the cutter.

For the preceding reasons, the face cutter was discarded and the drill was adopted as the cutting device. Because many stainless steel nails are driven into the plywood frame during fabrication of the filter, experiments were conducted carefully to develop the shape of the drill bit which is capable of cutting such materials as well as the plywood in a single pass.

The driving force and torque of the drilling were measured by cutting 3/4-inch plywood with drills of various shapes of face and at various speeds. This experimental work was conducted on a radial drilling machine equipped with instrumentation such as load cells, etc. The arrangement is illustrated in Figure 2.

Test Results

(1) Cutting was increased and driving force decreased by minimizing the size of the web and chisel edge.

(2) There was some variation in the results of torque measurement. The maximum torque was 17 kg/m.

(3) Extent of wood flakes generated is shown in Figure 3.

(4) No degradation was observed in either the cutting performance or of the face of the drill after cutting plywood along with stainless steel nails.

Results above dictated a drill size of 60 mm. in diameter, an operating speed of 750 rpm., and a shape of drill face illustrated in Figure 4 as best for cutting.

2. System Study of Processing

The main purpose of this stage of the procedure is to separate the filter into chips of wood, a couple of nipples, and medium with asbestos separators. It consists of the following mechanisms for fully automatic processing.

(1) Handling mechanism

This is to carry the filter to the holding mechanism from the receiving device within the containment.

(2) Holding mechanism

This will hold the filter during cutting of front and back plywood plates and to rotate it for the next procedural step.

(3) Clamping mechanism

This will grasp the nipple for progressive movement of the filter, and added stability in conjunction with the clamping mechanism, during the cutting process.

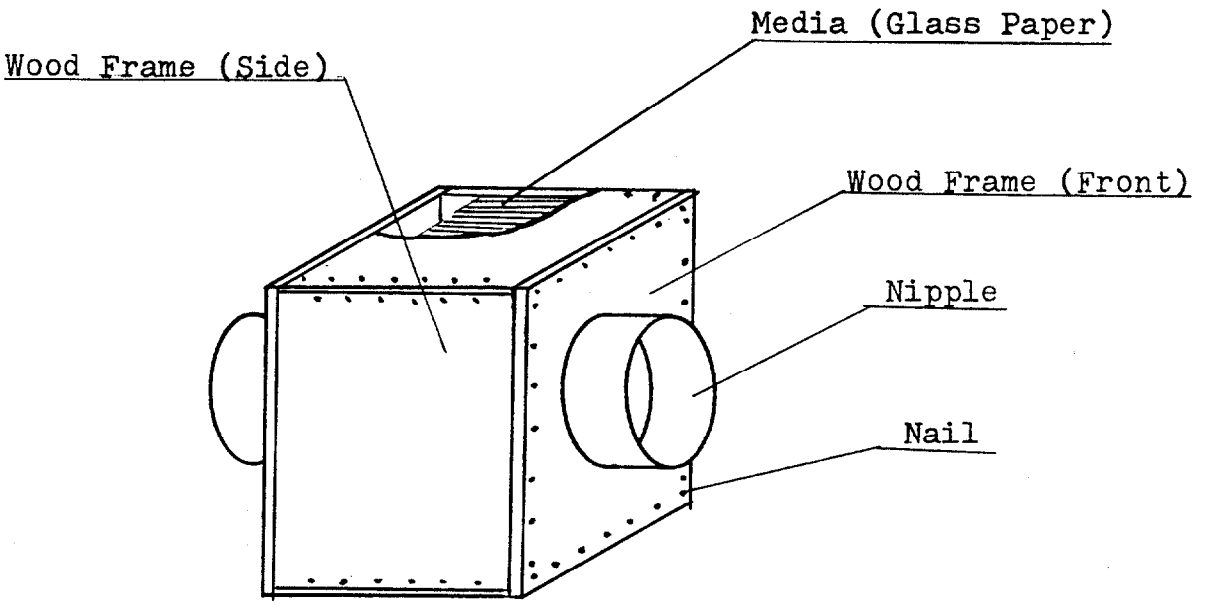

Nipple-Connecting Type of HEPA Filter

Figure 1

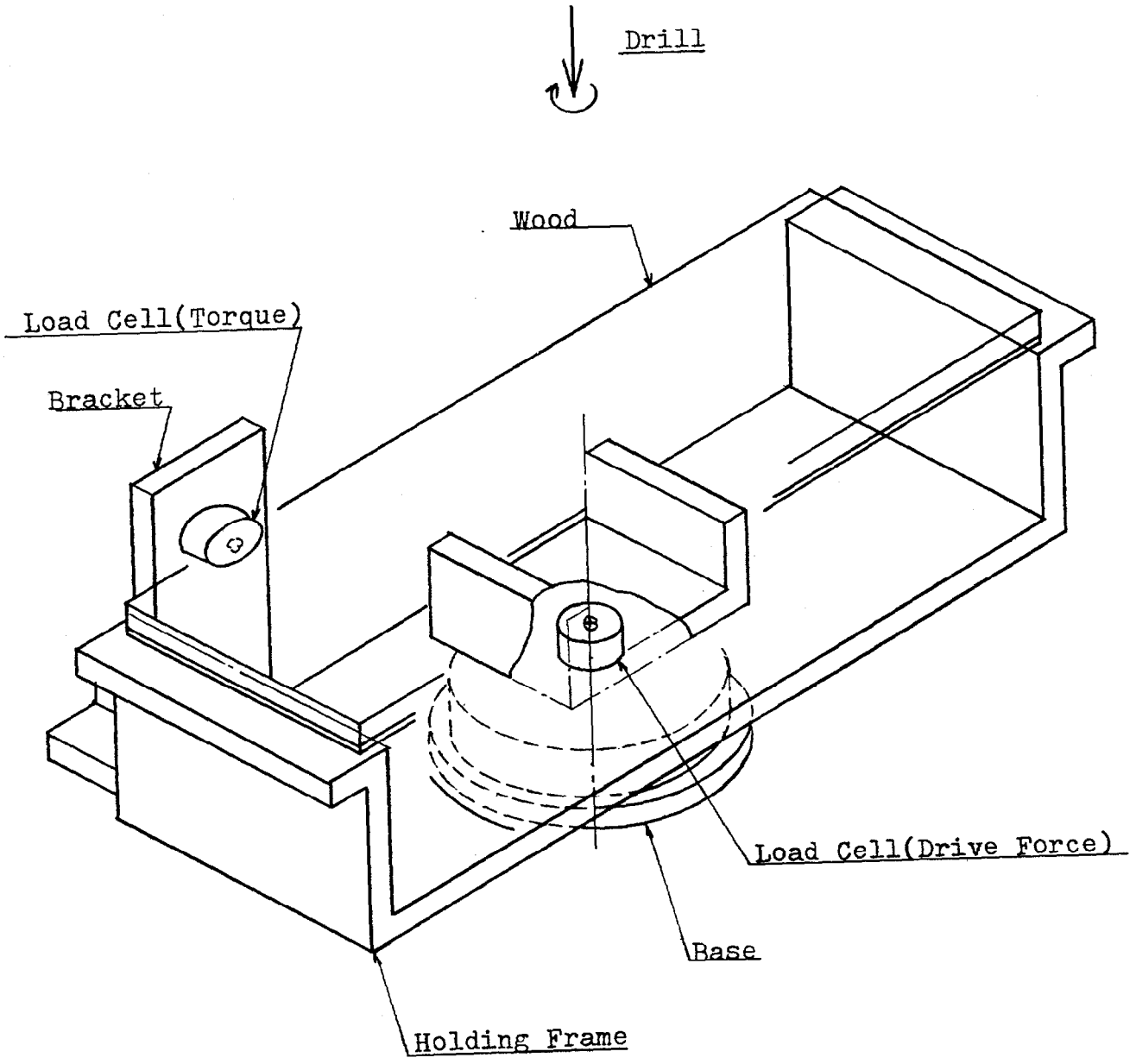

Torque and Driving Force Testing Jig.

Figure 2

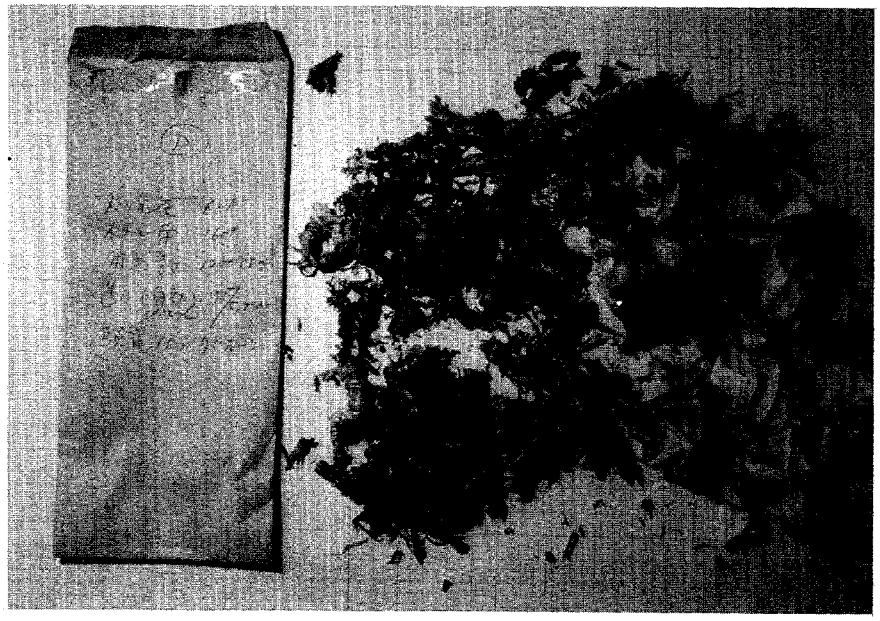

Plywood Chips

Figure 3

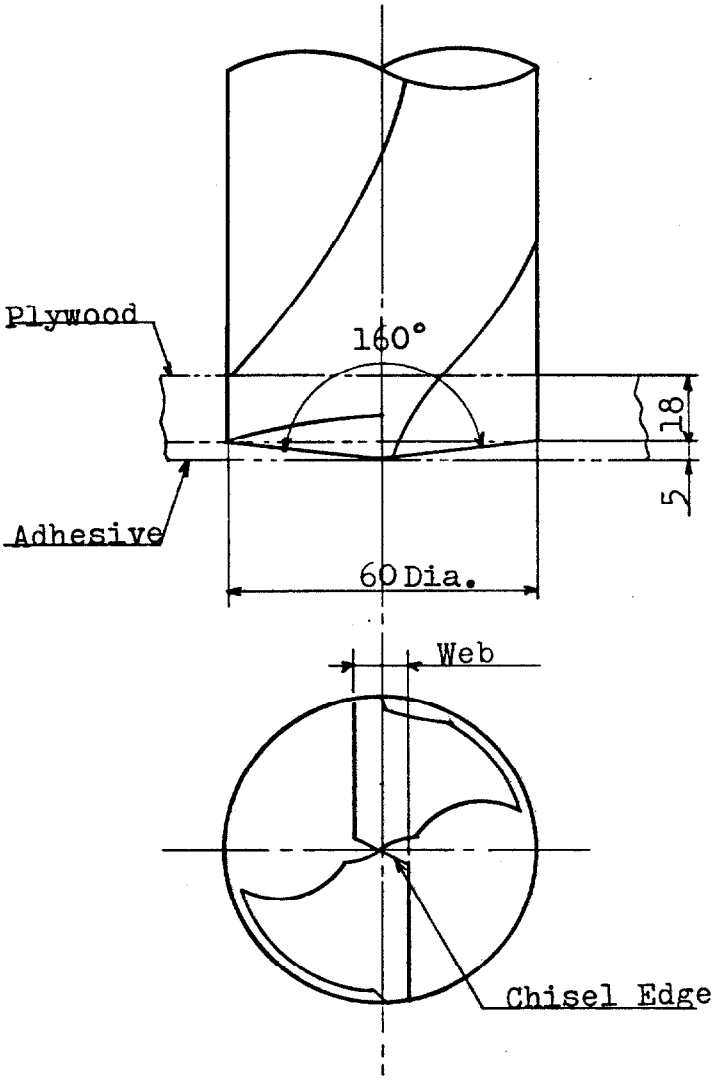

60mm Dia. Drill

Figure 4

(4) Cutting mechanism

From the viewpoint of the cutting period and for compact design, four heads, two each drilling in both the horizontal and vertical direction, were adopted.

(5) Waste handling mechanism

This will remove separated elements, wood chips, nipples, and medium together with separators for the next stage of operation.

(6) Dust collecting devices

These will collect the fine wood dust generated during the cutting process. This prevents the build-up of dust on the inside faces of clear glove box panels which obscures the operation.

(7) Control system

This feature will control operation of each stage of operation by means of a microcomputer, limit switches, and other sensing devices.

IV. Simulation Test

The prototype machine with almost the same functions as the production machine was built based upon the results of preliminary experiments on drill cutting. The model glove box (made of vinyl sheet) was erected around this machine. Not only did we confirm the function, and rigidity such as in the cutting, holding, and clamping mechanisms, but we likewise studied the functions of the total system. These involve the dispersion of wood flakes and fine dust and the adhesion of dust to inside the machine enclosure panels, and the performance of maintenance from outside of the glove box, which is very difficult to learn in experiments on individual components.

1. Components of the prototype machine

The handling mechanisms for carrying in and -out, as well as devices for dust collection, were not designed. Design was unnecessary because of the availability of commercial products and well-known methods. The outline of the prototype machine is shown in Figure 5.

(1) Cutting mechanism, Figure 6

This mechanism consists of two horizontal drill heads for cutting front and back plates of the filter. Two vertical drill heads cut away the four sides of the filter. Each head is powered by a motor and drive gears. Cutting is done according to the patterns shown in Figures 7, 8, and 9. Drills of the prototype machine are 60 mm. in diameter. The Morse Taper shank drill is shown in Figure 4.

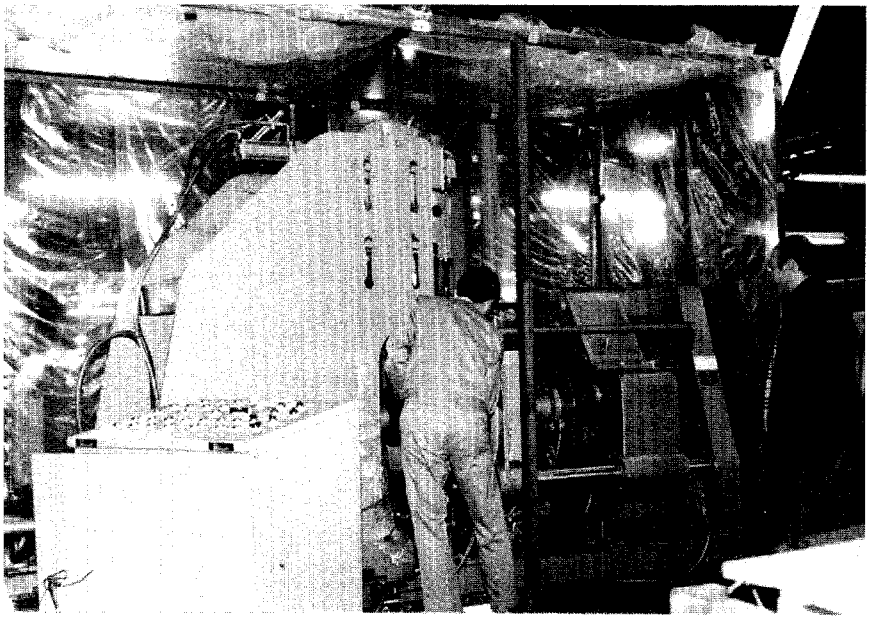

Prototype Machine

Figure 5

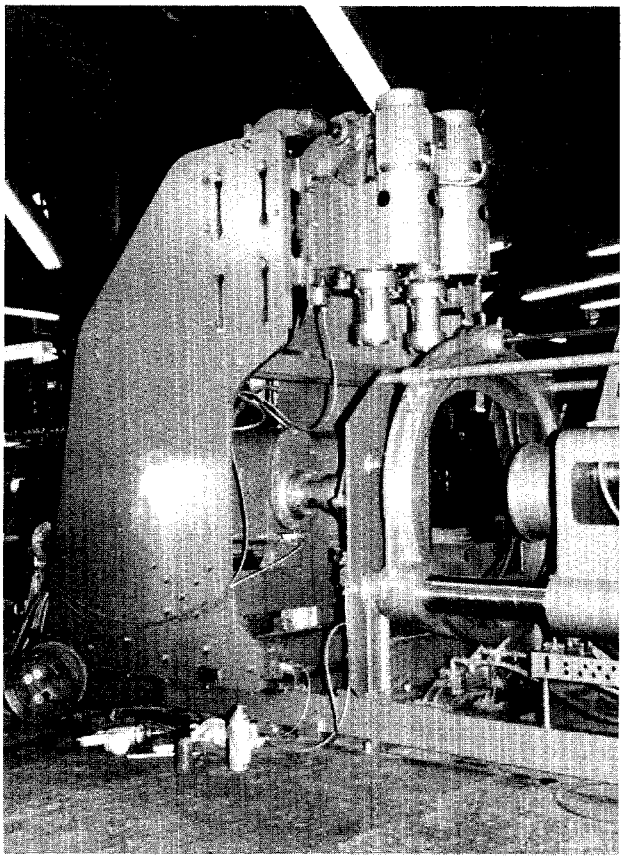

Cutting Mechanism

Figure 6

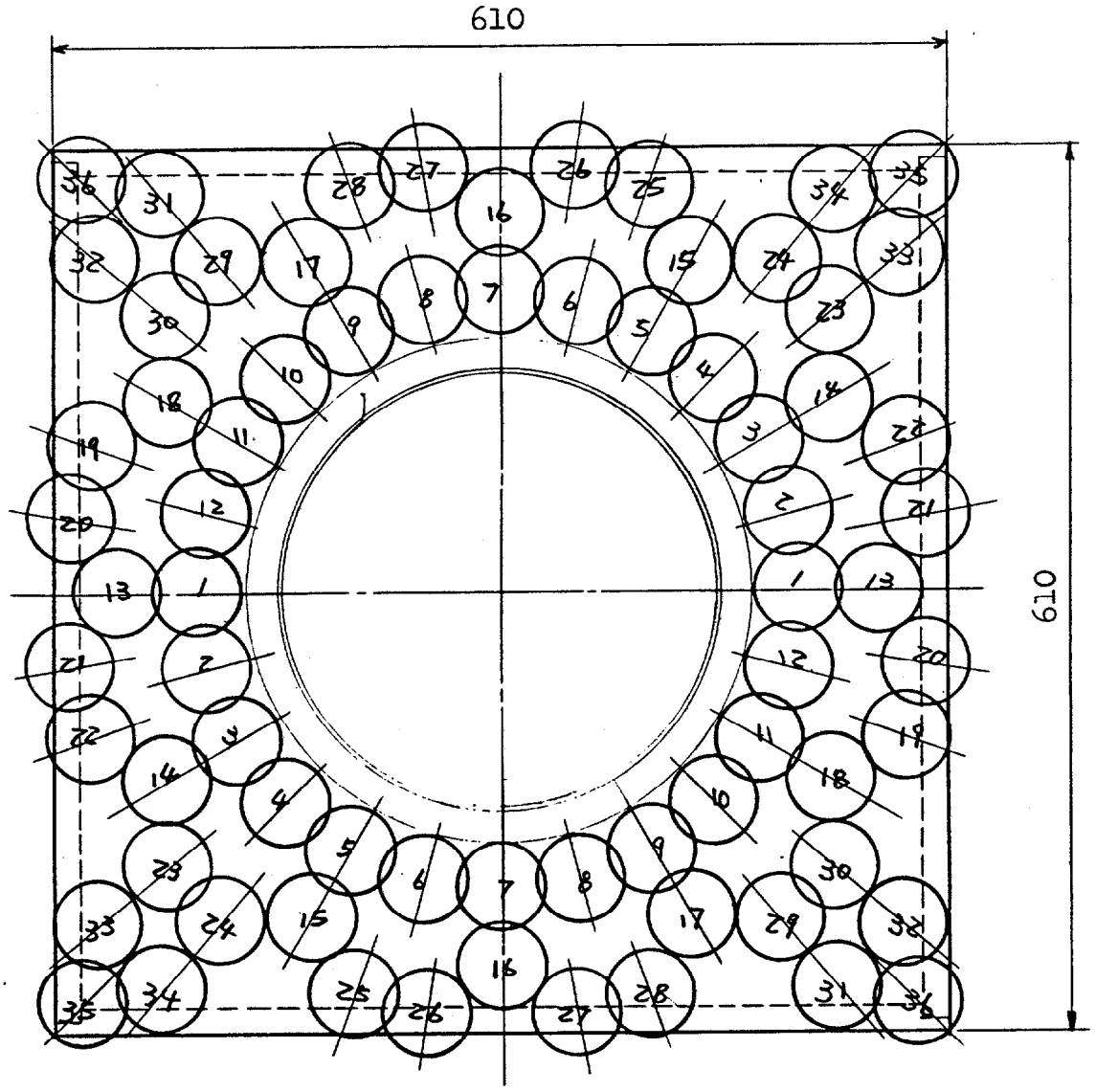

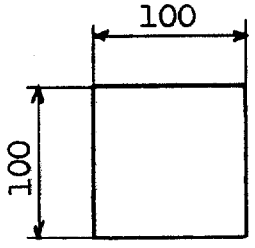

Scale Reference 10cm SQ

Size 5 Cutting Pattern (Front)

Figure 7

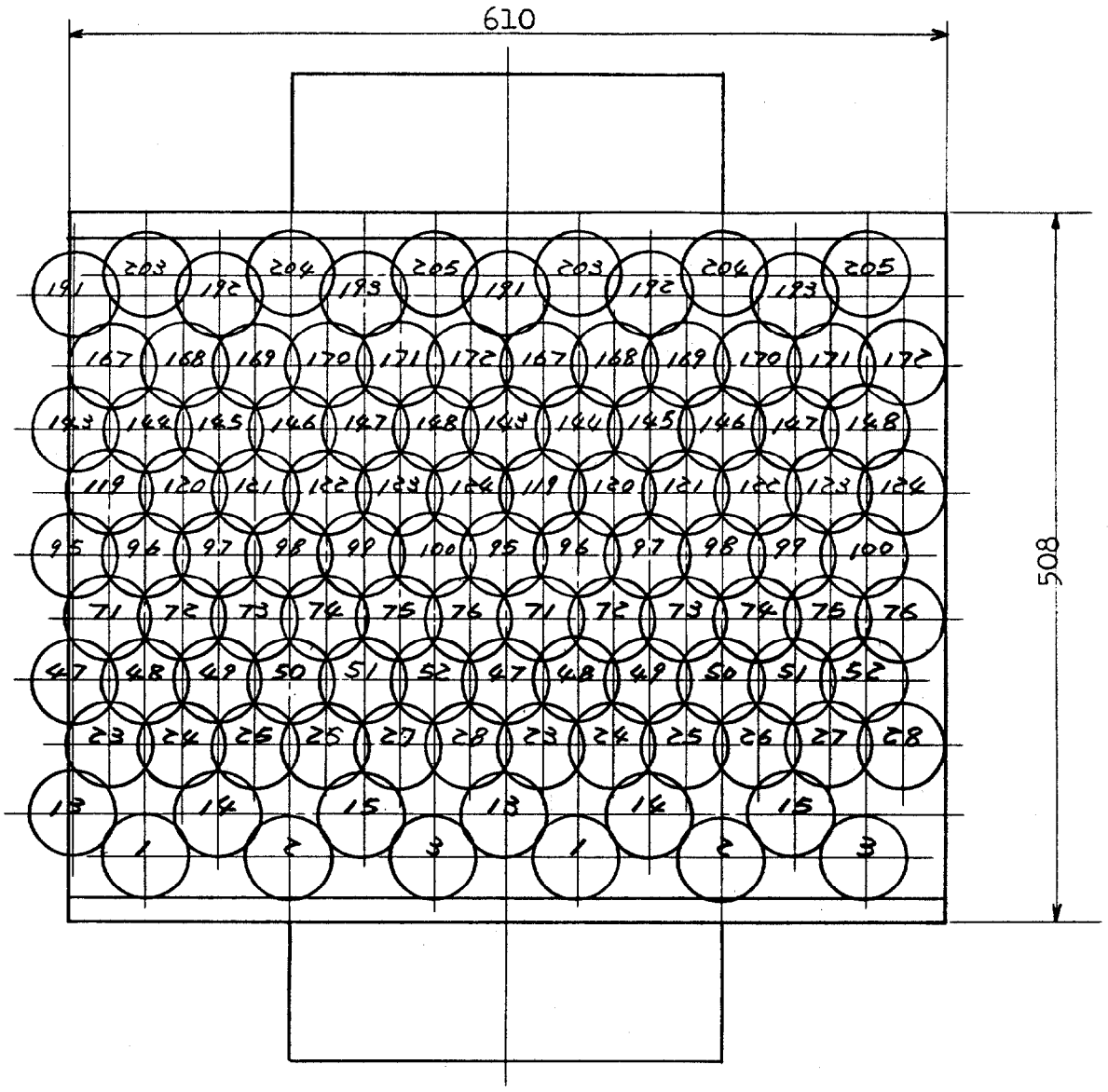

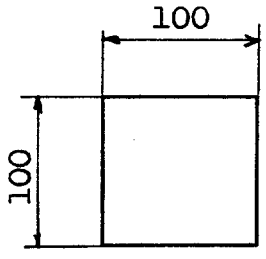

Scale Reference 10cm SQ

Size 5 Cutting Pattern (Four Sides)

Figure 8

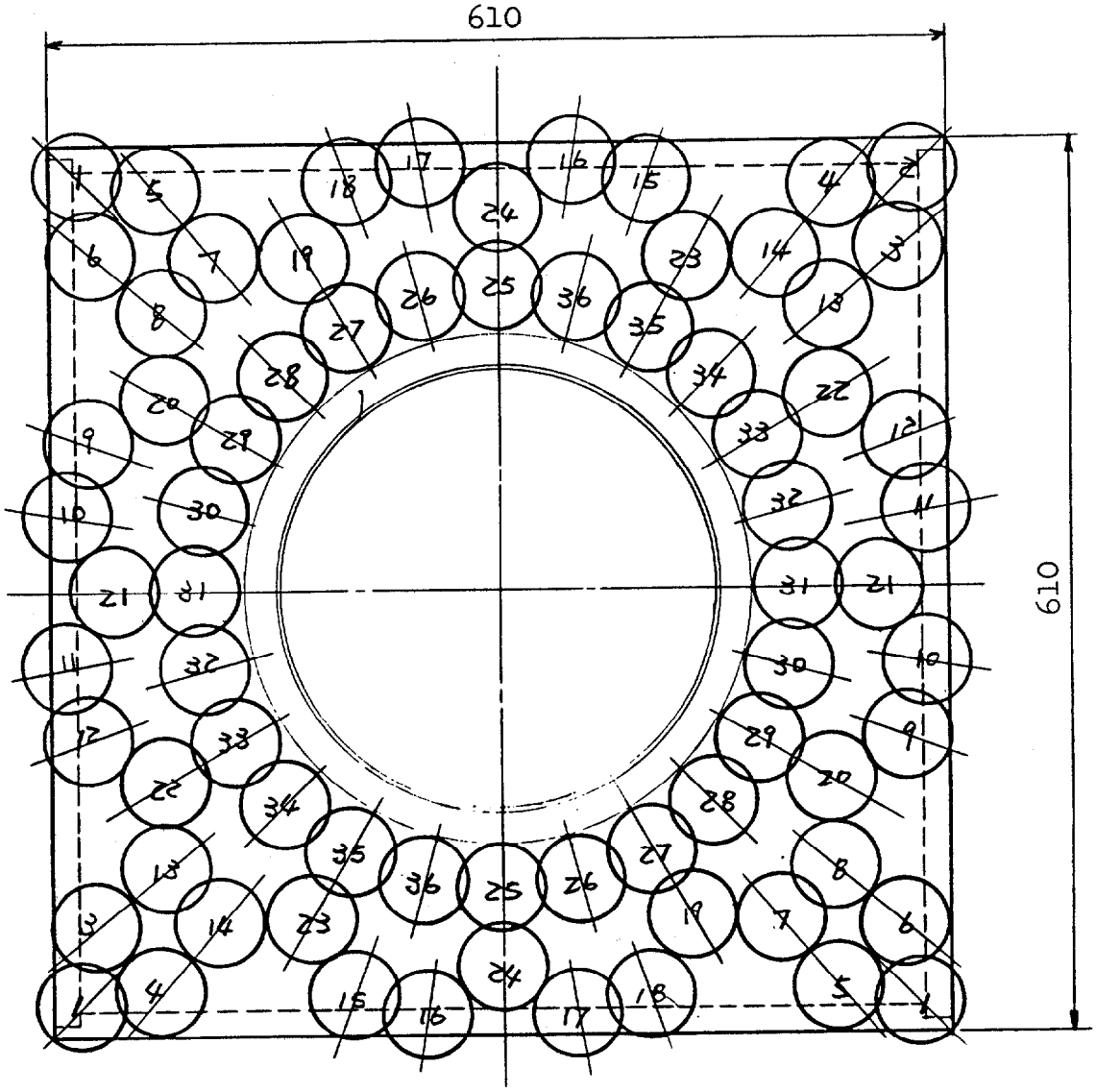

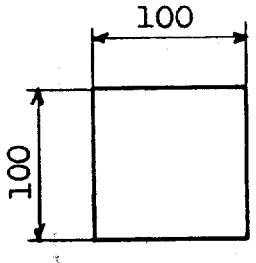

Scale Reference 10cm SQ

Size 5 Cutting Pattern (Back)

Figure 9

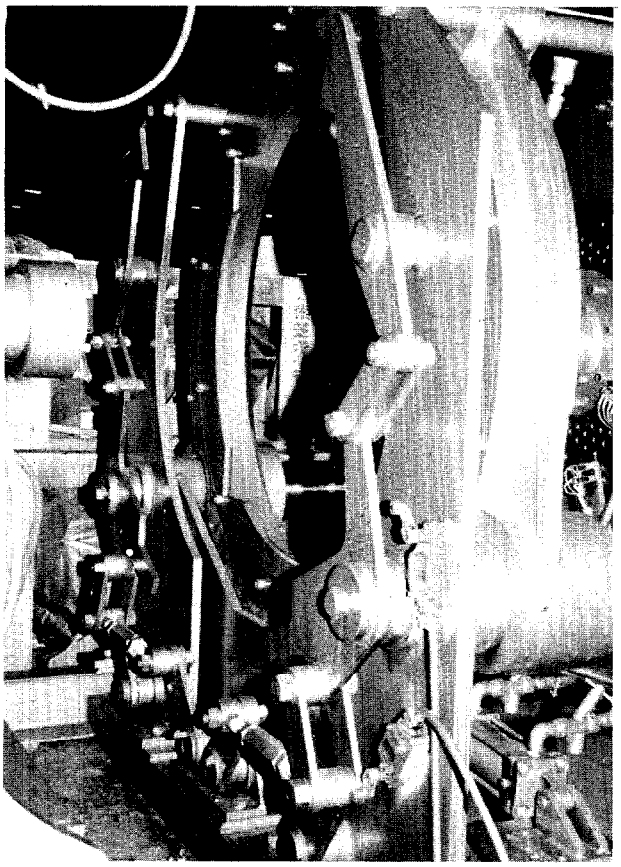

Holding Mechanism

Figure 10

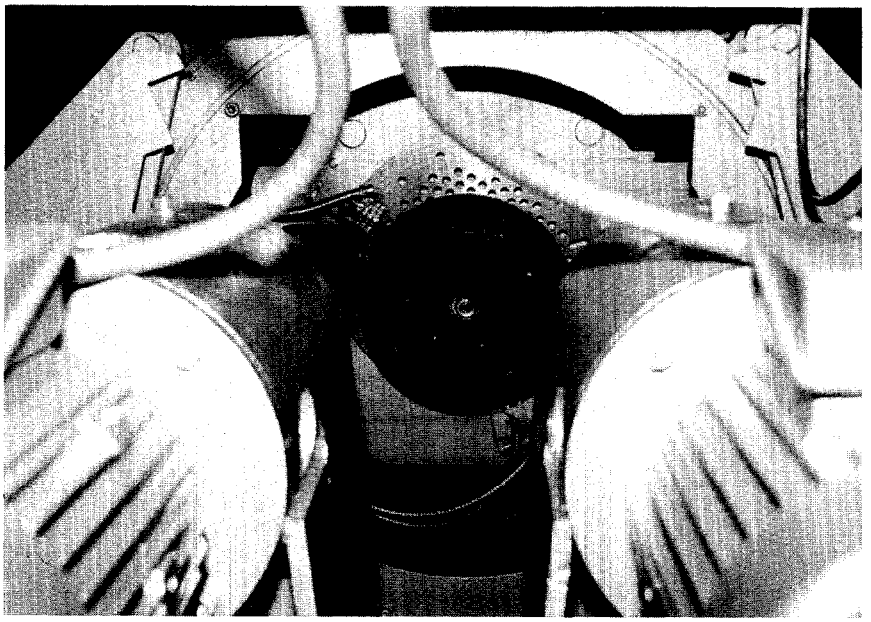

Clamping Mechanism

Figure 11

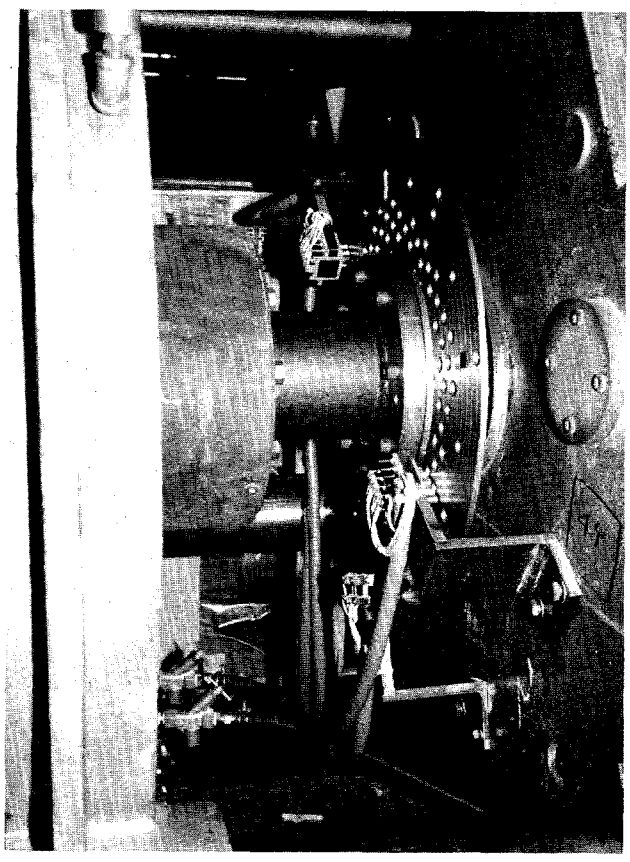

Programming Plate

Figure 12

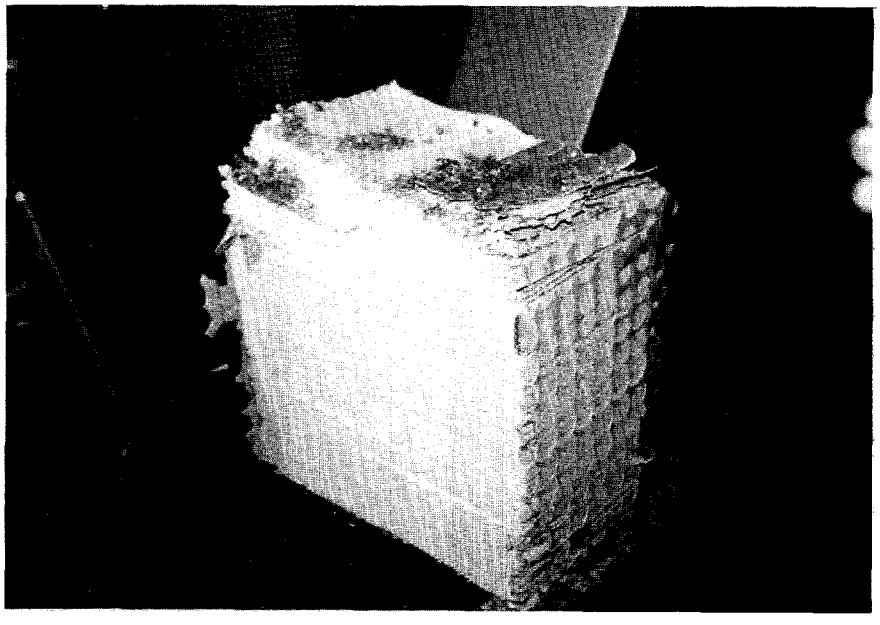

Medium and Separators
(Frame Removed)

Figure 13

(2) Holding mechanism, Figure 10

This mechanism performs dual functions. One holds the filter at four of its corners by right and left links actuated simultaneously by air cylinders. This prevents the filter from vibrating and twisting during the cutting process. The other function revolves the filter according to the pattern for cutting end plates and turns it 90° for cutting sides.

(3) Clamping mechanism, Figure 11

The clamping mechanism is comprised of the nipple-clamping head and its driving gears. One nipple is clamped in the cutting process, which further stabilizes the work in conjunction with the holding mechanism. This also moves the filter forward at the fixed rate specified for the cutting pattern.

(4) Control system

Manual and automatic control are provided so that all of the functions can be tested separately throughout the mechanism without stopping. The automatic control is operated by the microcomputer which receives signals from the programming plate and limit switches. The sensors and programming plate are shown in Figure 12.

(5) Cutting pattern

The cutting pattern is preset to minimize cutting time and volume of wood flakes. Tracks of the drills overlap each other so that there will be no failure of cutting in case of deterioration of a drill bit.

2. Test Results

(1) Cutting

No. 1 End plates

Plywood was cut off and the nipples were separated without any problem.

No. 2 Four sides

The top and bottom plywood plates were removed without difficulty. Two sides required more drilling depth because of absence of support below by the filter medium. Direction of medium pleated across separators varies support from one side to another. Medium and separators were separated as a block covered with adhesive, Figure 13.

(2) Clamping mechanism

The filter was held stable throughout the processing.

(3) Cutting pattern

The cutting was done automatically in accordance with the fixed program. Consequently, satisfactory performance was obtained from this pattern.

(4) Volume of wood flakes

The volume was 0.17 m^3 in performing the operation on a Size 5 filter.

3. Evaluation of the prototype machine

Resulting from operation of the prototype machine, the filter was separated satisfactorily into wood chips, nipples, and medium, as expected in the design stage. The basic function of each mechanism and total function as a system were almost satisfactory. In design of the production machine, however, the holding mechanism and the control system will be improved for greater safety and for reduction of the cutting period.

V. Design of the Production Machine for Processing a Plutonium-Contaminated HEPA Filter

The production machine was designed based upon the study and evaluation of results obtained from experiments with the prototype machine.

1. Components of the production machine

Complete assembly drawings of the production machine and its processing flow chart are shown in Figures 14 and 15.

(1) Filter handling mechanism

From a glove box adjacent to the containment, the filter is borne over the cutting mechanism on a tray-type container to reach the holding mechanism.

(2) Holding mechanism, Figure 14

A scroll chuck mechanism, instead of the link mechanism of the prototype machine, was supplied for the production machine. Better rigidity for the cutting process is expected by holding four corners of the HEPA filter frame with the scroll chuck. The mechanism also has the capability of adjusting to keep the nipples of the filter at the center line of the machine.

(3) Clamp mechanism

The clamping mechanism is actuated by a chuck powered by oil pressure rather than air pressure. Respective clamping heads are provided for Size 5 and Size 3 filters.

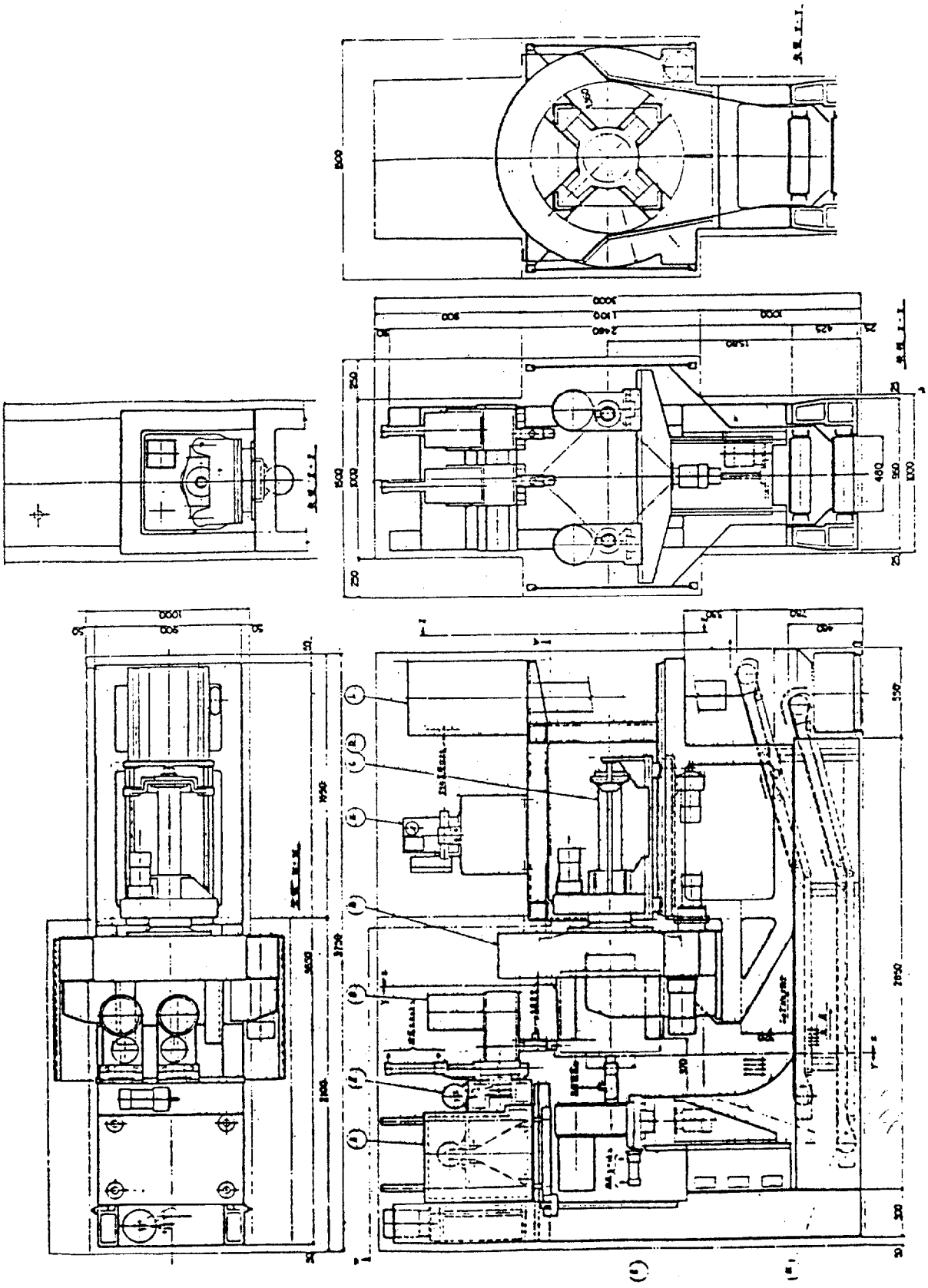

Figure 14 Assembly Drawing

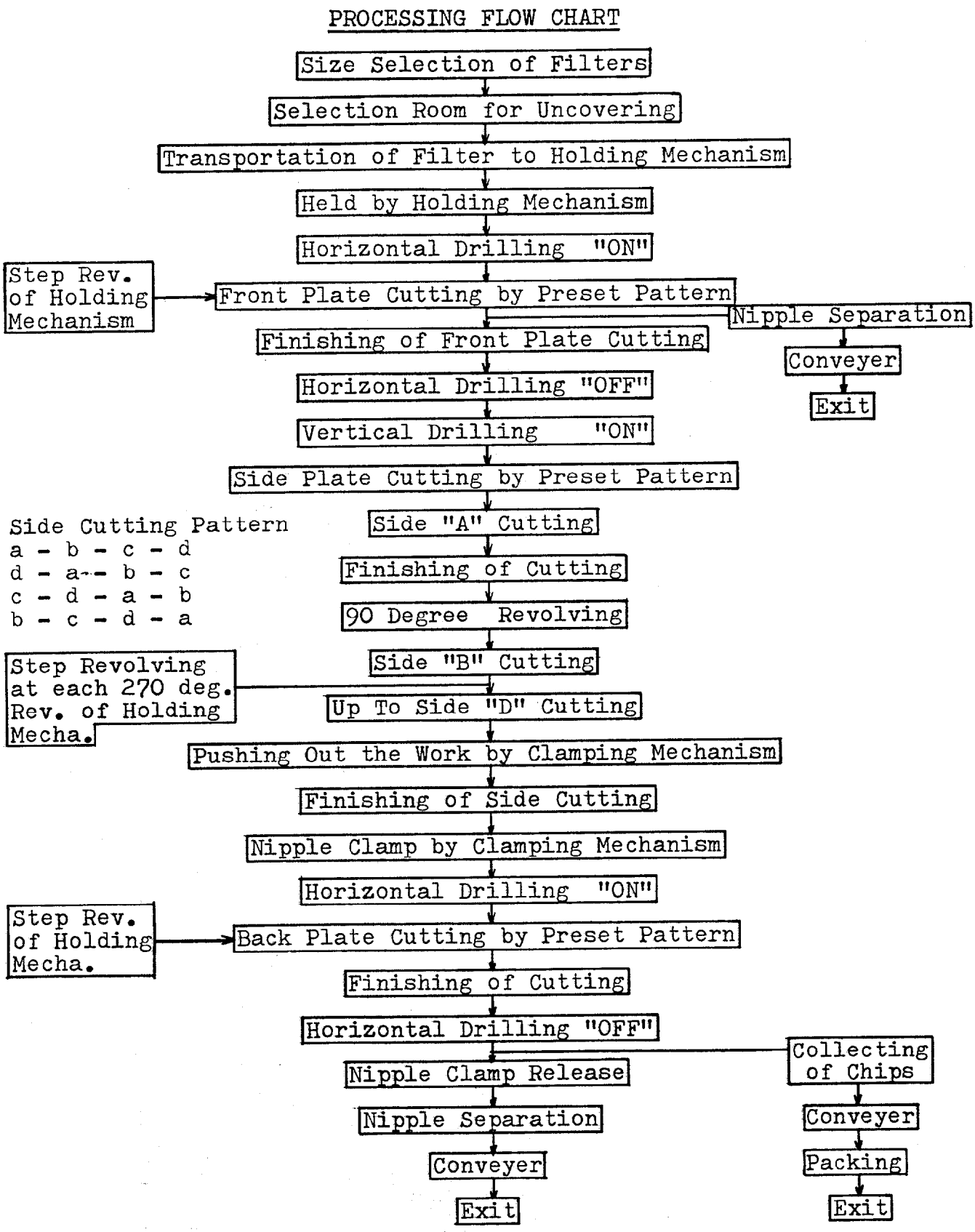
PROCESSING FLOW CHART
Size Selection of Filters
Selection Room for Uncovering
Transportation of Filter to Holding Mechanism
Held by Holding Mechanism
Horizontal Drilling "ON"
Step Rev. of Holding Mechanism
Front Plate Cutting by Preset Pattern
Nipple Separation
Conveyer
Exit
Finishing of Front Plate Cutting
Horizontal Drilling "OFF"
Vertical Drilling "ON"
Side Plate Cutting by Preset Pattern
Side Cutting Pattern
a - b - c - d
d - a - b - c
c - d - a - b
b - c - d - a
Side "A" Cutting
Finishing of Cutting
90 Degree Revolving
Side "B" Cutting
Step Revolving at each 270 deg. Rev. of Holding Mecha.
Up To Side "D" Cutting
Pushing Out the Work by Clamping Mechanism
Finishing of Side Cutting
Nipple Clamp by Clamping Mechanism
Horizontal Drilling "ON"
Step Rev. of Holding Mecha.
Back Plate Cutting by Preset Pattern
Finishing of Cutting
Horizontal Drilling "OFF"
Collecting of Chips
Nipple Clamp Release
Conveyer
Packing
Exit
Nipple Separation
Conveyer
Exit
Finishing of One Cycle

Figure 15

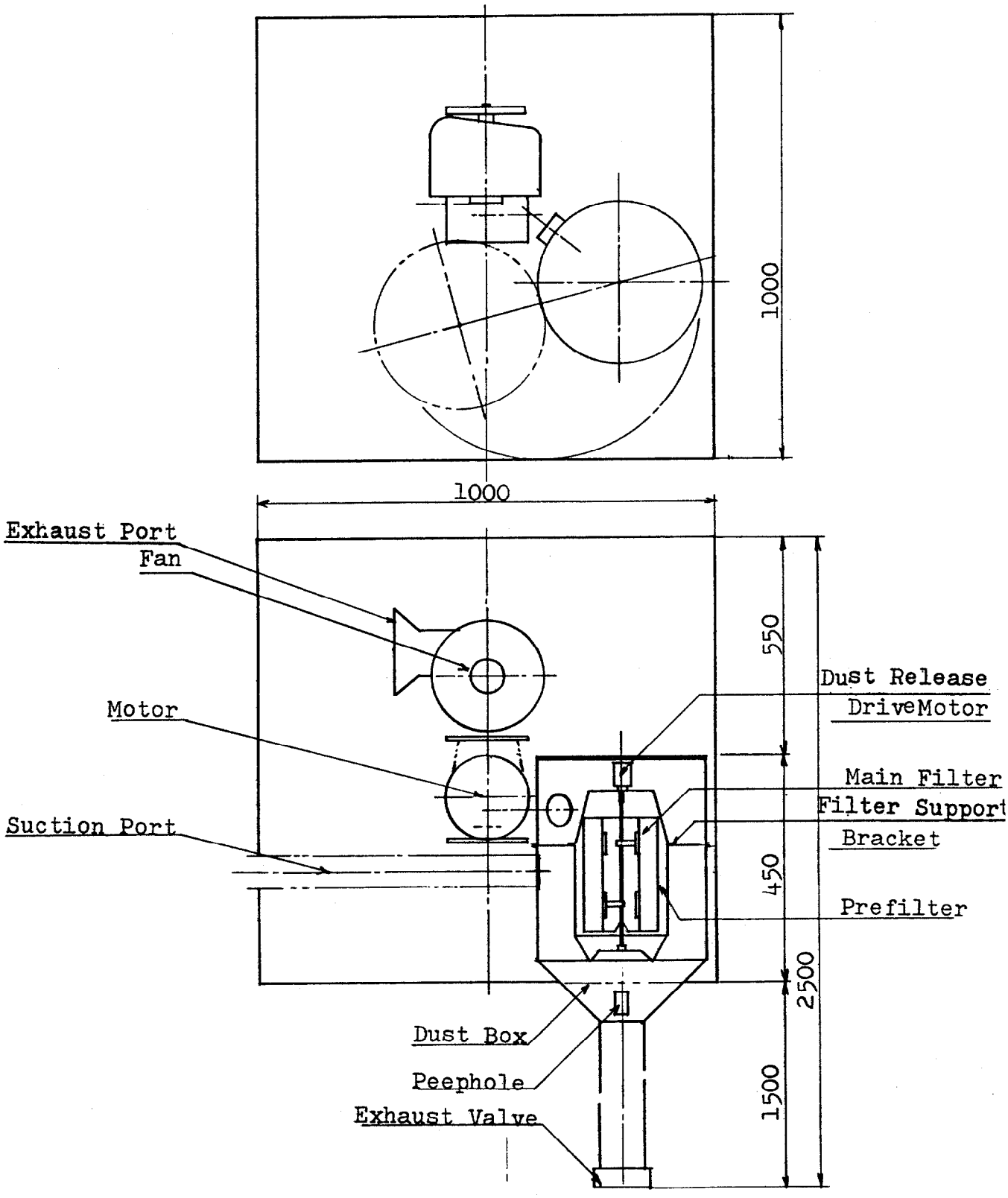

Dust Collecting Devices

Figure 16

(4) Cutting mechanism

Two drill heads and twin spindles will be employed for cutting in the vertical direction and similar equipment will cut in the horizontal direction.

(5) Separating and filter-handling mechanism for processed elements

This arrangement provides a twin-belt conveyor. The upper belt is a screen type bearing nipples, medium, separators, and wood chips. The wood chips will pass through the screen and be carried out by the lower belt.

(6) Dust collecting devices

Cylindrical dust collecting heads are installed for every drill to intake the dust scattered during the cutting operation. Dust will be exhausted to a cyclone comprising the first stage. Particles passing the cyclone will be collected by a unit filter, Figure 16. The life span of this filter will exceed 10,000 hours at the maximum flow rate of 180 m^3/hr.

(7) Driving and control systems

Insufficient force is exerted by a small size of cylinder driven pneumatically. Therefore, the production machine was designed for operation by hydraulic oil to assure adequate power. Opening and closing of chucks, and movement of the work during cutting, will be actuated by an oil-powered cylinder. Each mechanical function is controlled by a microcomputer. As a consequence, the production machine can be operated automatically throughout the processing.

(8) Processing capacity

The period to process one Size 5 filter is 55 minutes and processing a Size 3 filter consumes 30 minutes.

(9) Containment

The production machine must be installed inside of a containment. Part of the holding mechanism was widened because of a revolving ring of large diameter. The dimensions of the containment are 3.75 meters long, 1.5 meters wide, and 3 meters high. Ports for maintenance were provided with gloves mounted in the acrylic panels of the containment.

VI. Conclusion

Many studies and much research work was repeated and two prototype machines were built before designing the production version of the processing system for plutonium-contaminated HEPA filters. The nipple-connecting type of HEPA filter can be separated into wood chips, nipples, medium and separators without difficulty and the processed material is in satisfactory form and condition. Two problems, however, remain to be solved.

(1) Reduction of processing time

The use of a larger drill must be studied to reduce cutting time. The major part of the processing period is used in cutting away the four sides of the filter. A drill bit of larger diameter appears to be the solution.

(2) Development of a new drill for longer life

Drill bits deteriorate after long use and must be replaced. It is therefore desirable to identify or develop a new drill with high resistance to wear. In addition, a grinding machine should be installed exclusively for drill bit sharpening. Attainment of these objectives should minimize secondary waste from these sources.